REPORT OF AD HOC COMMITTEE

on

ENVIRONMENT MODIFICATION EXPERIMENTS IN SPACE

to the

National Aeronautics and Space Administration

March, 1968.

Report of Ad Hoc Committee

on

ENVIRONMENT MODIFICATION EXPERIMENTS IN SPACE

by

D.A. Tidman* (Chairman)
University of Maryland

R.A. Helliwell*
Stanford University

W.N. Hess
NASA Manned Space Craft Center, Houston

E. Hones*
Los Alamos Scientific Laboratoris

C.F. Kennel*
University of California, Los Angeles

L.M. Linson*
AVCO Everett Research Laboratory

C.E. McIlwain*
University of California at San Diego

T.G. Northrop
Goddard Space Flight Center

H.E. Petschek*
AVCO Everett Research Laboratory

March, 1968.

* The work of these authors was supported in part by National Aeronautics and Space Administration Grant NsG 220-62.

CONTENTS

The chapters in this report have been arranged in the order of topics dealing with injection of energetic particles, neutral plasmas, and waves, respectively.

Contents continued

Contents continued

Contents continued

1. INTRODUCTION

Since the discovery of the radiation belt in 1957 and the discovery of the general nature of the earth's magnetosphere over the ensuing few years, there has been a period of extensive mapping of this environment. We now have a fairly detailed picture of the particle fluxes, plasmas, and fields in the space around the earth and are also starting to acquire some understanding of the nature and intensity of the various electromagnetic waves in this region.

Clearly however there is much work that needs to be done to elucidate this picture - particularly in revealing the physical mechanisms that maintain the environment the way it is and control dynamic phenomena occurring in it.

In this report we suggest that a different kind of effort, which is more manipulative of the environment, would aid in obtaining a fundamental understanding of these basic mechanisms.

In order to obtain a quantitative understanding of many magnetospheric phenomena it would be very instructive to carry out controlled "active" experiments in space. We have in mind experiments in which the environment is modified in a controlled and temporary way. By studying the results of such modifications we can isolate the physical variables that are involved and start to

understand the basic dynamics of magnetospheric processes.

Naturally occurring events like magnetic storms or auroras are almost biological in their complexity, with several processes occurring simultaneously. Passively observing such phenomena (as has been done to date) is similar to the study of taxonomy where one observes the gross features of a biological specimen and classifies it. Conducting controlled geophysical experiments on the other hand is analogous to the study of physiology where one studies a part of a biological system and understands its functions and properties. The ability to isolate variables in such a complicated system plays an important role in gaining this understanding.

It should also be pointed out that a detailed understanding of the dynamics of field, particle, and plasma processes in the neighborhood of the earth is expected to have (and indeed already has had) an important impact on astrophysics. Many of the processes that are hypothesized to occur on the Sun, in the Solar System and beyond, are similar to those occurring in the magnetosphere. A detailed understanding obtained from our "local" environment in space will thus help to clarify our understanding of more distant astrophysical phenomena.

In this report we have listed a number of specific ideas that were examined by the committee. These involve experiments with injected electron beams, ion beams, and plasmas produced using

ments could look for unexpected results.

(iii) Many of the experiments done to date which passively map the environment suffer because it is difficult to distinguish between space and time variations in a quantity. Adequate separation of these variables is even more crucial in active experiments. For this purpose a two satellite system with one "slaved" to the other (i.e., with a controllable distance between them) would often be desirable.

---

(1) University of Minnesota Proposal to NASA entitled "Electron Radar Technique as a Probe of the Trapped Radiation Belts". NASA control number 24-005-008-(111), Principal Investigator Dr. J.R. Winckler.

(2) Lockheed Proposal to NASA entitled "Proposal to develop injection experiment for Apollo Flight". Tech.Report No. LMSC-894635, Aug. 1966. NASA control number 05-138-111-(112). Principal investigator, Dr. W.L. Imhof.

Table of Experiments

The weight estimates in the table include the contribution from power supply requirements which are high in some cases. Information on weights and characteristics of power sources available on Apollo and Apollo application missions is included in an Appendix of this report.

Experiment	Weight	Orbit	Expected Results	Possible Effects	Measurements	Principal Difficulties
Electron accelerator for geomagnetic field mapping. (See page 9)	∿ 300 lbs.	200 miles, inclination ∿ 90°	(a) feasibility of field mapping. (b) role of drifts of beam. (c) propagation characteristics of beam in space	Generation of waves by instabilities.	Conjugate point optical ground measurements. RF detectors above ionosphere. Wave frequency measurements in 100 kc → 10 Mc range.	Instabilities may diffuse and de-energize the beam. A maneuverable subsatellite is desirable for measurements.
Generation of artificial Van Allen belt: (a) 300 keV-5 MeV electrons. (b) Ions (10 MeV protons or 7 MeV α-particles) (c) Positrons (d) Lockheed Expt. (see page 35)	1000 lbs. ? "	equatorial circular "	Generation of detectable fluxes and study evolution in L, α, and energy E. Low L-shell diffusion.	"	Partical detectors to measure L, α, E. Wave detection. "	Probably need more than one satellite to make measurements. Injection instabilities may scatter α and E on injection
Destabilize Van Allen belts with electrons of energy ∿ 50 keV. They may verge on instab. in this range for much of the time. They could perhaps thus be held in a marginally stable state.	10^4 lbs.		Fill belt to unstable limit and observe waves. Observe natural changes for marginally stable belts.			Injection instabilities. Large currents require neutralization of charge accumulation on satellite.

Experiment	Weight	Orbit	Expected Results	Possible Effects	Measurements	Principal Difficulties
Increase nightime electron density in the ionosphere at auroral latitudes. (see page 87)	Several hundred pounds.	Ballistic rocket flight in the auroral zone; maximum height 125 km.	A change in the conductivity and currents in the ionosphere. Interference with radio communications. Increased precipitation of electrons.	May trigger an aurora. May create a whistler duct.	Measure n_e by radar. All sky cameras, ground magnetometers, VLF detectors.	
Ion tracer experiments			Trace magnetic $\underline{B}$ and $\underline{E}$ drifts.		Ground based optical. Topside sounder or radar for low clouds.	Cloud diffusion. Injection instabilities. Chemical efficiency of bomb burst ionization. Disturbances of $\underline{E}$, $\underline{B}$.
(a) Ion engine	100 lbs.	300 km	"			
(b) Chemical bursts.	100 lbs.	300 km → greater than $10\ R_E$.				
(See page 125)						

Experiment	Weight	Orbit	Expected Results	Possible Effects	Measurements	Principal Difficulties
Whistler wave injection in space. Coherent waves of controllable frequency with power modulation available. (See page 170)	10^3-10^4 lbs.	L=3-4 and L=6.6 stationary equatorial crossings desired.	Wave growth and damping results. Triggering or supression of natural emission. Electron acceleration, precipitation, and phase bunching.		Detect waves on ground and on satellite. Energy spectrum and pitch angle measurements of electrons interacting with wave.	Antenna size ($\sim$ 5 km ??)
<u>Mass Injection</u> Auroral Zone	$\sim$ 100 lbs	L $\sim$ 6	Disturb convection pattern, modify ionospheric currents, create whistler duct.	Precipitation of particles, aurorae, VLF emissions.	Ground magnetometer, cameras, VLF detection & transmission, riometer, satellite ion detector in cloud.	Predicting ionization times of injected material
Tail (See page 161)	10^4 lb	Tail $R_{\sim} 30\ R_E$	Reduce energy input for $\sim$3 hrs, modify convection and ionospheric currents globally.	Precipitation of particles, aurorae, VLF emissions, modification of trapped particle fluxes, ring current changes.	Complete magnetosphere monitoring.	

2. THE GENERATION OF ARTIFICIAL AURORAE

Wilmot N. Hess

National Aeronautics and Space Administration

Manned Space Craft Center

Houston, Texas

(i) Introduction

The objective of this experiment is to generate an aurora by injecting an intense enough stream of electrons into the geomagnetic field parallel to a field line so that they will enter the atmosphere, deposit their energy and produce an auroral spot. To do this at first we will use a small electron accelerator on an Aerobee 350 rocket.

TABLE 1

The brightness of auroras varies from below the visual threshold to a brightness which produces an illumination on the ground equivalent to full moonlight. Forms are rated in brightness according to the International Brightness Coefficient (IBC).

IBC	I	II	III	IV
Visual Eq. Brightness	Milky Way	thin moonlit cirrus clouds	moonlit cumulus clouds	full moonlight
Intensity (OI) 5577A (Kilorayleighs)	1	10	100	1000
Intensity N_2^+ 1st Neg 3914A KR	1	10	100	1000
Energy Deposition ergs cm^{-2} sec^{-1}	3	30	300	3000

Table 1 from T.N. Davis[1] shows the energy flux required to make different brightness aurorae. Let us consider the requirements to generate an IBC III aurora which should be easily measurable. Using 100 m as the radius of the auroral spot produced we get the input energy requirement of

$$E = \left(300 \frac{\text{ergs}}{\text{cm}^2\text{-sec}}\right) \pi \, (10^4 \text{ cm})^2 \simeq 10^{11} \frac{\text{ergs}}{\text{sec}}$$

We know auroral forms of $\sim$ 100 m width occur naturally. This width should be dominated by coulomb scattering so we should be able to produce a spot of this size or even less artificially.

Let us consider a beam pulse of 0.1 second length -- probably longer than necessary for spot detection. If we use 10 Kev electrons we will require a charge of

$$Q = \frac{10^{10} \text{ ergs}}{1.6 \times 10^{-8} \text{ ergs/electron}} = 0.6 \times 10^{18} \text{ electrons} = .1 \text{ coulomb.}$$

Such an electron beam can be generated by an accelerator that can be flown.

It seems possible to generate an IBC III aurora with a pulse of electrons.[2] What good would it be? There are several scientific experiments that can be accomplished using this capability.

(ii) Possible Experiments

(1) Study of Magnetic Field Line Geometry

By shooting an electron beam up along a field line in one hemisphere and having it hit the atmosphere and produce an aurora in the other hemisphere one can study the large-scale structure of the geomagnetic field (see Figure 1). By observing the spot locations and spot shapes for a series of pulses put out at about one second intervals, we can tell if the electrons are traveling in an orderly fashion or are being disturbed perhaps by various magnetic or electric fluctuating fields.

By observing what happens to the pulses emitted as the satellite moves to high latitudes, one can try to understand the high latitude magnetic field geometry. Boundary current or tail current distortions of the geomagnetic field could be investigated this way. In the polar regions, it should be possible to distinguish between the closed magnetosphere of Beard, Mead, et al, and the open magnetosphere of Dungey and Petschek, et al, by studying field line shapes. These studies will be most valuable conducted at large L values. This method of studying field line shapes, complements single point vector measurements as are commonly made from spacecraft. Here we determine the large-scale field geometry -- a quite different matter.

(2) Determination of Conjugate Point Locations

By using a low altitude satellite, shooting the accelerator beam up a field line, an auroral spot can be made at the other end of the field line -- the conjugate point to the satellite location.

Using ground-based observations at the conjugate point the auroral spot location can be determined to 1 km or better. This is about a factor of 100 better than can be done by present methods of determinig conjugacy. Such an improvement should enable several natural conjugate phenomena to be studied in more detail. It would be interesting here to study polar cap conjugacy and also the diurnal and seasonal variation of conjugate point locations. Approximate conjugate point locations are shown in Fig. 2.

(3) Field Line Length Measurement

By measuring the time it takes the electron beam to go from one end of a field line to the other end, the field line length can be determined. Using a 10 Kev electron beam of $v/c = \beta = .2$ at $L = 6$ where the field line length is about 10^5 km the beam transit time is

$$t = \frac{10^{10} \text{ cm}}{.6 \times 10^{10} \text{ cm/sec}} = 1.6 \text{ sec} \quad .$$

This transit time can be given approximately by

$$t = .055 \frac{L}{\beta} \text{ seconds} \quad .$$

This time is not a sensitive function of the electron's pitch angle, varying only about 3 % for $0 < \alpha < 60°$. Measurements at large L are most important where transit times will be of the order of 1 se-

cond or maybe more. By measuring transit time as a function of L (for example on a low altitude polar orbiting vehicle) one can find field line lengths and also study discontinuities that might occur in transit time vs. L curves if, for example, polar cap field lines that go into the geomagnetic tail don't connect back to the earth.

(4) Measurement of Large Scale Electric Fields

It is commonly held that there are quite large electric fields in the magnetosphere. The SD current system in the polar regions is thought by many to result from a potential of about 30 kilovolts across the polar cap. If there are such large potentials they should be measurable by their effects on the electron beam. The electron beam will be subject to the magnetic field line curvature drift of velocity

$$v_c = \frac{mcv^2}{B_e R} \quad .$$

It will also be subject to an electric field drift if the electric field is perpendicular to the magnetic field, given by

$$v_{\mathcal{E}} = \frac{c\mathcal{E}_\perp}{B} \quad .$$

In order to separate out the electric field drift to measure $\mathcal{E}_\perp$ a series of pulses of different energies can be shot from the acce-

lerator. Using a dipole magnetic field and $\mathcal{E}_\perp = 10^{-8}$ statvolts/cm, corresponding to 30 kilovolts across the polar cap, the displacements due to $v_{\mathcal{E}}$ and v_c from traveling from one hemisphere to the other for $L = 6$ for a 10 Kev electron beam are

$$X_c = \int \frac{mcv^2}{B_e R} \left(\frac{dl}{v}\right) = 6 \text{ km East}$$

$$X_{\mathcal{E}} = \int \frac{c\mathcal{E}_\perp}{B} \left(\frac{dl}{v}\right) = 1.3 \text{ km North} \quad .$$

Due to the different velocity dependences of $X_{\mathcal{E}}$ and X_c we should be able to separate out these two drifts quite easily and measure values of the electric field down to values given roughly by

$$\int \mathcal{E}_\perp (\mathcal{L})\, d\mathcal{L} > V_{beam} \quad .$$

A measurement of $\mathcal{E}_{||}$ may also be possible by observing at what altitude the artificial aurora is produced and seeing if it is consistent with the beam energy or not. These measurements will be especially interesting in the auroral zone. Ground-based observations of the spots with an accuracy of $\sim 0.1°$ seem necessary here.

Vertical luminosity profiles calculated by Maeda[3] for different energy electrons are shown in Fig. 3. The ability to measure the bottom edge of the profile and thereby the electron energy

at the top of the atmosphere is what makes it possible to measure $\mathcal{E}_{\parallel}$. If the vertical profile is inconsistent with the beam energy, then an electric field $\mathcal{E}_{\parallel}$ may be present.

(iii) The Wallops Feasibility Test

It is necessary to show that the idea of producing auroral spots with a space-borne accelerator is feasible. There are several things that could go wrong. We expect to fly an electron accelerator on an Aerobee 350 Rocket from Wallops Island in July to show that the idea works.

a./ The Electron Accelerator

The accelerator will be a set of nine electron guns each with a single accelerating grid. The guns will be opened in flight and pulsed with voltages varying from 1.25 kilovolts to 10 kilovolts and with controlled currents from 1.5 ma to 500 ma. Most pulses will be 0.1 second long but about every 10 pulses a long pulse of 1.0 second at full power will be put out to enable the observers on the ground a good chance to see the spot. The accelerator is being constructed by Ion Physics Corporation under the direction of Mr. William Beggs.

b./ The Auroral Spots

Dr. Martin Berger and Mr. Steve Seltzer of the Bureau of Standards have performed a two-dimensional Monte Carlo calculation of the electron interaction with the atmosphere including secondary

production. They have in this way calculated energy deposition profiles. These can be used to show how big and how bright the spots ought to be. Assuming a 0.5 % luminous efficiency and integrating horizontally through the luminous region we have made horizontal luminosity profiles for electrons of 12.5 Kev, 6.25 Kev, 3.12 Kev and 1.56 Kev as shown in Fig. 4. We see here that the spots are typically $\sim$ 50 m wide and $\sim$ 20 km long. The luminosities are given in kilorayleighs (1kR = 10^9 protons/cm^2_{source}-sec). We have not tried to calculate a spectrum but we expect that much of the light will be at $\lambda = 5577\text{Å}$ and at $\lambda \sim 3914\text{Å}$ and in the other typical auroral lines. If the spots are viewed at an angle and not side-on or horizontally, then the luminosity increases by $\frac{1}{\cos \varepsilon}$ where ε is the angle off horizontal.

c./ The Rocket Potential

The rocket will try to charge up with a + voltage when the electron beam is shot out. In order to prevent the rocket potential from interfering with the beam ejection, this potential must be kept small. This could be accomplished by ejecting an ion beam (or plasma beam, maybe) but this seemed like a hard development problem and also somewhat uncertain when finished. Questions about power requirements and turn-on times made this look marginal. We decided to solve this problem by a more brute force method of collecting enough current from the ionosphere to balance the beam current. In order to do this, we are going to deploy an aluminized mylar foil

80 feet in diameter. This foil has an inflatable outer rim and spokes and is being built by Scheldahl who built the Echo Balloons. (See Figure 5). Assuming that the ionosphere density is 10^5 elec/cm^2 a thermal current of $\sim$ 1 amp will be collected by the foil. This should mean that the potential on the rocket should be $V \sim \frac{kT_e}{e}$ and it should be $\sim$ .1. Dr. Gene Maier will fly a faraday cup on the rocket to see that the vehicle potential is reasonable. This will be swept through a considerable range of voltages during the beam pulse to see that the vehicle potential is reasonable. This can be done by measuring the energy of the infalling electrons.

d./ The Rocket Payload

A layout of the Aerobee 350 is shown in Fig.6. The nose cone is ejected in flight and the deployable foil and experiment section is pumped down before launch and deployed just after nose cone ejection. The rocket is despun, turned around and brought to rest parallel to a magnetic field line by the Attitude Control System before the current collecting foil is deployed. Data is telemetered back to the ground but because we are afraid of RF interference during the pulse we will also tape record the data and play it back after the experiment is over. A beam-on pulse will be telemetered and distributed to ground observers. Figure 7 shows a rough sequence of events and times in more detail.

e./ Ground Based Optical Equipment

The primary method of spot measurement is by using cameras on the ground. To do this, we will have the following equipment.

(1) Neil Davis from Alaska will have three TV systems taking movies at three stations.[4] These will be similar to those he has used before for natural auroral studies.

(2) Bob Young from SRI will have an image intensifier camera taking movies at the same site Davis is at.

(3) Al Belon from Alaska will use one TV system to spectroscopy on several auroral lines.

(4) Don Heath from Goddard will use the 31" Baker Schmidt telescope at Wallops with beam splitters and several photometers to do spectroscopy on several auroral lines.

(5) J.T. Williams and Roy Proctor from SAO at Wallops will probably run the SAO Super Schmidt cameras at Wallops to take still pictures of the spots. Using about one minute exposures and Royal-X Pan recording film they can photograph 14th magnitude stars this way so they ought to see our spots well.

(6) Grady Hicks from NRL will use a TV system he built to take movies at a fourth camera site. This should provide very good triangulation data.

(7) Gordon Sheperd from Saskatchewan will use optical gear to measure the N_2^+ rotational temperature of the spots.

f./ Electron Density Measurements

From Berger's and Seltzer's calculations, we get the ex-

pected electron density in the auroral spots directly (see Figure 14 to 17). Electron densities of $\sim 10^7$ elec/cm^2 should be measurable. Oliver Bartlett will attempt this using a radar reflection technique involving a 27 mc radar.

(iv) Problem Areas

a./ Beam Propagation

The electric fields associated with the beam itself may cause some trouble in the beam propagation. One dimensional calculations assuming no ambient plasma show that the beam can get into trouble. However, realistic 2D calculations seem to show that the problem is not serious. We will continue to worry about it for some time till the calculations are complete. The fact that the ambient density $n_e \sim 10^5$ is larger than the beam density $n_b \sim 10^4$ seems comforting.

b./ Plasma Instabilities

This may really be serious. A system of two counter-streaming fluids is unstable if the streaming velocity is larger than the beam thermal velocity. Any density or velocity perturbations in one beam couple to the second beam and then back on the first beam due to the electric field involved. The initial disturbance can grow as a result of this.

The dispersion relation

$$1 = \sum_i \frac{\omega_{pi}^2}{(\omega - v \cdot k)^2}$$

relates the angular frequency ω of a perturbation to the disturbance's wave number k and the streaming velocity v and the plasma frequency ω_{pi} of particle type i. Buneman[5] has discussed this dispersion relation and shown that for electrons flowing through stationary ions the system is unstable and perturbations on a 10 Kev electron beam grow a factor e in a distance of about 100 meters. For electrons flowing through stationary electrons the growth length is even less.

The analysis says the beam will be unstable but it does not say what will happen to it. There is no good non-linear theory of the ultimate properties of an unstable beam. The best thing to do here is to ask what experiments show about propagation of electron beams through plasmas. Apel[6] at APL has observed wave trains form in an electron beam traveling through a plasma.

From a study of the dispersion relation for this system Apel can predict the growth rate and frequencies of the observed instabilities. Based on this, he can predict what instabilities should occur for the auroral beam. But he cannot predict what the beam properties will be when its properties have been changed enough to be stable. The fact that natural aurorae occur is encouraging at this point.

In order to study this business of beam instability, we will perform two experiments. Dr. Sigi Bauer and Dr. Leo Blumle of GSFC will fly a swept frequency radio receiver on a second rocket

launched at nearly the same time as the Aerobee 350 is launched. Also, Dr. Bob Helliwell and Dr. John Katsufrakis of Stanford will operate a VLF receiving station on the ground at Wallops. Both of these experiments will try to detect waves from our electron beam. If as much as 1 % of the beam energy goes isotropically into RF at the plasma or gyro frequency, it should be easy to detect.

(v) Future Experiments

The experiments we ultimately want to carry out using this particle beam technique for field mapping involve sending the beam a long distance out into the magnetosphere. The reason for this, is that almost all interesting problems dealing with the static geomagnetic and geoelectric field are high latitude problems (> 60°). When the electron beam penetrates into regions of weak magnetic field where trapped electron lifetimes are short, the electron beam may get into trouble. Petschek and Kennel suggest that the short electron's lifetime is due to resonant scattering by whistlers. The natural Van Allen belt particles are limited in flux by an instability which produces whistlers, scatters the particles and dumps them. In this theory whistlers amplitudes observed on OGO 1 seem large enough to be in agreement with this theory. These same whistlers will scatter the beam electrons and cause them to become more isotropic and therefore become trapped. This might decrease the flux entering the atmosphere at the other end of the field line enough so that the auroral spots would not be detectable. The observation that

the Van Allen belt electron flux seems to be isotropic even inside the loss cone for $L > 4$ and especially during magnetic disturbances, seems to say that electrons can be appreciably scattered in pitch angle in a single bounce. If the low energy electron lifetime at $L \sim 6$ is roughly $\tau \sim 10^3$ sec as Kennel and Petschek believe, then an appreciable part of the accelerator electron beam should reach the other hemisphere. The bounce time for particles going some distance into the tail is $\tau_B \sim 10$ sec so:

$$\tau_B << \tau \quad .$$

This means that the electron beam technique should work even for $L \sim 6$ but it is uncertain.

a./ Ion Beams

There are two reasons why this field mapping experiment might benefit from the use of an ion beam rather than an electron beam.

(1) An ion beam should be a more sensitive indicator of large scale quasi-static electric fields. The displacement from a field line given earlier due to electric fields is:

$$x_\varepsilon = \frac{c}{v} \int \frac{\varepsilon_\perp}{B} \, d\ell \quad .$$

The fact that the velocity appears in the denominator means that a

beam of heavy ions with low velocity will give a larger displacement and therefore a more sensitive measurement of $\varepsilon_{\perp}$.

(2)An ion beam may not be plagued by as many troubles in moving from hemisphere to hemisphere as an electron beam will. Proton precipitation is not a common occurrence in the radiation belt except at the auroral zone. It seems that the protons may not be subject to some wave-particle disturbances (such as whistler interactions) that electrons experience. If this were the case, then beams of ions could propagate over paths that electrons could not and therefore the use of ion beams might enlarge the region of applicability of the experiment.

There is one reason why the ion beam technique might not work. The luminous efficiency of such beams is not known well at all. It is uncertain whether a 50 kw ion beam will produce enough light on interacting with the atmosphere to allow ground photography.

FIGURE CAPTIONS

Figure 1. Sketch of an electron accelerator sending an electron beam along a field line to the opposite hemisphere.

Figure 2. Approximate Conjugate Point Locations.

Figure 3. Vertical luminosity profiles of an electron beam interacting with the atmosphere for an isotropic beam and a vertical incidence beam of several energies (after Maeda).

Figure 4. Horizontal luminosity profiles of an electron beam interacting with the atmosphere for a vertical incident beam for several energies (from data of Berger and Seltzer).

Figure 5. Sketch of rocket-borne accelerator with electron collector foil displayed.

Figure 6. Layout of Aerobee 350 rocket showing payload.

Figure 7. Approximately flight profile of Aerobee 17.03.

Figure 8. Density profiles of the electron blob made by 1/2 coulomb of 6.25 Kev electrons striking the atmosphere vertically.

REFERENCES

1. T.N. Davis, The Aurora, in Introduction to Space Science.

2. An earlier feasibility study of artificial aurora production (Dyce, Johnson, Passel, DASA 1396, July 1963, The Feasibility of Generating an Artificial Aurora Using a Rocket-Borne Electron Accelerator) arrived at similar numbers of the total light output from artificial auroral spots. They used 10 kw beam power at 0.3 % efficiency to get $\sim 10^{20}$ photons/sec generated. Using a spot area of 3×10^8 cm^2 this gives 3×10^{11} photons/ cm^2 - sec = 300 kilorayleighs, which is close to our estimate. They studied the detectability of the spot using a 6° aperture photometer and found a signal/noise ratio about 1. On the basis of this, they concluded the experiment was very difficult to perform. But using new equipment with high resolution such as T.N. Davis' television system, the spots should be very easy to observe.

3. K. Maeda, Diffusion of Low Energy Auroral Electrons in the Atmosphere JATP 27, 259, 1965.

4. T.N. Davis, and G.T. Hicks, Television Cinemaphotography of Auroras and Preliminary Measurements of Auroral Velocities, JGR, 69, 1931, 1964.

5. Buneman, O., Instability, Turbulence and Conductivity in Current Carrying Plasma, Phys. Rev. Let., 1, 8, 1958.

6. Apel, J., and A.M. Stone, Experiments in Wave Interactions Between Plasmas and an Electron Stream in a Magnetic Field, Proceedings of 7th International Conference on Phenomenon in Ionized Gases, Belgrade, 1965.

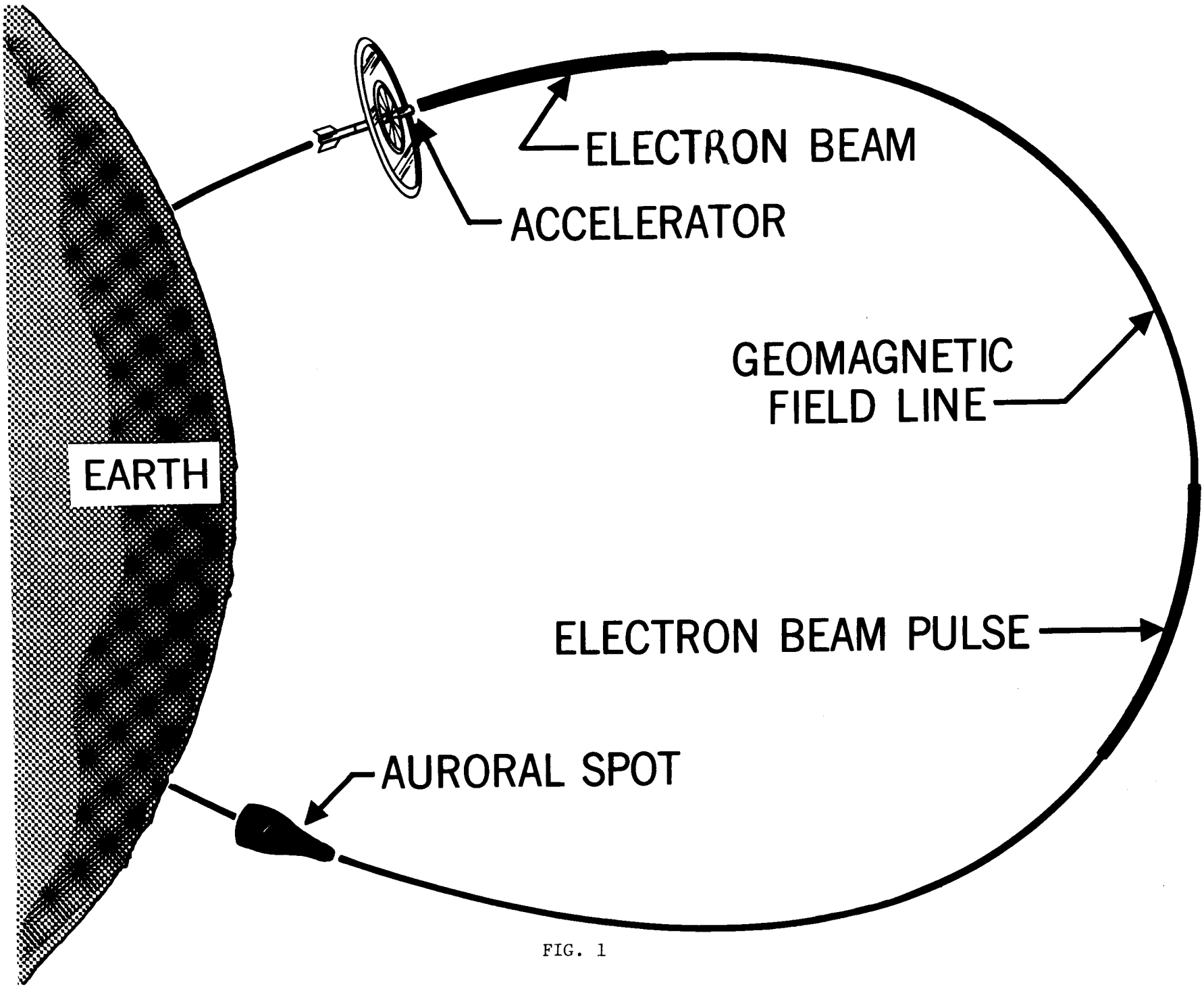
ELECTRON BEAM
ACCELERATOR
GEOMAGNETIC
FIELD LINE
EARTH
ELECTRON BEAM PULSE
AURORAL SPOT

FIG. 1

Fig. 2

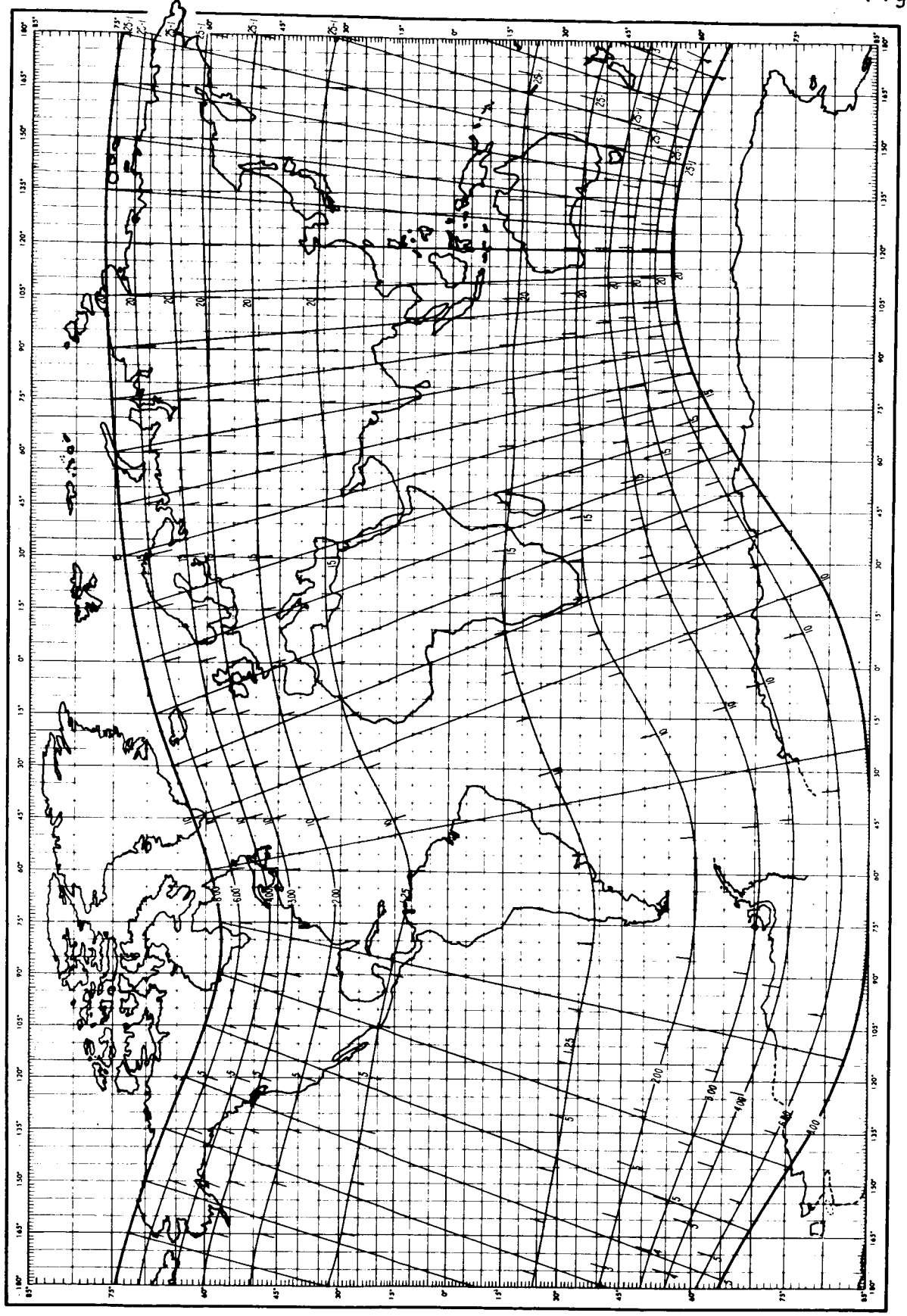

NASA
S-68-26109

Fig. 3

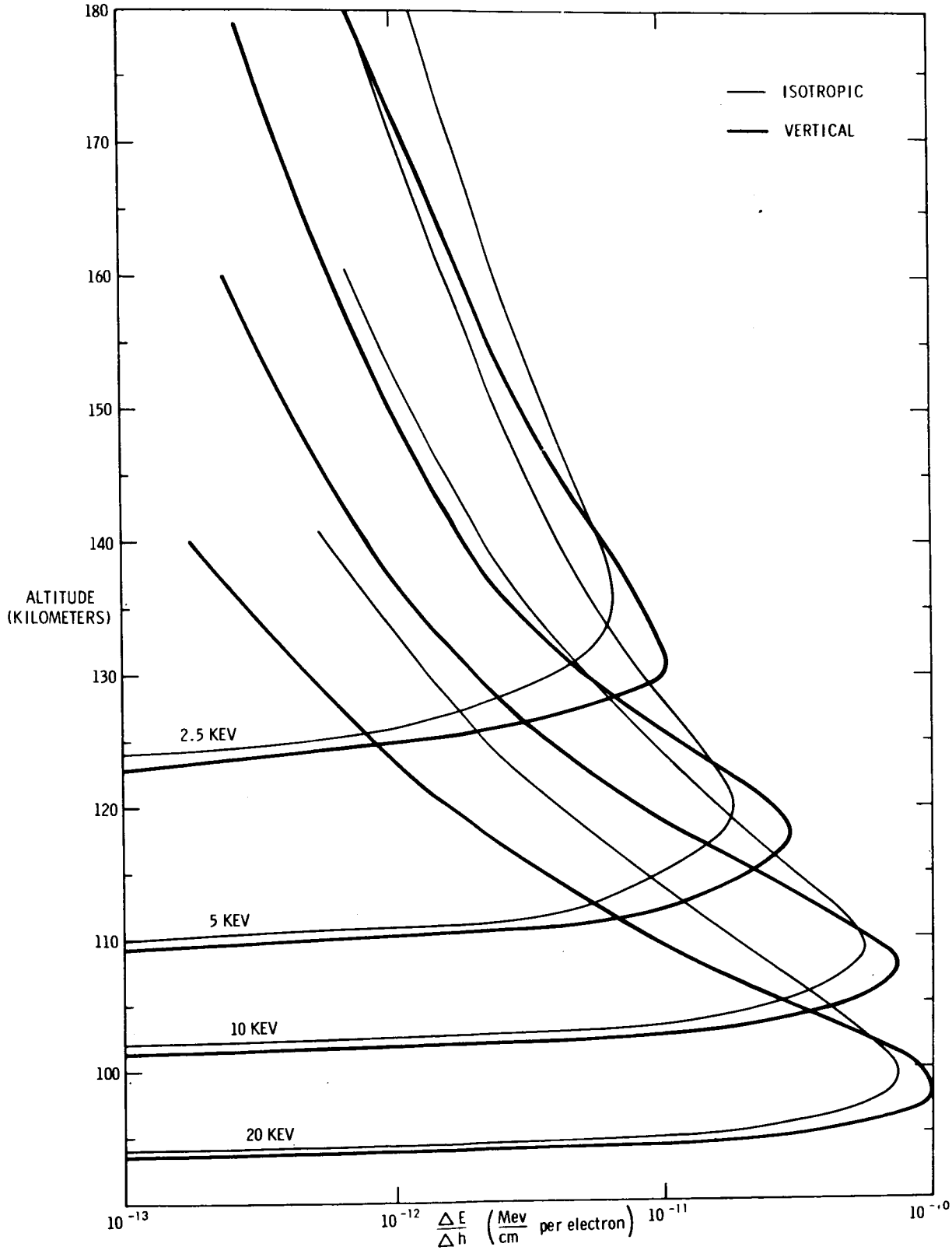

NASA
S-68-26102

Fig. 4

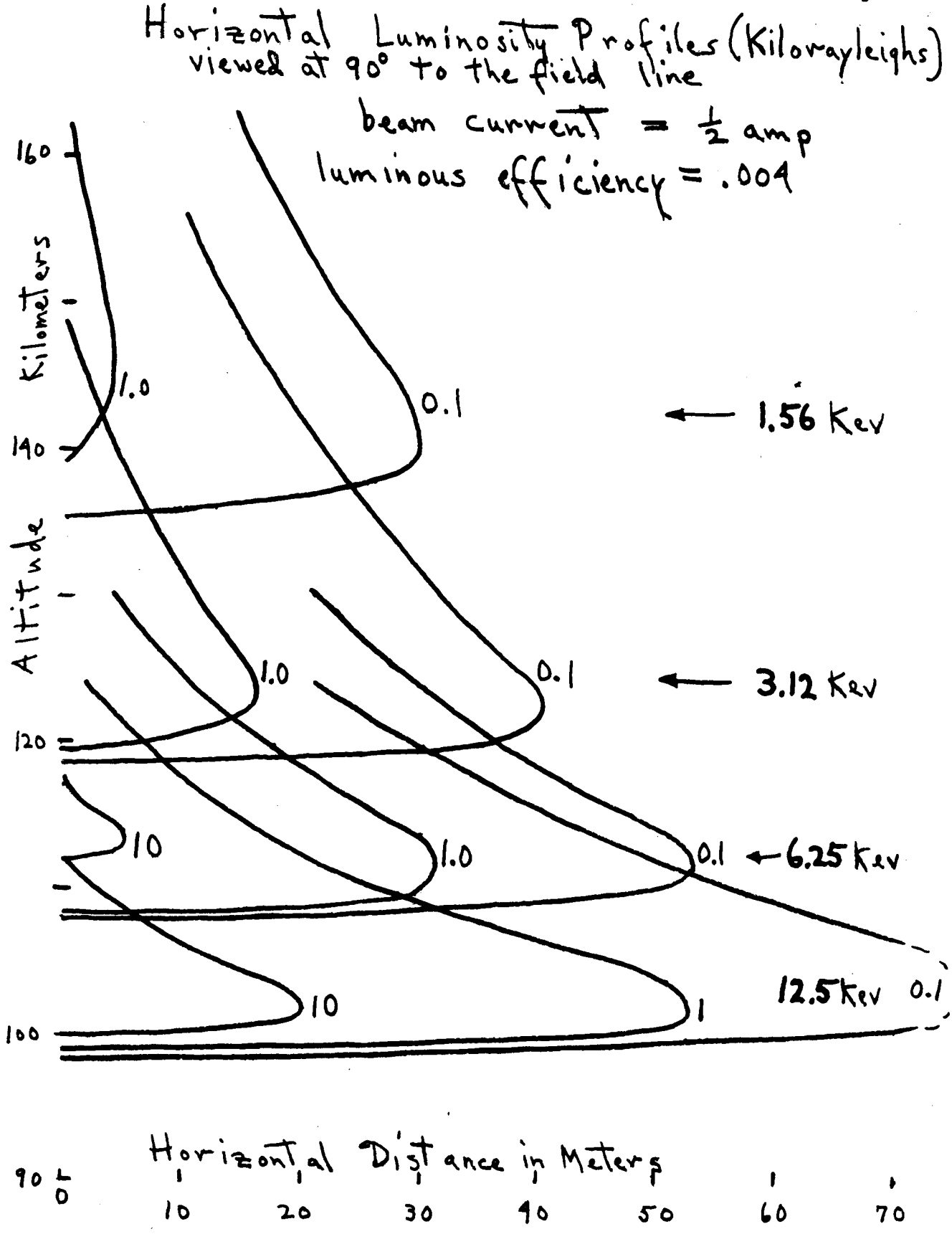

NASA
S-68-26099

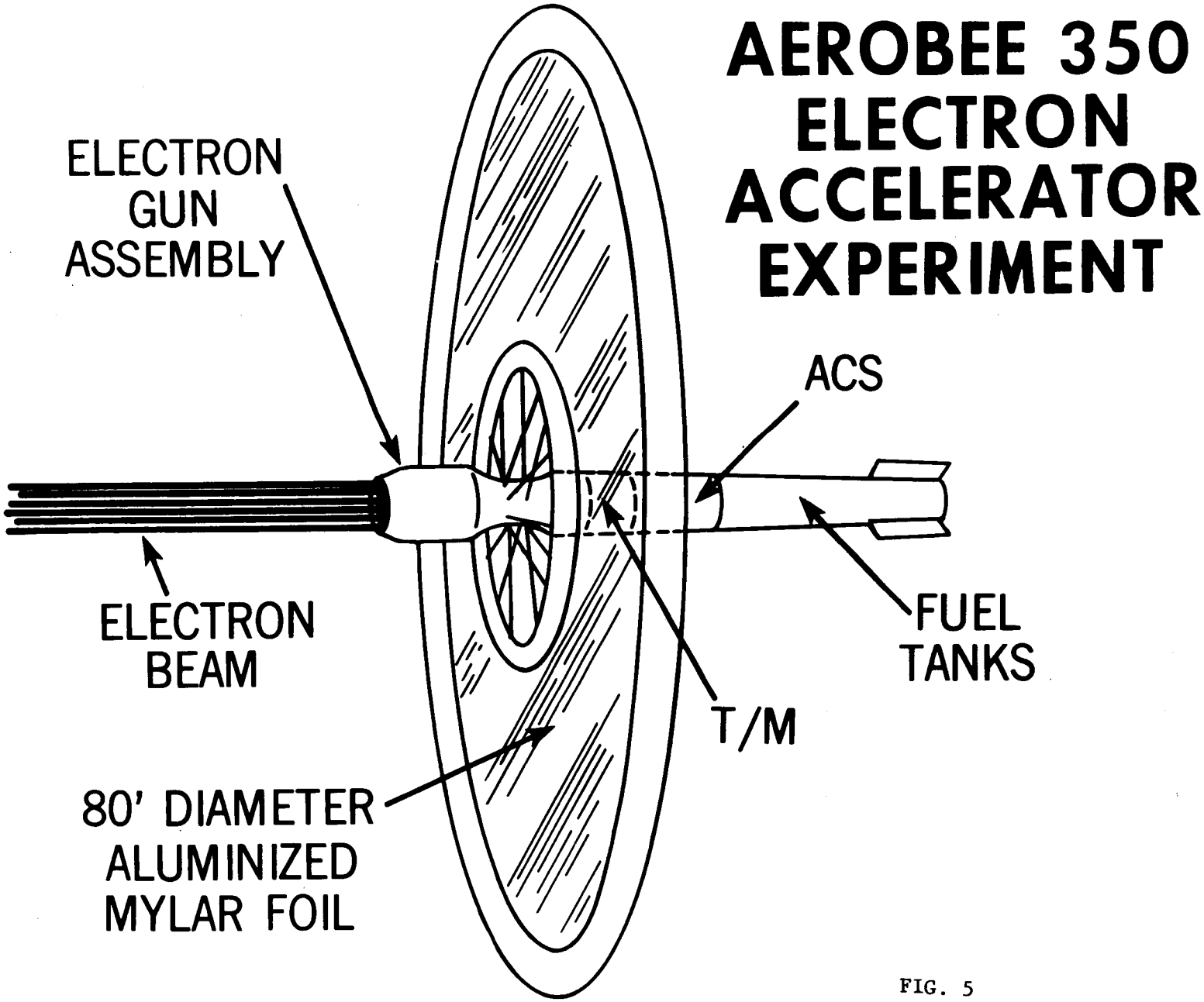

FIG. 5

Fig. 6

AEROBEE 350 SOUNDING ROCKET VEHICLE
GT-17.03

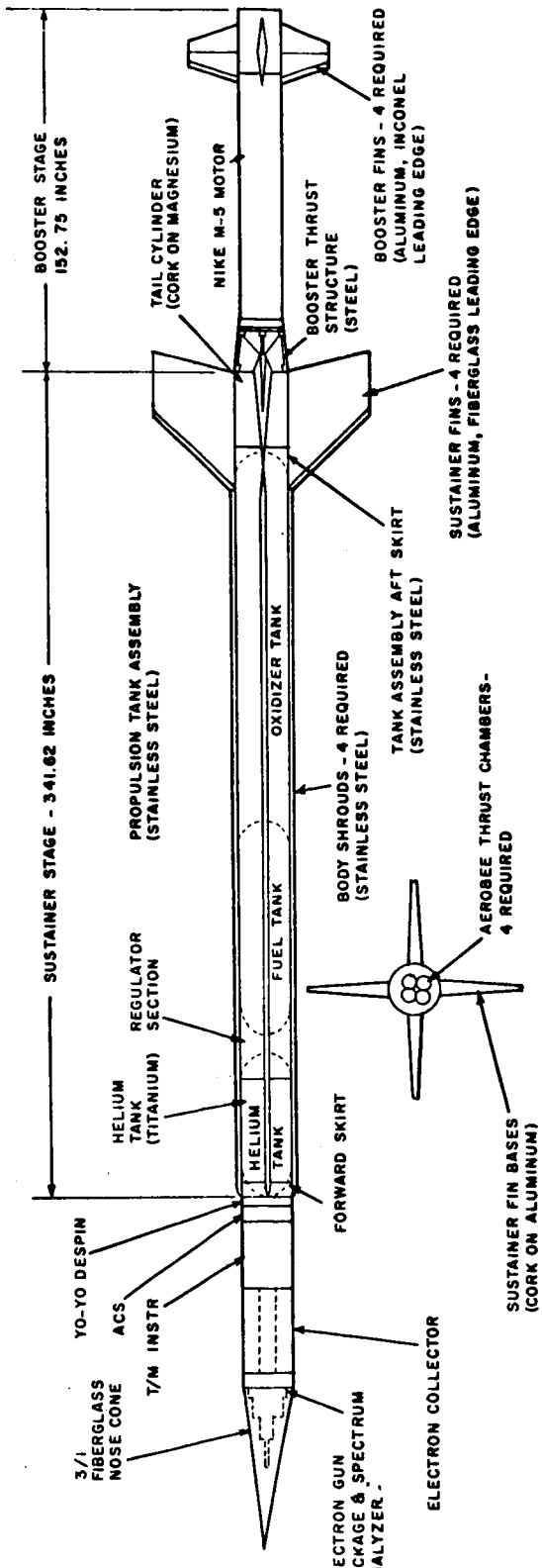

NASA
S-68-26104

FIG. 7

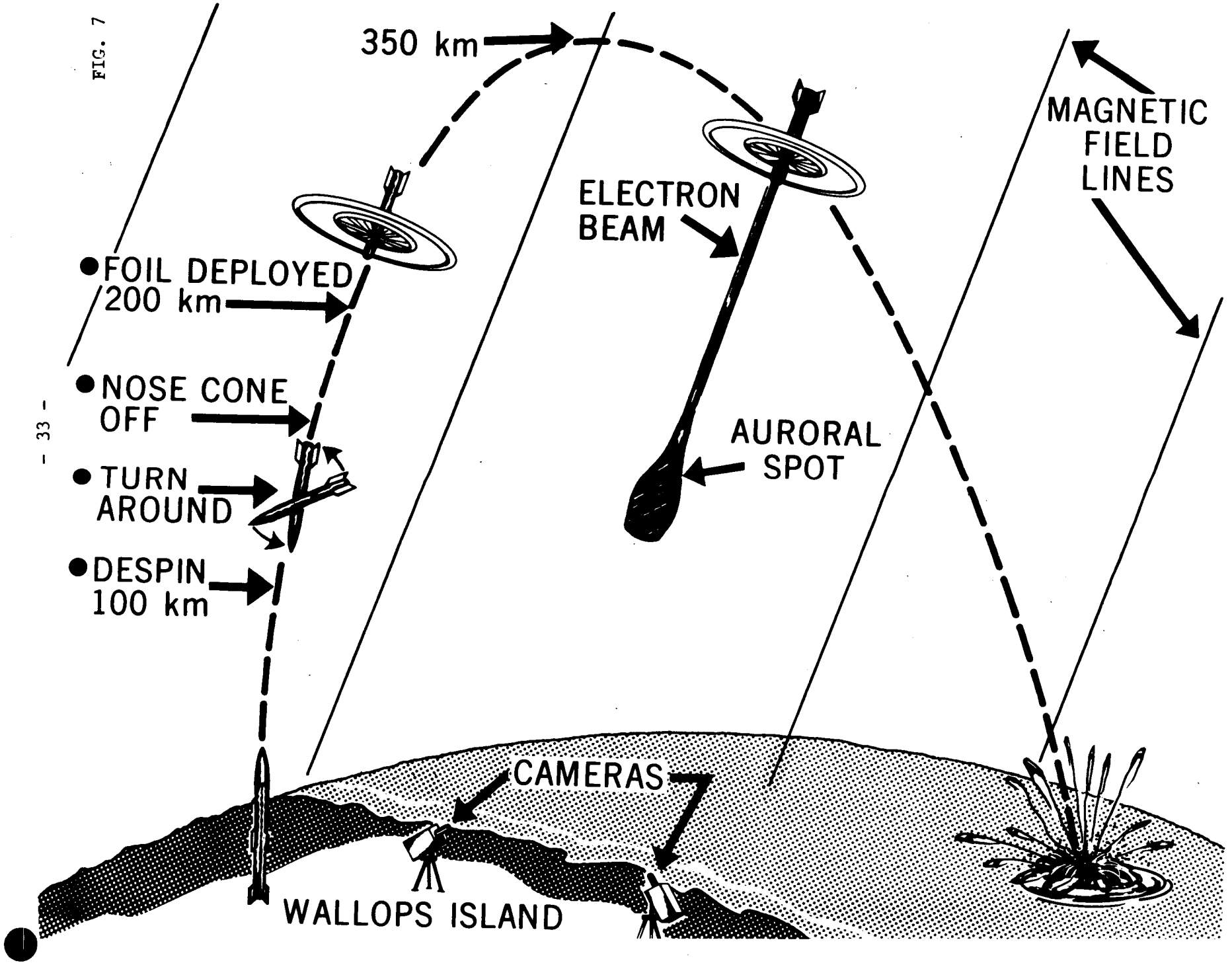
350 km
MAGNETIC FIELD LINES
ELECTRON BEAM
FOIL DEPLOYED 200 km
NOSE CONE OFF
TURN AROUND
DESPIN 100 km
AURORAL SPOT
CAMERAS
WALLOPS ISLAND

Fig. 8

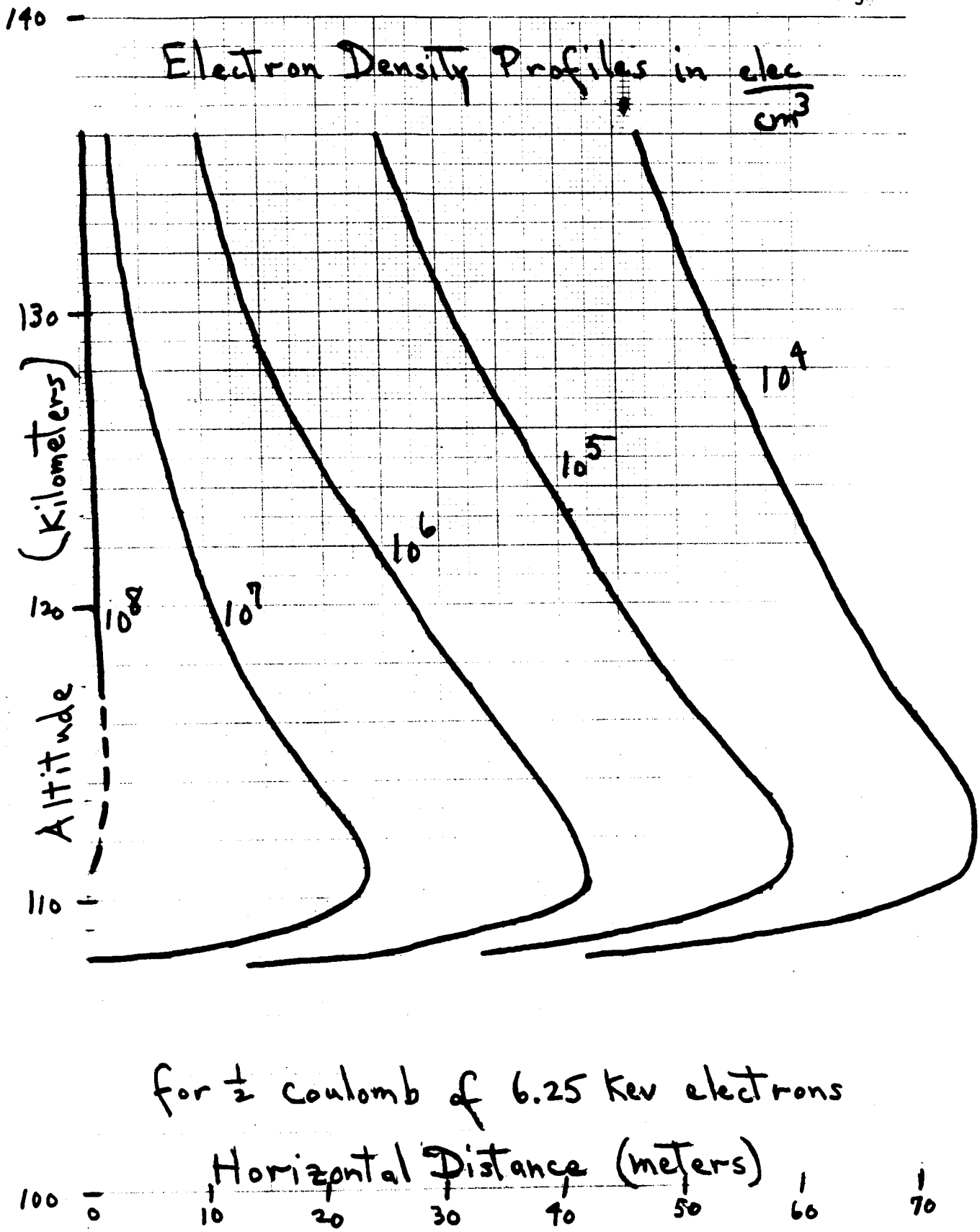

for ½ Coulomb of 6.25 Kev electrons

NASA
S-68-26103

3. ARTIFICIAL VAN ALLEN BELT

Charles F. Kennel

University of California

Los Angeles, California

ABSTRACT

It may be possible to create an artificial Van Allen belt by deep space injection of high energy electrons into the Earth's magnetic field. We calculate in very crude terms the powers and currents required to inject electrons faster than they are removed by natural processes. A 300 Kev belt at L = 3, with a radial extent of 1 Earth radius, would require a continuous injection of a few kilowatts and a few milliamps for a week. A power supply module weighing roughly one ton will provide sufficient power. A 1/10 Earth radius belt would require a 200 lb. power supply.

(i) Introduction

We magnetospheric physicists may be on the verge of a change. We have studied our chosen subject with a highly sophisticated and extensive array of passive detectors and have established the salient phenomenological features of the magnetosphere. For instance, we now know, simply from experience with our data, what typical radiation doses in space are, where the magnetospheric

boundary is likely to be on a given day, and so on. At a deeper level, we have succeeded in generating several theoretical notions which may increase our understanding of the magnetosphere; we now have some ideas about the structure of the Earth's bow shock wave and magnetospheric boundary, about the radial and pitch angle diffusion of high energy particles, and the generation of some of the radio emissions observed. (In one or two cases, there might even be an overlap of experiment and theory, though never enough to convince the detractors of a given theory and usually not enough to satisfy the proponents.) All in all we have basic knowledge of magnetospheric phenomenology, a reliable and flexible array of passive measuring instruments and a growing fund of theoretical ideas, but we don't yet know how the magnetosphere really works.

While there is presently extensive interest in making passive measurements, this area does seem to have a finite life expectancy. Presumably, the catalog of significant phenomena is not endless, however it may seem at the present time.Already there is a growing effort to test our theoretical ideas, such as they are, against observation. In several cases, this requires more precise and fine scale measurements than was previously necessary. Our necessarily limited informational capabilities force us to choose what is important to measure. As a result, theorists henceforth will probably have to be coupled more directly into ongoing experimental programs than has previously been the case. Already one sees signs of this, and a new generation of young people, the first

trained specifically in space plasma physics, is ready to begin professional life with an integrated understanding of magnetospheric physics.

Increasing our fundamental understanding through passive measurements alone could well be arduous, time-consuming and expensive. Not only will satellite instrumentation have to be sophisticated, but so also will those scientists who interpret the data. (The variability of the magnetosphere strains everyone's understanding.) Of course, what one would like to do is reproduce in space the controlled conditions of earth-bound laboratories, actively perturb the space plasma to see what happens, and do it over and over again. Clearly, this is not possible in entirety. However, we were surprised during the course of this study to find how much certain selected pieces of the magnetospheric environment may be open to our partial control. We need only choose our perturbations to dominate the competing natural magnetospheric processes for a while. In this paper, we shall discuss the possibility of making an artificial Van Allen belt by injecting more electrons than are there naturally.

We should like to draw a distinction between several types of environmental modification experiment. For instance, in the context of Van Allen Injection, one might inject small but highly controlled particle fluxes for use as tracers. These do not modify the environment in any essential way but are a valuable experimental technique. At intermediate injection fluxes, the perturbations become more important and the results confusing. Finally, when one injects

so many electrons artificially that the natural injection sources do not play a significant role at all, he has created a partially controllable artificial Van Allen belt.

The injection process will introduce many new elements of physics not present in the unperturbed environment, for example, beam-plasma interactions in the environment of the injection satellite. While such processes must be understood, we should like to emphasize the aim of creating an artificial space plasma in order to study naturally occurring geophysical processes. This requires an experiment of geophysical scale where the essentially extraneous perturbations due to the injection process may be neglected. Finally, while we might be able to control part of the Van Allen belts, we cannot control the entire magnetosphere. Thus, we only can go part way from our present status of a primarily observational subject akin to astronomy to the laboratory precision of modern physics. Nevertheless, partially controllable magnetospheric experiments are an innovation in technique which should lead to clearer physical understanding and many new ideas, and extend the meaningful capabilities of our present array of passive detectors.

(ii) Artificial Van Allen Injection

a./ Introduction

Because available power in space is limited, we must choose our perturbations carefully. If our aim is to inject electrons, it is advantageous to inject them at high energies (where the natural fluxes are small and untrapping lifetimes are long) and over a small spatial

volume. A realistic Van Allen belt fills an entire drift shell around the Earth. Thus we ought to limit the volume of an artificial Van Allen belt only by localizing injection to within certain radial limits. While the injection volume is smallest on low L-shells near the Earth, most of the geophysical activity occurs on high L-shells. Similarly, while Mev electrons have flow fluxes and long lifetimes, much of the interaction with plasma turbulence occurs at lower electron energies. Thus we must compromise our desire to study an "interesting" portion of space and the particle energy spectrum with our natural desire to get away with as little injection power as possible.

We shall outline here one such tradeoff, whereby continuous injection of 300 Kev electrons for one week or more can create an artificial Van Allen belt comparable in intensity with observed fluxes. This appears to be technically feasible, though it requires a reorientation of payload design towards higher on-board power, power storage, and voltage capabilities. Nowhere do we pretend that we have done a full scale engineering feasibility study; rather we shall present some simple arguments and estimates which suggest that a more careful examination of Van Allen injection ought to be undertaken.

b./ Scaling Law

Electrons will be injected in a "lunoid" - a figure of rotation about the Earth's magnetic dipole axis having an inner boundary given by the magnetic line of force intersecting the magnetic equatorial plane at a geocentric distance LR_E , and an outer

boundary by the line $(L + \Delta L)\ R_E$. A cross-section has the shape of a partial phase of the moon. The volume V^* of the lunoid is crudely

$$V^* = 2\pi\ L^2\ \Delta L\ R_E^3 \approx 10^{27} \left(\frac{L}{3}\right)^2 \Delta L\ \text{cm}^3$$

$$\text{where } R_E \approx 6 \times 10^8 \text{ cm} \approx 1 \text{ Earth radius} \quad . \qquad (2.1)$$

For very circular satellite orbits, $\Delta L \gtrsim 0.1$ might be attainable. (W.N. Hess, private communications).

If the observed omnidirectional flux in a given energy range is $J(E)$, the fractional number density of these particles is roughly $J/(2E/m)^{\frac{1}{2}}$ where m is the electron mass. The total number of electrons N in the lunoid is then

$$N \approx 5 \times 10^{16} \left(\frac{L}{3}\right)^2 \Delta L\ J(E) \sqrt{\frac{100\ \text{Kev}}{E}} \qquad (2.2)$$

The total energy ε of the electrons in an energy band of width E is roughly

$$\varepsilon = 5 \times 10^2 \left(\frac{L}{3}\right)^2 \Delta L\ J(E) \sqrt{\frac{E}{100\ \text{Kev}}}\ \text{Joules} \quad . \qquad (2.3)$$

Geophysical processes lead to a finite lifetime $T_L(E)$ for the particles to remain in the lunoid. They may leave the lunoid by precipitation to the atmosphere, by radial diffusion, and pro-

bably by other unknown processes. The power delivered to space in order to maintain the flux J in the lunoid is roughly

$$P \approx \frac{5 \times 10^2}{T_L(E)} \left(\frac{L}{3}\right)^2 \Delta L \; J(E) \sqrt{\frac{E}{100 \text{ Kev}}} \qquad (2.4)$$

and the gun current I

$$I \approx \frac{10^{-2}}{T_L(E)} \left(\frac{L}{3}\right)^2 \Delta L \; J \sqrt{\frac{100 \text{ Kev}}{E}} \quad \text{amps} \quad . \qquad (2.5)$$

Let us now estimate the injection power and current required to create an artificial Van Allen belt of 300 Kev electrons between $L = 3$ and $L = 4$ ($\Delta L \gtrsim 1$) . The precipitation lifetimes for these electrons is the order of one week (5×10^5 seconds), (Williams and Smith 1965). The observed fluxes are the order of a few times $10^5/cm^2$ - sec. Thus, to match the natural injection processes requires a continuous injection power the order of a kilowatt for one week. Similarly, the injection current is the order of a milliamp.

The above powers and currents are within range of present technology. Using figures kindly supplied by W. Hess and P. Coleman (private communications), we find that 2000 lbs of oriented solar cells will provide 10 kw continuous power, allowing arbitrarily for a 10 % overall power efficiency between solar photons and 300 Kev electrons. Similarly, 2000 lbs of fuel cells will supply one kw for 45 days or 5 kw for 7 days. Moreover, ionospheric injection experiments already in progress (W. Hess, private communication) will use current collectors with areas comparable to the $10^3 m^2$ needed for satellite charge

neutralization within the plasmapause. (see section 4.2). While artificial Van Allen injection is not a small experiment, neither does it strain our weightlifting capabilities.

c./ Geophysical Significance

Here we outline some presently unsolved questions which a Van Allen injection facility might illuminate. Clever interpretation of ongoing passive measurements may find some of the answers before an injection experiment could be performed; however, new problems always arise. A controlled input source is extremely helpful in studying particle diffusion and loss processes. In this regard, three hundred Kev electrons are particularly interesting theoretically because they lie at the conjunction of three different diffusion mechanisms mentioned in the literature.

(1) 3rd Invariant Violation and Radial Diffusion

Several authors (Dungey, 1965; Falthammar, 1965, 1966 a and b; Nakada et al, 1965, and others) have suggested that low frequency perturbations (either electric or magnetic) which violate the 3rd adiabatic invariant, but conserve the first and second, diffuse particles radially inwards into the magnetosphere. Recently Cornwall (1967) has observed that a very large radial diffusion coefficient is required to maintain the observed Davis-Williamson (1963) protons against precipitation losses by self-excited ion cyclotron wave turbulence. He suggested that only Bohm diffusion, probably generated by low frequency drift waves, is sufficiently strong to explain the large proton fluxes at low L-shells electrons. Therefore, injecting

electrons will clarify the radial diffusion question. It might be interesting to program the injection so that azimuthally (longitudinally) asymmetric, mono-energetic fluxes are created. If radial diffusion is driven by drift period resonances with magnetospheric scale magnetic oscillations, the injected beam will spread out radially only after several drift times around the Earth. If the injected electrons spread out in less than a drift period, we must look to shorter period oscillations, (presumably Bohm diffusion) to drive radial diffusion.

(2) 2nd Invariant Violation

Cornwall (1966) and Roberts (1967) have recently suggested that 10 cps waves may precipitate electrons with energies > 10^5 ev. This would also cause significant radial diffusion.

(3) 1st Adiabatic Invariant Violation and "Parasitic" Pitch Angle Diffusion

Kennel and Petschek (1967) and Kennel (1967) have observed that while 300 Kev electron fluxes are too small to self-excite whistler turbulence, they too would be diffused in pitch angle and therefore precipitated should the more intense lower energy electron fluxes be unstable to whistlers. This "parasitic" diffusion mechanism is weak for mev electrons, but important for 300 Kev electrons. A study of the dependence of the diffusion and loss rates upon particle energy would help greatly to sort out the various diffusion mechanisms.

(iii) Test of Limit on Stable Trapped Particle Fluxes

Several recent theories (for instance, Kennel and Petschek, 1966, Cornwall, 1966, and others) suggest that trapped Van Allen electron fluxes are limited by the onset of whistler mode instability. Typical critical fluxes for this mechanism are $3 \times 10^7/cm^2$ - sec, roughly independent of the particle energy. Clearly, an injection experiment could test the critical flux limitation mechanism. Straightforward injection of very large fluxes require somewhat more power than that required to match the natural fluxes. For instance, to create a $3 \times 10^7/cm^2$ - sec flux of 300 Kev electrons would require delivery to space of

$$P \approx 5 \times 10^4 \left(\frac{L}{3}\right)^2 \Delta L \text{ watts} \qquad (3.1)$$

assuming that NO LOSS MECHANISMS INTERVENE, other than that which creates the 5×10^5 sec natural precipitation lifetime, until the stably trapped limit is reached, whereupon whistler instability just removes all the new electrons injected thereafter.

If the stably trapped limit is reached, VLF emissions ought to be observable near the equatorial plane, and be identifiable because they would have a lower frequency than any whistler noise arising from the lower energy electrons ($\gtrsim$ 40 Kev) which observations indicate are often near their critical flux.

The whistler marginal stability flux was calculated by Kennel and Petschek (1966) assuming the electrons had smooth energy

and pitch angle distributions. By injecting a "peaky" distribution, whistler instability (and indeed other kinds!) could be achieved at lower powers. These local instabilities would then smooth out the velocity distribution near the injection satellite, setting the stage for a test of the flux limitation for the smoothed distribution away from the satellite.

It is unlikely that we could match the geophysical sources of 40 Kev electrons. Assuming that 40 Kev electrons are near their stably trapped limit, so that $J(40\ \text{Kev}) \gtrsim 3 \times 10^7/\text{cm}^2$ - sec, and taking the observed precipitation lifetimes to be 10^{+3-5} seconds (O'Brien, 1962) we arrive at an injection power

$$P \gtrsim 10^{5-7} \left(\frac{L}{3}\right)^2 \Delta L \ \text{watts} \quad . \tag{3.2}$$

However, we could inject at times when the natural 40 Kev Van Allen electrons are slightly below their stably trapped limit, and when therefore, the 40 Kev lifetimes are long. We would then push the 40 Kev electrons to the edge of stability, sensitizing the electron distribution to small geophysical perturbations. The required power delivery would be a few tens of kilowatts if the lifetime of the stable 40 Kev distribution were one week. By creating or maintaining the trapped electron distribution near marginal stability, VLF activity should be greatly enhanced.

(iv) Discussion

Here we take up several points in no particular order of importance.

a./ Second Passive Satellite

Correlations with observations on other satellites well separated from the injection satellite would be extremely helpful. For instance, complications arising from injection could locally obscure the basic magnetospheric processes under investigation. These presumably would smooth out before reaching the second satellite. Furthermore, a second satellite on the same drift L-shell would give time resolution to better than a drift period. Since many processes may be faster than a drift period, a second satellite might be needed. Finally, the violent onboard processes accompanying injection may be incompatible with the requirements of sensitive passive measurements, in which case a second observing platform would be absolutely necessary.

b./ Problem of Satellite Charging

The simplest brute force method of neutralizing the charge on the satellite is simply to draw thermal electrons from the environment to replace those high energy electrons ejected in the beam. Within the plasma pause, we may expect an electron density of $10^2/cm^3$ and, perhaps a temperature of 1 ev, in which case the thermal current would be 10^{-10} amps/cm^2, so that a collecting area of 10^7 cm^2 $\approx$ (30 meters)^2 would neutralize a 1 ma injection current. Outside the plasmapause, electron densities and temperatures of $\sim 1/cm^3$ and $\sim 10^3$ ev might

be encountered, leading to a thermal current somewhat less than 10^{-10} amps/cm^2 and a slightly larger collecting area. For high power and current experiments, larger areas might also be required. We have not considered whether other more sophisticated satellite neutralization schemes might be feasible.

c./ Advantages of Deep Space Injection

A large range of pitch angles can be created. Ionospheric injection creates particles only within a small range of equatorial plane pitch angles, and thus would not create a Van Allen belt similar to the naturally generated one. There are indications that instabilities in or near the ionosphere may be responsible for many rapid fluctuations in electron precipitation rate. Presumably ionospheric beam injection would be a valuable tool for studying these processes. However, only deep space injection will enable us to study the geophysical processes affecting most of the trapped electrons.

d./ Significance of L=3-4 Injection

The injection power, and therefore payload weight, increase with increasing L. On the other hand, the interesting diffusion physics seems to occur at high L-shells. At low L-shells, however, the plasmapause appears to be the boundary of much geophysical activity. Presumably the plasmapause will swing back and forth under the artificial Van Allen belt with magnetic activity. Correlations of the various diffusion rates with plasmapause location would be extremely illuminating. However, it may be necessary to inject within the plasmapause for reasons of satellite charge neutralization (see 4.2).

It is important that injection occur at a sufficiently large L-shell that natural geophysical processes will remove the artificial Van Allen belt at the conclusion of the experiment. This criterion rules out injection for $L < 2$, where electrons injected by nuclear explosions had lifetimes the order of years. Similarly, electrons with energies above 1 mev also have long lifetimes, and an artificially created belt might not decay suitably quickly at high energies.

e./ Injection at High L-shells

In this L-shell range, we would sample auroral and sub-storm activity. In addition at quite times, injection of electrons would test which L-shells are closed. Furthermore, by injecting two pulses of different pitch angles, one nearly along the line of force, and one nearly across, one could test the splitting of drift shells due to magnetospheric distortion and the thereby ensuing pitch angle dependence of the drift orbits around the Earth.

(v) Summary

It may be possible to create an artificial Van Allen belt. Considerations of power suggest that electrons with energies greater than 100 Kev ought to be injected since these have small fluxes and moderately long lifetimes. If necessary, one can save power by injecting in a thin lunoid, with $\Delta L \gtrsim 0.1\ R_E$. In order to neutralize the satellite charge with a thermal electron collector of modest area, it may be necessary to inject within the plasmapause. Beam powers and currents of roughly 1 kilowatt and milliamp respectively

may be sufficient. One ton or less of power could investigate various diffusion processes, trace out L-shells, and so on. However, it might barely test the theoretical limit on stably trapped electron fluxes, and therefore enhance VLF emissions throughout the radiation zone. Further development of power supplies and charge neutralization capability would open up a range of high energy experiments, including definitely testing the limit on stably trapped fluxes.

A sine qua non for many active geophysical experiments is the development of high onboard power and power storage capabilities. Once the requisite power is on board, a wide range of experiments will be accessible. Best use of the resources can probably be achieved by putting many high power experiments on the same platform. For instance, the same power may be able to inject meaningful fluxes of both electrons and waves. Clearly, such a coordinated wave-particle experiment would be of far greater value than the two individual experiments alone.

It is customary to conclude proposals for scientific research with an inspirational hortatory passage extolling in extravagant terms the technological fallout destined to follow (as B follows A) a given fundamental investigation. We feel constrained by form to do so. Looking deep into the future, suppose it turns out that a small investment of injected electrons knocks the whole Van Allen belt over the edge of instability to create a large ionospheric blackout, this would have obvious implications for communications in general and defense in particular. Conversely, if we really

learn how the Van Allen belt works, we might understand how to prevent radio blackouts, with a concurrent improvement in radio communication. For the present, it seems reasonable to state that the possible creation of an artificial Van Allen belt is worth studying with more care than in this very preliminary discussion. Not only should its feasibility be investigated, but members of the space physics community ought to be encouraged to extend the list of meaningful possible experiments.

ACKNOWLEDGMENTS

The author is indebted to J.M. Cornwall, F.C. Coroniti, L.M. Linson and H.E. Petschek for their many useful comments.

REFERENCES

Cornwall, J.M. "Micropulsations and the Outer Radiation Zone" J. Geophys.Res. 71, 2185-2199, 1966.

Cornwall, J.M. "Diffusion Processes Influenced by Conjugate Point Wave Phenomena", Paper presented to "Conjugate Point Symposium", Boulder, Colorado, June 1967, to be published in Radio Science.

Davis, L.R. and J.M. Williamson, "Low Energy Trapped Protons", Space Res. 3, 365-375, 1963.

Dungey, J.W. "Effects of Electromagnetic Perturbations on Particles Trapped in the Radiation Belts", Space

Science Reviews, 4, 199, 1965.

Falthammar, C-G. "Effects of Electric Fields on Trapped Radiation", J. Geophys. Res., 70, 2503-2516, 1965.

Falthammar, C-G. "On the Transport of Trapped Particles in the Outer Magnetosphere", J.Geophys. Res.71, 1487-1491, 1966a.

Falthammar, C-G. "Coefficients of Diffusion in the Outer Radiation Belt", Radiation Trapped in the Earth's Magnetic Field,ed. B.McCormac, D.Reidel Co.,Helland, 1966b.

Kennel, C.F. and H.E. Petschek, "A Limit on Stably Trapped Particle Fluxes", J. Geophys.Res., 71, 1-28, 1966.

Kennel, C.F. and H.E. Petschek, "Van Allen Belt Plasma Physics", AVCO report RR 259, to be published in Proceedings Second NATO Summer Institute of Plasma Physics, 1967.

Kennel, C.F. Remarks delivered to Boston College - Air Force Cambridge "Institute of Magnetospheric Physics", June, 1967.

Nakada, M.P. and J.W. Dungey and W.N. Hess, "On the Origin of Outer Belt Protons", J. Geophys.Res., 10, 3529-3532, 1965.

O'Brien, B.J. "Lifetimes of Outer Zone Electrons and Their Precipitation into the Atmosphere",J.Geophys.Res., 67, 3687-3706, 1962.

Roberts, C.S. Remarks delivered to Boston College-Air Force Cambridge, Institute of Magnetospheric Physics, June, 1967.

Williams, D.J. and A.M. Smith "Daytime Trapped Electron Intensities at High Latitudes at 1000 km", J.Geophys. Res., 70, 541-556, 1965.

APPENDIX

Dr.Hess has recently made more detailed calculations of some aspects of the problem discussed in this paper and these are presented below:

4.0 ARTIFICIAL VAN ALLEN BELT

4.1 Introduction

In the previous section we discussed the possibility of driving the Van Allen belts all the way to instability. Here we consider a more gentle steady state experiment. By going to higher particle energies, the particle fluxes become lower and their natural life times much longer (since they are not on the edge of the instability) so that it becomes considerably easier to generate fluxes of electrons comparable with the observed naturally generated fluxes.

4.2 Geophysical Significance

The dynamics of high energy Van Allen electrons is one of the less well understood aspects of Van Allen belt physics. At least three mechanisms have been suggested which could alter the high energy electron distribution.

4.2.1 3rd Adiabatic Invariant Violation

Quasistatic magnetic field fluctuation can alter the electrons' 3rd invariant causing L-shell diffusion. Since this also energizes particles, it would be important to watch changes in the L-shell and energy profile of the injected electrons.

4.2.2 2nd Adiabatic Invariant Violation

Roberts has suggested that bounce period fluctuations may be responsible for the finite lifetimes of high energy Van Allen electrons. This will lead to diffusion primarily in the parallel

velocity component. Correlations with the 10 cps whistler spectrum and the injected electron distribution should be an important part of such an injection experiment.

4.2.3 Second Harmonic, First Invariant Violation

It has been suggested that high energy electrons are precipitated due to second cyclotron harmonic interactions with whistlers generated by lower energy ($\gtrsim$ 40 kev) electrons which are often, if not always unstable. This will lead to pitch angle diffusion.

4.3 Experiment Requirements

The observing time available to study the injected particles is limited by their lifetimes. The natural lifetimes of trapped particles measured at high latitudes by satellite 1963-38c is roughly one week $\sim 10^6$ sec at L = 3 and maybe one day $\sim 10^5$ sec at L=6 .

To consider how many particles we must inject in order to do a reasonable experiment let us consider what volume we must fill with particles. The volume from the surface of the earth to an L shell is:

$$V = 4\pi \int_0^{\pi/2} \sin\theta d\theta \int_{r_e}^{Lr_e \sin^2\theta} r^2 dr = V_e \left[-\cos\theta + \frac{\cos\theta}{\sin^6\theta}\left(1-\cos^2\theta + \frac{3}{5}\cos^4\theta - \frac{1}{7}\cos^6\theta\right)\right]$$

From this equation we can determine the volume between neighboring L shells separated by 1,000 km at the equator. These are given in Table I below.

L	V	R(1 Mev)	R(10 Mev)
3	2.2×10^{27} cm^3	4.1 km	29 km
4	3.7×10^{27}	10.0	70
5	5.7×10^{27}	20.0	140
6	8.9×10^{27}	33.0	235

Also shown in Table 1 above are the gyroradii of 1 Mev and 10 Mev electrons. It is obvious the region of space we are filling is much larger than the gyroradius of the particles involved and will probably be dominated by the motion of the satellite from which the particle injection is originated.

Let us assume that we want a signal to noise with the filled lunoid (the figure of revolution which is cross section is two field lines) of 10 to 1. That is, the injected flux should be ten times the average natural flux for the L shell under consideration at the equator. Average fluxes may of course,be a bad choice due to the substantial fluctuations in the outer Van Allen belt but we must choose some index of flux. Vette has collected data on outer belt omnidirectional electron fluxes n and Table II shows his values for n for several L values in energies. Figure 1 shows Vette's AE2 outer belt electron flux map which has been used to generate Table II.

TABLE 2

Average Natural Omnidirectional Fluxes

L	250 Kev	1 Mev	5 Mev	10 Mev
3	1.1×10^5	1.6×10^4	4	$\sim 10^{-3}$
4	2×10^6	4×10^5	4.5×10^3	~ 0.3
5	4.5×10^5	5×10^5	10	$\sim 10^{-4}$
6	2.2×10^6	1.1×10^5	10^{-2}	$\sim 10^{-9}$

Using Table I and II with a signal to noise of 10 to 1 we can calculate the required total number of injected particles N given by

$$N = \frac{10n}{c} V$$

This is shown in the Table III below.

L	250 Kev	1 Mev	5 Mev	10 Mev
3	8×10^{22}	1.2×10^{22}	$*7 \times 10^{18}$	$*7 \times 10^{18}$
4	2.4×10^{24}	4.8×10^{23}	5.5×10^{21}	$*1.2 \times 10^{19}$
5	9×10^{24}	1×10^{24}	1.9×10^{19}	$*1.9 \times 10^{19}$
6	6.6×10^{24}	3.3×10^{23}	$*3.0 \times 10^{19}$	$*3.0 \times 10^{19}$

* - These values are based on $n = 10$. The values from Table 2 are less than this. This value was chosen to keep a reasonable counting rate for a reasonable detector.

THE LOG B-L FLUX MAP OF THE AE2 ENVIRONMENT.

The Contours are the Omnidirectional Flux Above 0.5 MeV .

The dotted contour for 1 electron /cm^2-sec

represents the limit of the map at low

altitudes.

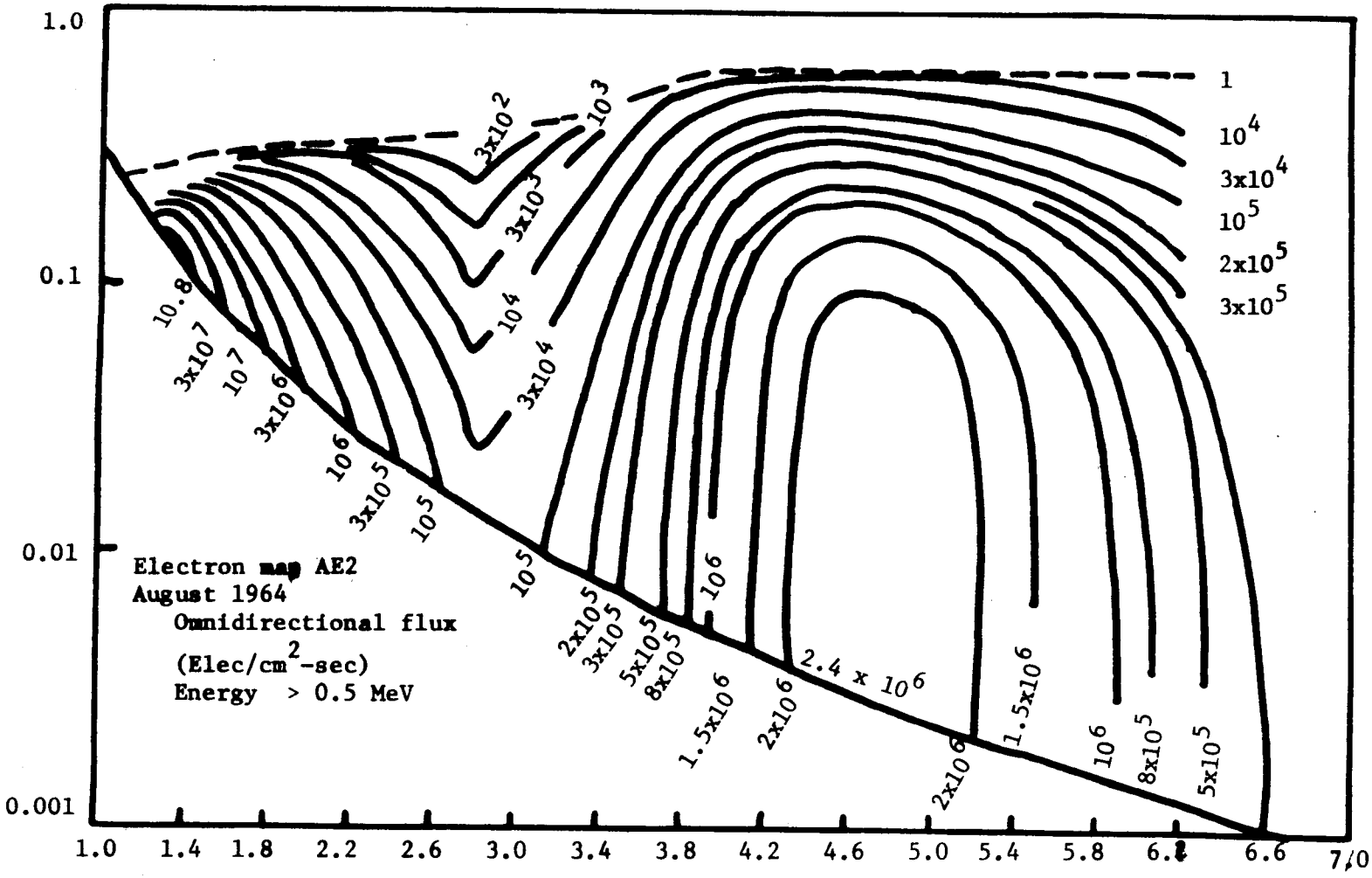

FIGURE 1

Table III determines the type of accelerator required to carry out a particular experiment. It is probably appropriate to do experiments at several L values and at several energies because the physical processes important probably will vary with both of these parameters.

Also, one could do either (a) continuous particle acceleration which would require a source strength of $\frac{N}{\tau}$ particles /sec where τ is the average lifetime measured by 1968-38c (b) pulsed injection where the total number of particles is produced is a time $t << \tau$. The pulsed source experiment is probably easier to interpret because one can study the time evolution of the pulse but it requires a larger power accelerator.

4.4 Illustrative experiments

Let us now consider a few possible artificial injection experiments:

(a) Continuous injection of 350 Kev electrons at L = 3.

The total number of particles required from Table III is $N = 8 \times 10^{22}$. The total energy required to fill the Lunoid is $W = 3 \times 10^{9}$ joules. Using a particle lifetime = $\tau = 5 \times 10^{5}$ sec the power required to maintain the artificial belt against natural geophysical losses is $P = \frac{W}{\tau} = 6$ kilowatts. This power is within the capability of current large spacecraft. The required accelerator current here is I = 25. milliamps. It may be difficult to limit the width of the Lunoid filled with particle to 1000 km in this case because the continuos injection of the beam from a circular orbit satellite will probably spread the particles more than that.

(b) Pulsed injection of 10 Mev electrons at L= 6.

The Marquardt Corporation[1] has written a report entitled "A Design Concept for Electron Injection in Space" which studies this particular problem. They conclude that the injection of $N = 3 \times 10^{19}$ electrons could be accomplished in one and one-half hours using a travelling wave linac. The payload weight including accelerator and power source is 850 lbs $\pm$ 10 percent. The linear accelerator has been fairly well designed in this Marquardt report. They have worked on this problem for several years for the Air Force. They suggest the use of two-cycle reciprocating engine utilizing hydrogen and oxygen for the power source. They suggest that the accelerator be C-band because equipment at this frequency readily available. The RF source for the accelerator was chosen to be a three megawatt magnetron having three kilowatt average power level. It might also be possible to produce a tube comparable to this having average power levels of 12 kilowatts or more. The amount of work that has been done on this accelerator shows that such a system is clearly feasible and that it could be done with a reasonable development program.

(c) Pulsed injection for several different conditions.

The Marquardt Corporation has also done a parametric design study based on the design on the instrument discussed in case (b) above and using various scaling laws to arrive at the capability

---

(1) The Marquardt Corporation, Report MR 20, 381, "A Design for Electron Injection in Space", November 1, 1966.

of a linac having characteristics different from that given in (b). Table IV below lists the various alternate designs they have produced. Design No. 1 is the one discussed in case (b) above.

TABLE IV

Alternate Designs for Electron Injection Experiment

	Current Amperes	Energy Mev	Average Beam Power, Kw	Operating Time Hours	Number of Electrons Injected	Total System Weight, Pounds
1.	10^{-3}	10	10	1.5	3×10^{19}	900
2.	10^{-2}	10	100	0.15	3×10^{19}	3870
3.	10^{-2}	10	100	1.5	3×10^{20}	5705
4.	3×10^{-3}	10	30	1.5	9×10^{19}	1900
5.	10^{-3}	10	10	0.5	10^{19}	760
6.	5×10^{-4}	10	5	1.0	10^{19}	690
7.	2×10^{-3}	5	10	1.5	6×10^{19}	850
8.	2×10^{-3}	5	10	0.5	2×10^{19}	710
9.	5×10^{-4}	5	2.5	0.5	0.5×10^{19}	460
10.	3×10^{-3}	10	30	0.5	3×10^{19}	1479

4. PLASMA EFFECTS OF ELECTRON BEAMS INJECTED INTO SPACE

Derek A. Tidman

University of Maryland
College Park, Maryland

(i) Introduction

In this report we discuss some of the phenomena that might occur when a beam of energetic electrons is injected into space. Instabilities are expected to play an important role giving rise to radial and longitudinal diffusion of the beam electrons. The emission of unstable waves from the beam into the surrounding plasma will also constitute an important energy loss by the beam. In view of the complex nature of these phenomena we have only attempted to make speculative and crude estimates of their magnitude for various situations. A partial list of papers that deal with aspects of electron beam problems is given at the end of this report.[1-8] It is clear that many theoretical investigations could usefully be undertaken to clarify the propagation characteristics of energetic particle beams in space.

It is useful to distinguish between three regions of the beam (see Fig.1.). Region 1 is close to the electron gun where we assume that a quasi-steady state has been reached after the beam has been on for a relatively long time. In this region

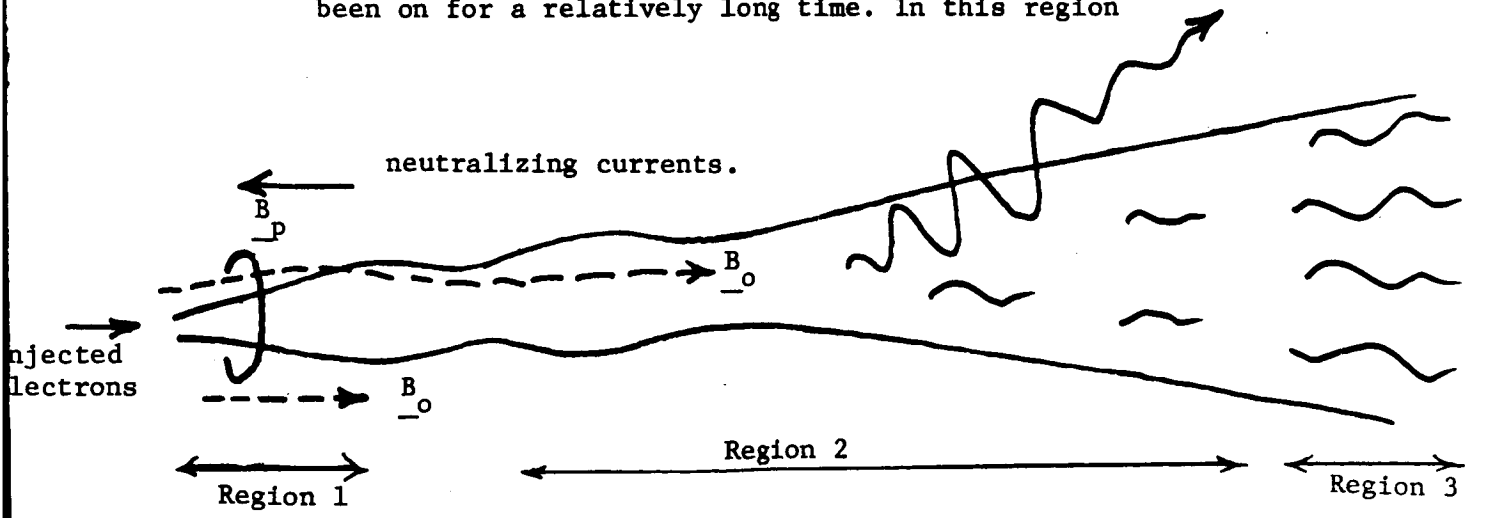

Figure 1.

the beam expands from its injected radius R_σ to a new radius R under the force of electrostatic repulsion and (more importantly) the pressure of its rapidly increasing perpendicular temperature (the particles may also be injected as a cone of flux). Geomagnetic flux may be pushed aside temporarily in the course of this rapid expansion but will soon diffuse back into the beam through wave-particle scattering a little farther along the beam. Currents also flow to the satellite, principally along $\underline{B}_o$, to balance the beam current.

Region 2 is the region in which the beam has become established some distance from the gun. It is expected to be a "noisy" region due to various plasma modes which have been excited to a non-thermal level by instabilities - or because the system is verging on instability. This turbulence causes further slower radial diffusion of the beam. It also leads to the emission of waves from the beam into the surrounding plasma. This emission contributes to the energy loss of the beam. Such waves couple the beam energy into the surrounding medium causing an effective "viscous" drag. The velocity distribution of beam electrons is expected to emerge from region 1 into 2 as a smeared-out distribution, contrasting with the injected monoenergetic beam.

Another consequence of turbulence in the beam is that stochastic acceleration[3] of a few beam electrons to very high energies may occur. There is some laboratory evidence that this phenomenon occurs when beams interact with plasmas. If it does occur, then a precursor of very energetic electrons may be detectable ahead of the beam.

Region 3 is the leading edge of the beam which is continually progressing into new regions of undisturbed ionospheric plasma. In this region the effects of velocity dispersion in the beam are particularly important. Fast electrons tend to outrun the slow ones at the front edge thus regenerating a "double-humped" velocity distribution of electrons in this region. The resulting increased instability in the front may oppose the spatial separation of the fast electrons from the slow ones (through wave-particle scattering) and perhaps lead to a sharp front -- analogous to an electrostatic shock. Beam electrons catching up to the front may also therefore tend to accumulate near the front of the beam due to their inability to outrun it. Only a very few highly energized electrons may outrun the beam if the stochastic acceleration mentioned previously occurs. However this picture is speculation and proper calculations need to be done to explore these phenomena.

These three regions will now be discussed separately. Instabilities of the gross MHD type that might tend to amplify kinks in the beam, etc., will not be discussed, and we shall principally be concerned with microinstabilities. The MHD instabilities however will undoubtedly also be present.

(ii) Region 1: Initial Expansion of Injected Beam

Consider a beam of electron density n_{BO}, radius R_o, and velocity U injected along the magnetic field $\underline{B}_o$. We assume that the beam has been on for some time and that due to its high energy density at injection it has swept out the ionospheric plasma inside the

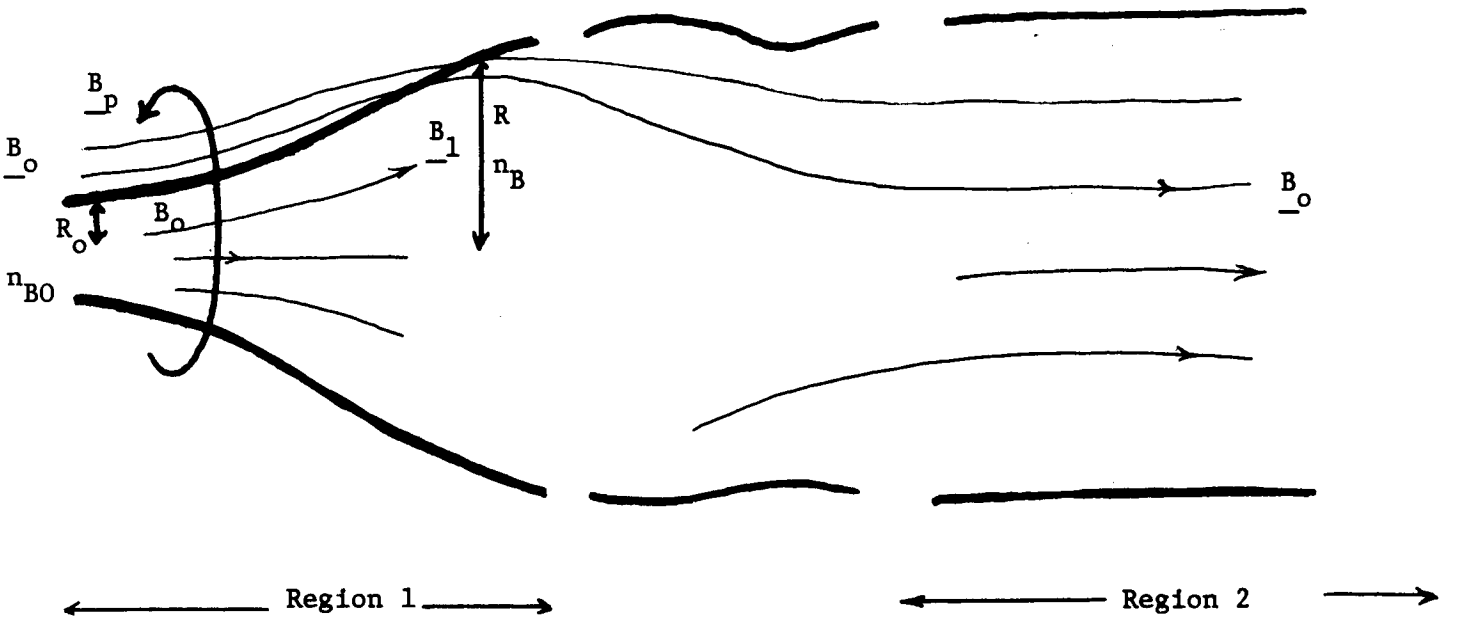

Figure 2.

cylinder of radius R_o . The ambient magnetic field however passes through the satellite and exists in this region with intensity $\underline{B}_o$ (Fig.2.).

The beam rapidly expands with increasing x , thus diluting the electron density to n_B , and causing some ordered radial motion $U_\perp$ and thermal motion $V_\perp$ of the beam electrons. Viewed end - on the beam electrons drift in an azimuthal direction inside the beam as shown with a drift velocity

$$v_D = \frac{cE}{B} \quad . \tag{1}$$

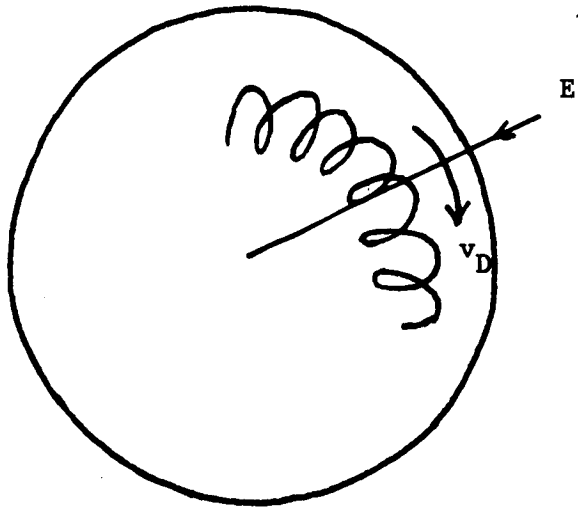

Figure 3.

The magnetic field inside the beam at expanded radius R is

$$B_1 \sim B_o \left(\frac{R_o}{R}\right)^2 , \qquad (2)$$

and the electric field at the outer edge of the cylinder is

$$E \sim e n_B R , \qquad (3)$$

and potential differences between axis and edge,

$$\Delta\phi \sim \frac{e n_B R^2}{4} . \qquad (4)$$

The above estimates assume that B_1 and n_B are constant across the radius of the cylindrical beam, and

$$n_B \sim \left(\frac{R_o}{R}\right)^2 \quad n_{BO} \quad . \tag{5}$$

As the beam expands the electron acquire an ordered radial velocity $U_\perp$. The contribution of the electrostatic field to this expansion energy is

$$\int_{R_o}^{R} dR\, eE = e^2 n_{BO} R_o^2 \ln\left(\frac{R}{R_o}\right) = \frac{1}{2} m U_{\perp E}^2$$

$$\text{i.e.,} \qquad U_{\perp E}^2 \sim \frac{2e^2 n_{BO} R_o^2}{m} \ln\left(\frac{R}{R_o}\right) \quad . \tag{6}$$

It is expected that the beam will overshoot its' final equilibrium radius after expansion and undergo a few damped radial oscillations.

Another feature of the injected current is that a "pinch" magnetic field B_p will be produced, where

$$B_p \cong \frac{2J_{Total}}{cr} \tag{7}$$

outside the beam $(r > R)$, and

$$B_p \sim \frac{2\pi R n_B U_e}{c} = \frac{2\pi R_o^2 n_{BO} U_e}{cR} \tag{8}$$

at the surface of the beam.

Now we shall obtain an estimate for the final "quasi-equilibrium radius" R for the beam after its' expansion by making use of a radial pressure balance for this condition. This is

$$\frac{B_1^2}{8\pi} + n_e m V_\perp^2 \sim \frac{1}{8\pi}\left(B_o^2 + B_p^2\right) + n_o K T_o \quad , \tag{9}$$

where n_o , T_o are the density and temperature of the ionospheric plasma and $V_\perp$ is the perpendicular thermal velocity of the beam, i.e.,

$$B_o^2\left(\frac{R_o}{R}\right)^4 + 8\pi m V_\perp^2 n_{BO}\left(\frac{R_o}{R}\right)^2$$

$$\sim B_o^2 + 8\pi n_o K T_o + \left(\frac{4\pi^2 R_o^2 n_{BO}^2 U^2 e^2}{c^2}\right)\frac{R_o^2}{R^2} \quad .$$

Neglecting R_o^4/R^4 we find

$$\left(\frac{R}{R_o}\right)^2 \sim \left[\frac{8\pi m n_{BO} V_\perp^2 - \frac{4}{c^2}\pi^2 R_o^2 n_{BO}^2 U^2 e^2}{B_o^2 + 8\pi n_o K T_o}\right] \quad . \tag{10}$$

The quantity $V_\perp$ is not known. It will at least be as large as $U_{\perp E}$ since after radial expansion the radial oscillations will - if present - probably damp and become thermalized. However $V_\perp$ may be much larger than $U_\perp$ due to scattering of parallel kinetic energy by turbulence generated in the beam in region 1. We shall set

$$V_\perp = \alpha U \tag{11}$$

and regard α as unknown but bear in mind that perhaps $\alpha \sim .1$.

Consider a beam with the following injection parameters. A pulse of 10^{18} electrons is injected in .1 sec. with

$R_o \sim 10$ cm.,

$U \sim 6.10^9$ cm.sec.$^{-1}$ (10 keV electrons),

$n_{BO} \sim 5.10^6$ cm.$^{-3}$

The dominant term in (10) is often the first one and for such situations

$$\left(\frac{R}{R_o}\right)^2 \sim \frac{4.5\ \alpha^2}{\left(B_o^2 + 8\pi n_o K T_o\right)} .$$

Choosing $B_o = .1$ gauss and $B_o^2 = 8\pi n_o K T_o$ gives

$$R \sim 20\ \alpha^2 \text{ meters} \tag{12}$$

It is interesting to note that the pinch field B_p is less than the geomagnetic field, i.e., $B_p \sim .3/Rcm$.

(iii) Comment on Neutralizing Currents.

A current $J = en_o A_{eff} U_c$ flows (principally along B_o) to the satellite to balance the beam current, where A_{eff} is the effective area of the satellite and U_c the conduction stream velocity. Provided $U_c < V_e$ = thermal velocity of ionospheric electrons, this current will flow with nearly zero resistance. However if $U_c > V_e$, instabilities arise which could provide a considerable resistance with attendant dissipation of this current in the surrounding medium. (It is in any case unlikely that an electric field could extend from the satellite into the surrounding medium capable of drawing electrons faster than V_e. This is because electrons are constrained to follow the magnetic field lines.) Thus to ensure that the beam current can be balanced by the plasma current we must satify the condition

$$en_o A_{eff} V_e > en_{BO} \pi R_o^2 U$$

i.e.,

$$A_{eff} > \pi R_o^2 \left(\frac{U}{V_e}\right) \left(\frac{n_{BO}}{n_o}\right) . \qquad (13)$$

For example if $T_e = 10^4$ °K so that $V_e = 3.10^7$ and $n_o = 10^5$ we have for the beam parameters below Eq. 11,

$$A_{eff} > 3.10^6 \text{ cm}^2 .$$

If $n_o = 10^6$, $A_{eff} > 3.10^5 \text{ cm}^2$.

(iv) Region 2: Instabilities and Diffusion of the Beam

Consider an infinitely long beam of radius R and velocity U along $\underline{B}_o$ with a distribution function as shown in Fig.4. at t = 0 . The electron distribution is the familiar bump-on-tail distribution but with the added complication of a finite geometry.

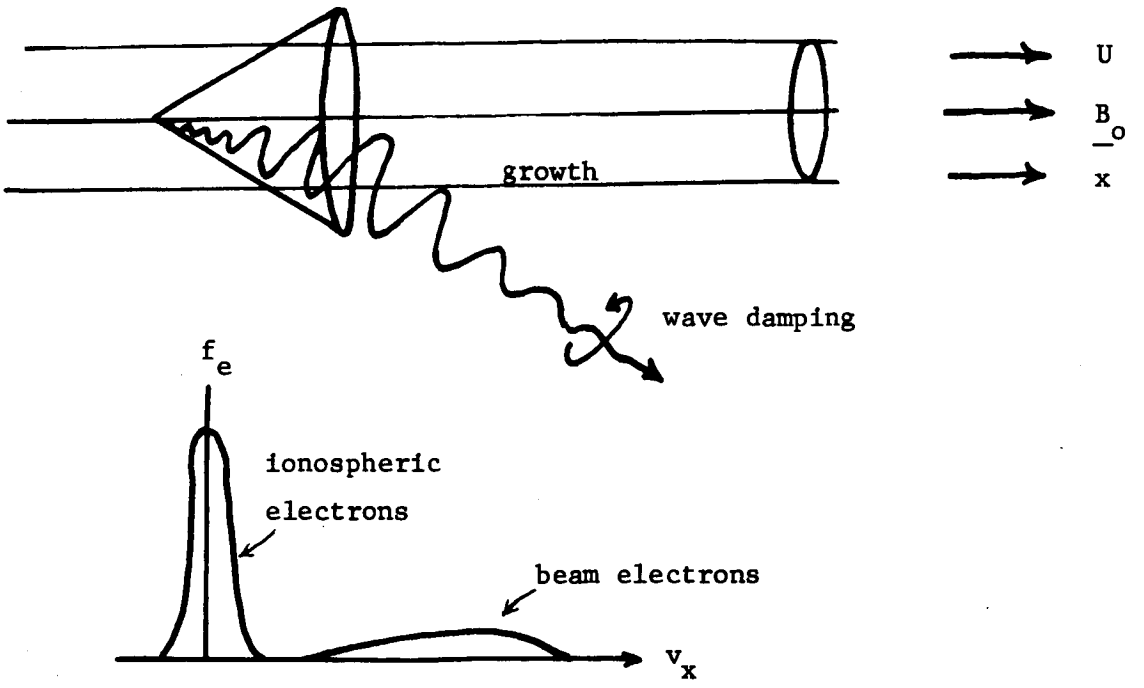

Figure 4.

Some of the questions of interest that arise for region 2 of the beam are:

(a) What is the spectrum of turbulence in the beam?

(b) How rapidly does the beam lose energy due to emission of plasma waves into the surrounding medium?

(c) What is the rate of radial diffusion of the beam due to wave-particle scattering?

(d) What disturbances - including electrostatic waves and radio emission - could be detected at large distances from the beam?

(a) Turbulence Spectrum

Various waves in the beam plasma will be unstable and grow in amplitude. They may grow until their amplitude is limited by non-linear effects or until they propagate out of the beam into the surrounding region of stable plasma. The problem of calculating the spectrum of turbulence in the beam is thus made particularly difficult since it is both a space and a time dependent nonlinear problem. This spectrum is however of central importance in that other processes are dependent on it. It may be necessary to measure the various spectral densities involved. For example waves detected at large distances from the beam give some information on the beam turbulence.

From considerations of linear theory it is simple to demonstrate that various waves will be unstable. Suppose for example we represent the beam and ionosphere electrons by the distribution

$$f_{oe} = \frac{\delta(v_\perp)}{\pi v_\perp} \left[\beta\delta(v_\parallel) + (1 - \beta)\, f_B(v_\parallel) \right] \tag{14}$$

with $\beta \cong 1$, and $\int f_B \, dv_\parallel = 1$, i.e., the beam distribution f_B has only parallel temperature and streaming ω.r.t. $\underline{B}_o$. It then follows (see Appendix) that the frequency $\omega = \omega_r + i\omega_i$, of cyclotron waves in the beam has an imaginary part given by

$$\omega_i = \frac{\mp\, \pi\Omega\omega_{eB}^2 f_B\left(\frac{\omega_r \mp \Omega}{k}\right)}{|k| \left[2\omega_r \pm \frac{\Omega\omega_e^2}{(\omega_r \mp \Omega)^2} \right]} \quad , \tag{15}$$

where the top signs apply for right circularly polarized waves and the bottom signs for left polarized waves, and $\omega_{eB}^2 = 4\pi n_B e^2/m$, $\omega_e^2 = 4\pi n_o e^2/m$. The infinite medium dispersion relations for waves propagating parallel to $\underline{B}_o$ were used to obtain (15). This is useful approximation for cyclotron waves in the beam with wavenumber $\underline{k}$ satisfying

$$k_\parallel >> k_\perp > \frac{2\pi}{R} \quad .$$

The dispersion relation relating the real part of the frequency, ω_r , to k is

$$\frac{c^2k^2}{\omega_r^2} = 1 - \frac{\omega_e^2}{\omega_r(\omega_r \mp \Omega)} \qquad (16)$$

where $\Omega = |e| B_o/mc$.

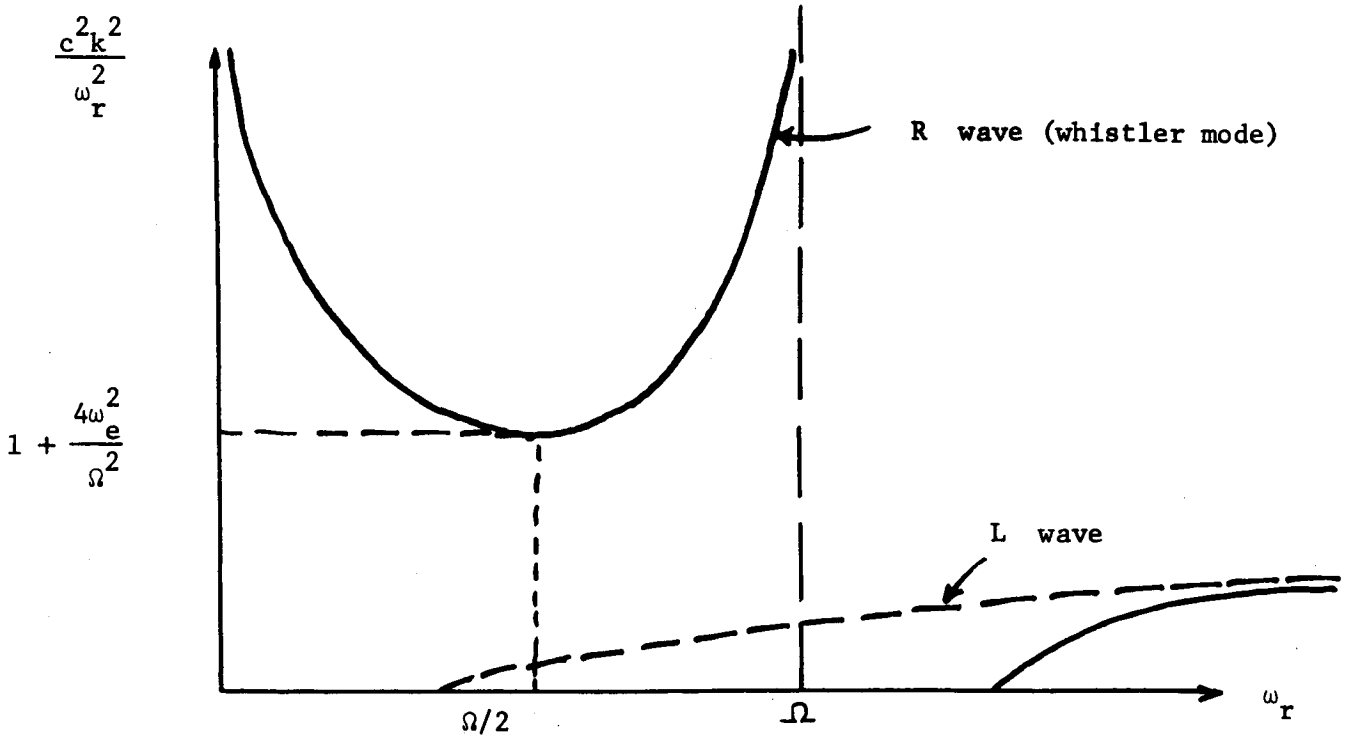

Figure 5.

If ω_i is positive the wave is unstable. For a beam propagating parallel to $\underline{B}_o$ as in Fig. 4. it is clear from (15) that only left-circularly polarized waves are unstable for a range of frequencies satisfying

$$2\left(\frac{\omega_r}{\Omega}\right)\left(\frac{\omega_r}{\Omega}+1\right)^2 > \left(\frac{\omega_e}{\Omega}\right)^2 \quad . \tag{17}$$

Similarly, electron plasma oscillations are unstable. Using the distribution (14) their growth rate is given by the familiar expression

$$\omega_i = +\frac{\pi}{2}\,\frac{\omega_e^3}{k^2}\,(1-\beta)\,\frac{\partial f_B}{\partial v_\parallel}\bigg|_{v_\parallel = \frac{\omega_e}{k}} \tag{18}$$

It is of interest to note that cyclotron wave growth depends on f_B, but electron plasma wave growth on its' gradient $\partial f_B/\partial v_\parallel$. Thus even if the bump-on-tail is completely flattened by wave-particle scattering as shown (Fig.6.), cyclotron waves will <u>still grow</u> and emerge from the beam.

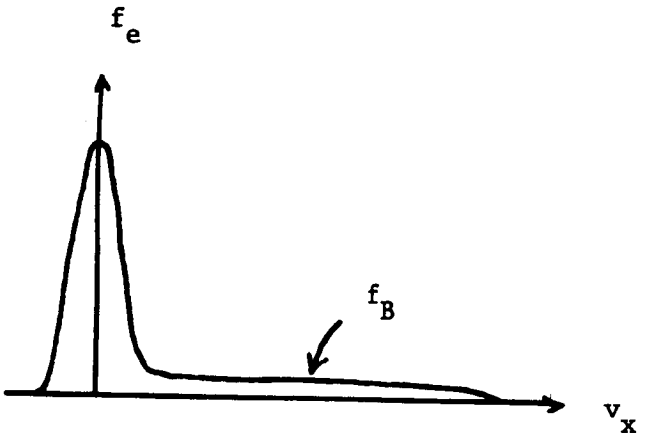

Figure 6.

Calculation of the spectral density functions, $\underline{\underline{S}}$, eg., for electric field fluctuations, is difficult. However one approach would be to use infinite medium quasilinear theory with a sink term $- S/\tau$ in the equation $dS/dt = 2\omega_i S - S/\tau$. Here τ is some average time it takes a growing wave packet to propagate out of the beam. A better approach would be to use the space and time dependent quasilinear equations directly.

A limited version of this latter approach has been published by Carnevale, Crosignani and Engelmann.[8] These authors consider a one-dimensional problem with only resonant wave-particle interactions and electrostatic waves included. The appropriate equations are,

$$\frac{\partial f}{\partial t} + v\frac{\partial f}{\partial x} = \frac{8\omega_e}{m}\frac{\partial}{\partial v}\left[\frac{1}{v^3}\left(\omega_i S_k\right)_{k=\omega_e/v}\right]$$

$$\frac{\partial S_k}{\partial t} + V_k \cdot \frac{\partial S_k}{\partial x} = 2\omega_i S_k$$

with ω_i given by (18). However their results are only applicable to short pulses of electrons of duration t_o such that the turbulence has a relatively small effect on the beam electron distribution, i.e., satisfying $\omega_i t_o < \ln \Lambda \sim 20$.

(b) Energy loss of the Beam Due to Wave Emission

We have seen that there will probably be a nonthermal spectrum of electron plasma oscillations and cyclotron waves in the beam together with other modes not discussed excited by azimuthal drift currents. A crude estimate for the rate of energy loss of the beam due to escape of such waves can be obtained by setting

$$\frac{d}{dt}\left(\pi R^2 n_B \frac{1}{2} m U^2\right) \sim \sum_\alpha 2\pi R V_{\perp\alpha} W_\alpha \quad , \tag{19}$$

where W_α is the energy density in mode α inside the beam, and $V_{\perp\alpha}$ its' group velocity perpendicular to the beam axis.

Defining a mean free path λ as the characteristic length

in which the beam radiates away all its energy we find

$$\lambda \simeq \frac{R\, n_B m\, U^3}{4 \sum V_{\perp\alpha}\, W_\alpha} \quad . \tag{20}$$

Consider for example electron plasma oscillations (either for case $\omega_e^2 >> \Omega_e^2$, or with $\underline{k}$ vectors nearly along the beam axis). Then $\omega^2 \simeq \omega_e^2 + k^2 V_e^2$ and $V_G \simeq V_e^2/(\omega/k) \simeq V_e^2/U$ for the most unstable waves. Assuming $V_{\perp\alpha} \sim 0(V_G)$ and that their energy density is $\langle \delta E^2 \rangle /8\pi$ we find

$$\lambda \simeq \frac{R}{4\beta} \left(\frac{U}{V_e} \right)^2 \quad , \tag{21}$$

where

$$\beta = \frac{\langle \delta \underline{E}^2 \rangle /8\pi}{n_B m U^2} \quad . \tag{22}$$

For example if $R = 20$ meters and $(U/V_e) = 10^2$, then

$$\lambda = 50/\beta \text{ km.} \tag{23}$$

If $\beta = 10^{-3}$, $\lambda = 50{,}000$ km, etc. The noise level in the beam, represented by β, is however unknown. However it would not be surprising to find the above value of β. Cyclotron waves will also contribute to the wave loss.

(c) Radial Diffusion of the Beam

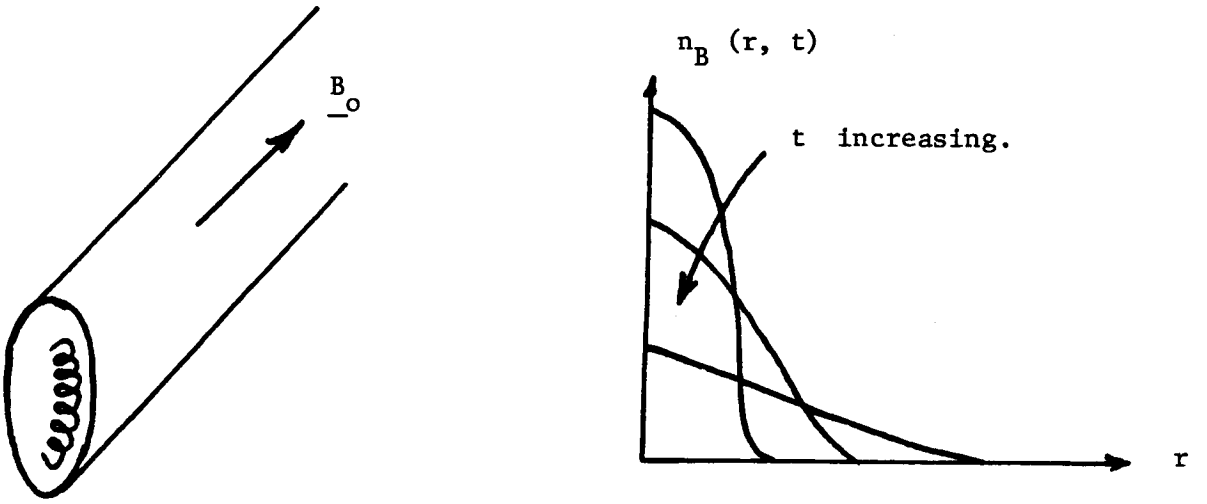

Figure 7.

Radial diffusion of the beam will occur as a result of wave-particle scattering. For an approximate description of this we make use of the diffusion equation for n_B with a diffusion coefficient $D_\perp$,

$$\frac{\partial n_B}{\partial t} = \underline{\nabla} \cdot \left[D_\perp(n_B)\ \underline{\nabla} n_B \right] \quad . \tag{24}$$

If the electrons undergo a random walk in which guiding centers take random steps of length a_e with frequency ν across the magnetic field, then $D \cong \nu a_e^2$. Setting $\nu = \Omega_e$, and $a_e = mcV_\perp/e\,B_o$ gives the Bohm diffusion coefficient

$$D_{\perp} = \frac{ckT_{\perp}}{eB_o} \quad . \tag{25}$$

For want of a better value for $D_{\perp}$ we shall use this one.

For the case of cyclindrical geometry the diffusion equation becomes

$$\frac{\partial n_B}{\partial t} = D_{\perp} \frac{1}{r} \frac{\partial}{\partial r} \left(r \frac{\partial n_B}{\partial r} \right) \quad .$$

which has a similarity solution

$$n_B = n_B \left(\frac{r}{\sqrt{t}} \right) \tag{26}$$

where $y = r/\sqrt{t}$ and n_B then satisfies

$$- \frac{y^2}{2} \frac{dn_B}{dy} = D_{\perp} \frac{d}{dy} \left(y \frac{dn_B}{dy} \right) \quad .$$

Setting

$$z = y \frac{dn_B}{dy}$$

then gives

$$z(y) = A\, e^{-y^2/4D_\perp} ,$$

so that finally

$$n_B\left(\frac{r}{\sqrt{t}}\right) = A \int_{\infty}^{r/\sqrt{t}} \frac{dy}{y}\, e^{-y^2/4D_\perp} .$$

Now the total number of electrons per unit length of the beam is

$$N = \int_0^{\infty} 2\pi n_B r dr = 2\pi A \int_0^{\infty} r dr \int_{\infty}^{r/\sqrt{t}} \frac{dy}{y}\, e^{-y^2/4D_\perp}$$

$$= 2\pi A \int_{\infty}^{0} \frac{dy}{y}\, e^{-y^2/4D_\perp} \int_0^{\sqrt{t}y} r dr = -2\pi A D t .$$

Thus,

$$n_B = \frac{N}{2\pi D_\perp t} \int_{\frac{r}{2\sqrt{D_\perp t}}}^{\infty} \frac{dx}{x}\, e^{-x^2} . \qquad (27)$$

The radius of the beam for large t can thus be defined roughly as

$$R \sim 2\sqrt{D_\perp t} = 2a_e \sqrt{\Omega_e t} \quad . \tag{28}$$

For example if $B_o = .1$ gauss then $\Omega_e \sim 10^6$, $a_e = mcV_\perp/eB_o \sim 10^3$ cm if $V_\perp = 10^9$ cm. sec.$^{-1}$, so that

$$R \sim 2.\ 10^6 \sqrt{t} \text{ cm.} \tag{29}$$

where t is in seconds. A typical transit time from point to conjugate point in the geometric field might be of order 1 sec. Thus for this case

$$R \sim 20 \text{ km.}$$

This figure is not very reliable. Bohm diffusion probably gives an upper limit to the diffusion rate across B_o and the radial diffusion may be somewhat less than this.

(d) Emission of Waves by the Beam.

Consider the disturbances detectable at large distances from the beam. These depend on the spectrum of waves excited by the beam and also their propagation properties in the ionospheric plasma. We now consider a few examples.

Electrostatic Waves

In regions where $\omega_e^2 >> \Omega^2$, or wave vectors are nearly along $\underline{B}_o$, electron plasma oscillations of the simple electrostatic type can be excited. They have a damping decrement $\omega_i \alpha \exp(- k_D^2/k^2)$. But the waves excited in the beam are principally waves with $\omega_e/k \sim U$. Thus once these waves propagate into the ionospheric plasma they suffer very little Landau damping since

$$\omega_i \alpha \exp \left(- \frac{U^2}{2V_e^2} \right) << 1 . \qquad (30)$$

One would expect therefore to sometimes find a far-field of electrostatic waves with only geometrical attenuation (αr^{-2}) emanating from the beam under some circumstances.

Similarly, practically undamped cyclotron waves will be emitted together with more complicated plasma modes.

Radio Noise

Combination scattering (mode coupling) of waves in the beam can excite electromagnetic waves at frequencies $\geq \omega_e$ capable of escaping from the beam. However such emission will be of smaller amplitude than the direct emission. However it may be important if one is attempting to detect waves at large distances from the beam eg., on the earth's surface.

For the case that $\Omega^2 << \omega_e^2$ the appropriate mode couplings are those of unstable electron plasma waves with thermal ion waves

or electron waves to emit electromagnetic radiation.

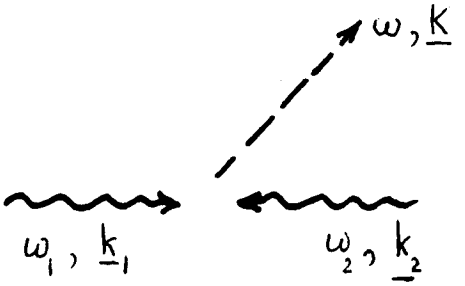

Frequencies and wavenumbers are conserved in such interactions, i.e., $\omega = \omega_1 + \omega_2$, $\underline{K} = \underline{k}_1 + \underline{k}_2$. But for $\omega \sim \omega_e$, $K \sim (V_e/c)k_D$, so that $\underline{k}_1 \cong -\underline{k}_2$. The two lowest order processes are thus as shown:

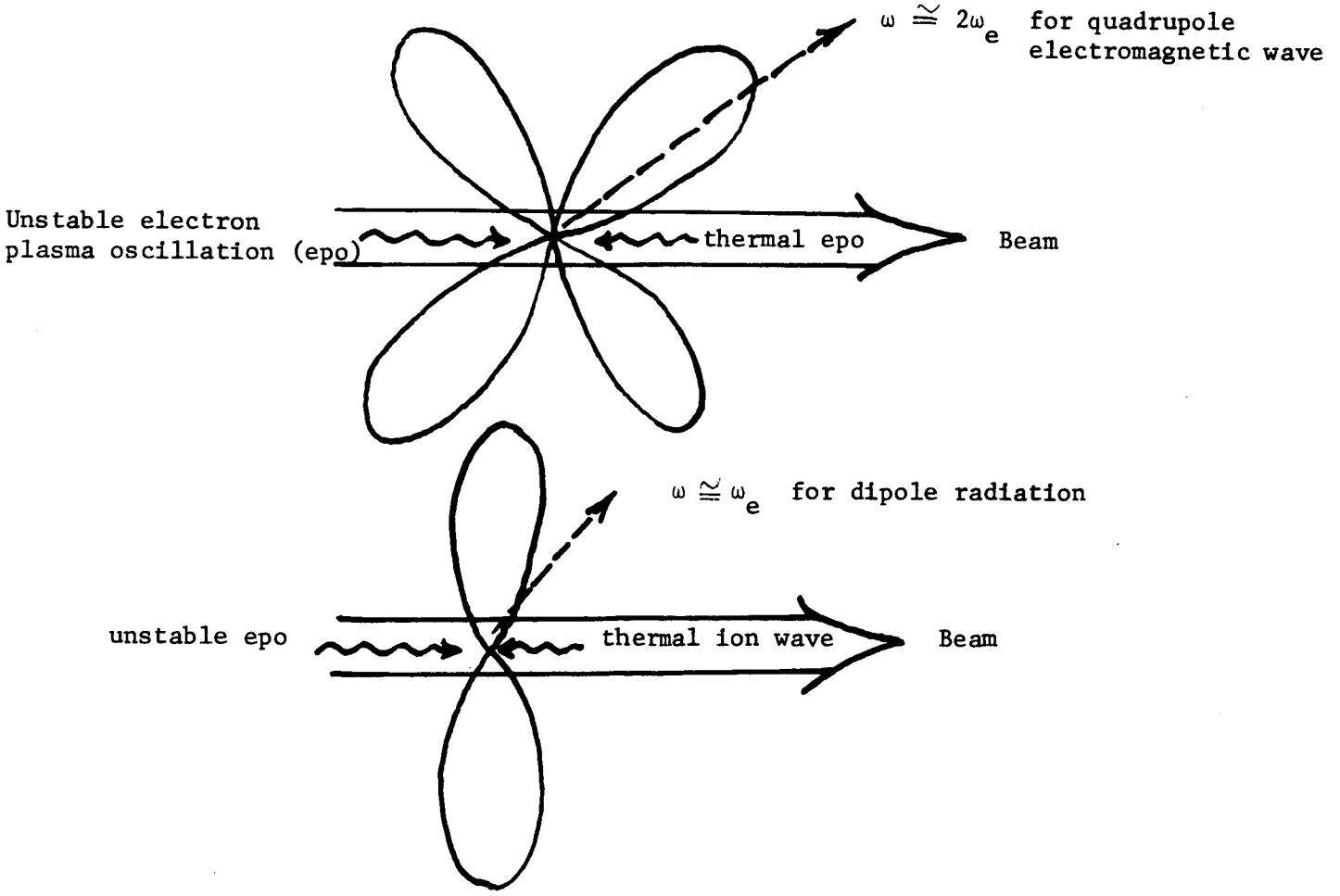

Figure 8.

The amplitude of these emitted radio waves is expected to be much less than that of the emitted electrostatic waves and other plasma modes. This is because the unstable electron plasma oscillations must scatter off thermal waves with $\underline{k}$ vectors antiparallel to the beam velocity U. Factors like $\exp(- U^2/2v_e^2) \cong 0$ are involved in the amplitude of such thermal fluctuations. However after the beam arrives at its mirror points, so that fast electrons are streaming in opposing directions in the beam, this radio emission might become more intense since nonthermal plasma waves of phase velocities $\omega/k \simeq \pm U$ will be generated to make the required head-on-collisions.

(v) Region 3: Comments on the Leading Edge of the Beam.

Consider a beam which has been stabilized against electrostatic instabilities, i.e., the bump-on-tail has been smeared out as shown in Fig. 9. Suppose at $t = 0$ it has a length L, i.e.,

$$f_e = f_{Max} + I(x, L)\, f_B(v_x) \quad , \tag{31}$$

$$I = 1 \text{ if } 0 < x < L \ ,$$

$$= 0 \text{ otherwise}$$

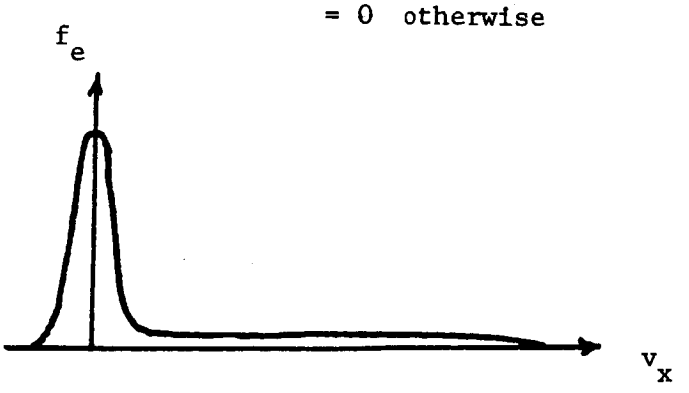

Figure 9.

If all forces are neglected and only free streaming of the beam particles is considered it follows that at $t > 0$,

$$f_e = f_{Max} + I(x - v_x t , L)\, f_B(v_x) \quad . \tag{32}$$

Due to velocity dispersion in the beam the front edge can now become a violently 2-stream unstable distribution as shown in Fig.10. Note the

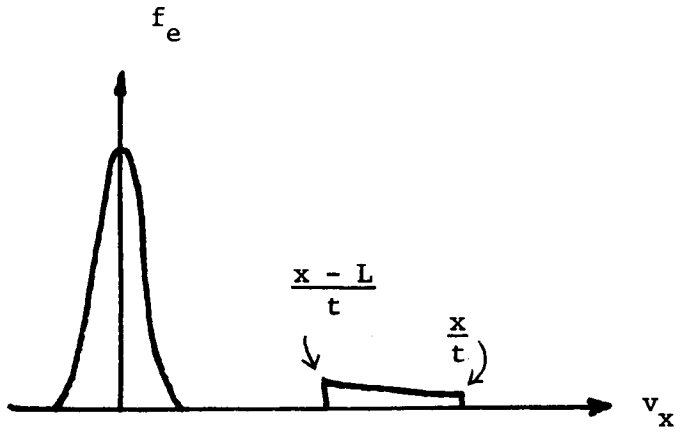

Figure 10.

beam occupies the velocity range $0 < x - v_x t < L$ at x, t, i.e.,

$$\left(\frac{x - L}{t} \right) < v_x < \frac{x}{t} \quad . \tag{33}$$

This rapid regeneration of instability at the leading edge of the beam is expected to make this a particularly turbulent region. The waves in turn will scatter particles thus opposing the separation of fast particles from slow ones.

This effect might tend to produce a sharp front on the beam in which region particles accumulate as they catch up to the front but fail to outstrip it. However, considerable radial diffusion might also take place. (Note, a 10 Kev electron beam pulsed at .1 seconds has a length $L \cong 6000$km.).

(vi) APPENDIX

Consider the dispersion relations for right (R) or left (L) circularly polarized cyclotron waves propagating parallel to $\underline{B}_o$,

$$\omega^2 - c^2k^2 + \pi\omega \sum_\alpha \omega_{p\alpha}^2 \int_{-\infty}^{\infty} dv_{\parallel} \int_0^{\infty} v_\perp^2 dv_\perp \frac{\left(\frac{\partial f_{o\alpha}}{\partial v_\perp} - \frac{kv_{\parallel}}{\omega} \frac{\partial f_{o\alpha}}{\partial v_\perp} + \frac{kv_\perp}{\omega} \frac{\partial f_o}{\partial v_{\parallel}} \right)}{(\omega - kv_{\parallel} \pm \Omega_\alpha)} = 0 \tag{A1}$$

where integrals continued as defined from $\mathrm{Im}(\omega) > 0$, $\Omega_\alpha = e_\alpha B/mc$ for α^{th} species and k is along $\underline{B}_o$, and signs go with electric field

polarization as shown.

We choose to consider a hot tenuous beam of electrons (with only parallel temperature) traversing a cold plasma. To describe this choose

$$f_{oe} = \frac{\delta(v_\perp)}{\pi v_\perp} \left[\beta\, \delta(v_\parallel) + (1 - \beta)\, f_B(v_\parallel) \right] \qquad \text{(A2)}$$

with $\int_0^\infty \delta(v_\perp) dv_\perp = 1/2$, and f_B the beam distribution. Thus (A1) becomes

$$\omega^2 - c^2k^2 - \omega\omega_e^2 \int_{-\infty}^{\infty} dv_\parallel \frac{\left(1 - \frac{kv_\parallel}{\omega}\right)\left[\beta\delta(v_\parallel) + (1 - \beta)\, f_B(v_\parallel)\right]}{(\omega - kv_\parallel \pm \Omega)}$$

$$\cong \omega^2 - c^2k^2 - \frac{\omega\omega_e^2\, \beta}{(\omega \pm \Omega_e)} - \omega\omega_e^2(1 - \beta) \int_{-\infty}^{\infty} dv_\parallel \frac{\left(1 - \frac{kv_\parallel}{\omega}\right) f_B}{(\omega - kv_\parallel \pm \Omega_e)} = 0 \ . \qquad \text{(A3)}$$

The beam electron distribution will be treated as a bump-on-tail that contributes to the small imaginary part of ω , but not to its real part, i.e., we set $\omega = \omega_r + i\omega_i$ and treat f_B and ω_i as small. Further,

$$(\omega - kv_{\|} \pm \Omega_e) = - k^{-1}\left[v_{\|} - \frac{(\omega_r \pm \Omega_e)}{k} - \frac{i\omega_i}{k} \right]^{-1}$$

$$\longrightarrow - \frac{P}{k\left[v_{\|} - \frac{\omega_r \pm \Omega_e}{k}\right]} - \frac{\pi i}{|k|}\,\delta\left[v_{\|} - \frac{\omega_r \pm \Omega_e}{k}\right] \quad . \qquad \text{(A4)}$$

Use this in (A3) and drop terms of $O(\omega_i^2)$. Thus

$$\omega_r^2 + 2i\omega_i\omega_r - c^2k^2 - \frac{\omega_e^2(\omega_r + i\omega_i)}{(\omega_r \pm \Omega_e + i\omega_i)} + \frac{\pi i \omega_r \omega_{eB}^2}{|k|}\int_{-\infty}^{\infty} dv_{\|}\,(1 - \frac{kv_{\|}}{\omega})\,\delta\left[v_{\|} - \frac{\omega_r \pm \Omega_e}{k}\right] = 0,$$

where $\omega_{eB}^2 = (1 - \beta)\omega_e^2 \equiv 4\pi n_B e^2/m$, i.e.,

$$\omega_r^2 - c^2k^2 - \frac{\omega_r \omega_e^2}{(\omega_r \pm \Omega_e)} \cong 0 \quad ,$$

and

$$2\omega_i\omega_r - \frac{\omega_i\omega_e^2}{(\omega_r \pm \Omega_e)} + \frac{\omega_r\omega_e^2\omega_i}{(\omega_r \pm \Omega_e)^2} + \frac{\pi\omega_r\omega_{eB}^2}{|k|}\left[1 - \frac{\omega_r \pm \Omega_e}{\omega_r}\right] f_B\left(\frac{\omega_r \pm \Omega_e}{k}\right) = 0 \ .$$

Finally, defining $\Omega = |\Omega_e|$ (since Ω_e is negative) we find

$$\omega_i = \frac{\mp \pi \Omega \omega_{eB}^2 f_B \left(\frac{\omega_r \mp \Omega}{k} \right)}{|k| \left[2\omega_r \pm \frac{\Omega \omega_e^2}{(\omega_r \mp \Omega^2} \right]} \qquad \text{(A5)}$$

where the top signs apply for the right polarized wave, and the bottom signs to the left wave.

REFERENCES

1. R.J. Briggs, Electron-Stream Interaction with Plasmas, Research Monograph No. 29., M.I.T. Press, Cambridge, Mass., 1964.

In this monograph the geometrical aspect of the beam-plasma problem is emphasized. However, principally zero-temperature beams are treated and the velocity-distribution function aspect is minimized.

2. J.R. Apel and A. Stone, Experiments on Wave Interactions Between Plasma and an Electron Stream in a Magnetic Field, Proceedings of Seventh Int.Conference on Ionized Gases, Vol.II. (Beograd 1966).

Experiments have been conducted on the UHF wave interaction between a plasma and an electron stream /1,2/ and comparisons made between the measured and calculated values of frequencies and wavelengths. The apparatus consists of a plasma source producing a plasma column one cm in diameter with n_e adjustable between 10^9 and 10^{13} cm^{-3}; an electron gun yielding 180 ma at 2000 volts, flowing coaxixally with the plasma; and a collimating magnetic field of 400 oersted intensity. The theory and measurements show the instability to be due to the interaction of the electron cyclotron wave in the plasma with the "plasma wave" in the beam.

3. J.R. Apel, Harmonic Generation and Turbulence-Like Spectrum in a Beam-Plasma Interaction, Phys.Rev.Lett. 19, HV511, 1-3.

The power spectrum of UHF emission from a pulsed, 3-μsec beam-plasma interaction has been found to contain peaks at harmonics of the fundamental interaction frequency up to $n = 7$, and to fall off with increasing frequency as $f^{-5.5 \pm 0.5}$. When an approximate correction for finite plasma diameter and probe response is included, the exponent becomes very nearly -5. This functional form indicates a turbulent wave-number spectrum going as k^{-5}, since the electron plasma waves most strongly excited by a beam have phase and group velocities nearly equal to the beam velocity v_b (here $k = k_z = k_{||}$). The observations cannot be accounted for using linear theory - say, the hot-plasma dielectric tensor - but suggest that appreciable nonlinear behavior and plasma turbulence occur early in the interaction.

4. T.H. Stix, Phys. Fluids 7, 1960 (1964), Phys.Fluids 8, 1415 (c) 1965.

A detailed examination is made of a large-amplitude beam-excited electron plasma wave, and of the acceleration to high energies of favored electrons by the electric field of this wave. In laboratory experiments x rays with energies greater than 100 Kev have been observed coming from a plasma in a magnetic field, typically 2000 G, penetrated by an electron beam, typically one ampere at 10 Kev. To account for the impressive energies reached by the electrons producing these x rays, an acceleration process is invoked in which individual steps of

coherent cyclotron acceleration are summed stochastically. The increase in the perpendicular energy of the favored electrons enhances their magnetic mirror confinement and enables the acceleration process to occur within a small volume of plasma. The overstable mode under consideration is the double-hump-excited electrostatic wave in a magnetic field, with $\underline{k}$ and $\underline{E}$ not quite parallel to $\underline{B}_o$. The wave frequency is close to the electron plasma frequency, the phase velocity is close to the beam velocity. It is electrons, often with low parallel energy, which feel the wave at their own cyclotron frequency (or a harmonic thereof) which are favored in the acceleration process. The rapid growth of the electric fields to the large amplitudes requisite for the acceleration mechanism is difficult to account for, however, since electron trapping would be expected to occur and the linearized Vlasov-equation theory loses validity. An efficient untrapping process is therefore invoked: The plasma is thought of as a conglomerate of wave regions which are individually coherent but mutually incoherent. As an electron passes from one coherent region to another it is subjected to a new electric field randomly phased with respect to the first. A short correlation length improves the ability to account for overstability growth to large amplitude, but lengthens somewhat the calculated time for electron acceleration. Computations show efficient acceleration when the electron plasma frequency is of

the same order or larger than the electron cyclotron frequency.

5. L.D. Smullin and W.D. Getty, Plasma Physics and Controlled Nuclear Fusion Research II, 815, IAEA, Vienna, (1966).

6. I. Alexeff et al, Plasma Physics and Controlled Nuclear Fusion Research II, 781, IAEA, Vienna, (1966).

7. J.R. Apel and A.M. Stone, Proceedings of Seventh Int. Conf. on Ionized Gases, II, Belgrad, 1966.

Experiments have been conducted on the UHF wave interaction between a plasma and an electron stream and comparisons made between the measured and calculated values of frequencies and wavelengths.

8. J. Uramoto, Tech. Report IPPJ-22, 1964 of Nagoya Univ., Japan: Energy Loss of an Electron Beam in a Plasma.

Energy loss of an initially uniform 11 Kev electron beam injected into a plasma is studied with an electrostatic analyser.

9. Interaction of an Electron Beam with a Collisionless Plasma, Phys. Fluids 10, 436 (1967).

The growth of electrostatic wave excitation in a collisionless plasma, interacting with an electron beam of finite length as well as the simultaneous modification of the beam are studied for weakly unstable situations. Using quasi-linear theory, explicit results as a function of space, of time, and of the plasma and beam parameters are obtained for the surface layer

where the relaxation of the beam effectively takes place. The effect on the beam of both unstable modes and resonant stable modes of thermal excitation is considered.

5. TRIGGERING AN AURORA

L.M. Linson* and H.E. Petschek*

AVCO Everett Research Laboratory

Everett, Massachusetts

ABSTRACT

The natural convective flow in the equatorial plane of the magnetosphere around $L = 6$ on the midnight side is responsible for auroral phenomena. We suggest that the disturbance created by line-tying a sufficient number of magnetic flux tubes in the lower ionosphere at auroral latitudes may trigger an aurora. The large electron cloud of order 10^3 km^3 and density of order 10^6 electrons cm^{-3} required is also useful for studies of the physics of the ionosphere. The necessary energy requirement and a preliminary evaluation of several methods which might be used to produce the desired ionization is discussed.

(i) Introduction

The purpose of this report is to suggest that a significant enhancement of the ambient electron density in the lower ionosphere at auroral latitudes may trigger an aurora. Even if this ultimate objective is not accomplished, the large electron cloud will

---

* Supported in part by NASw-1400

have scientific value by allowing studies of winds, diffusion, drifts, recombination, and effects on communications which would complement similar studies which have been conducted with the aid of smaller electron clouds. We shall estimate the necessary energy requirement and give a preliminary evaluation of several methods which might be used to produce the desired ionization.

The principal observations during an aurora consist of a significant degree of molecular and atomic excitation resulting in emission in the visible spectrum and deflections in magnetic field intensities measured at ground stations. The latter are believed to be due to currents in the vicinity of 120 km altitude which are the result of an increase in conductivity due to an enhancement of the ambient electron density. Both the molecular excitation and ionization are caused by high energy electrons (around 10 Kev) which precipitate along magnetic field lines from the equatorial region of the magnetosphere in the vicinity of L-shell equal to six. While it is not practical to consider supplying the energy which is dissipated during a natural aurora (of order 10^{10} watts for times up to 10^{4} sec) barring the use of nuclear sources, it may be possible to trigger such an event by a more modest expenditure of energy.

The suggestion is made that one might trigger an aurora by increasing the electron density and hence the conductivity in the auroral zone where the currents are observed to flow. The increased conductivity would couple the magnetic field line motion

more closely to the neutral atmosphere. The resulting disturbance in the magnetospheric convection may produce precipitation, as will be discussed below. Although the exact requirements are uncertain, a rough estimate indicates that an electron density of about 5×10^5 electrons cm^{-3} in a volume of about 100 km^2 by 20 km in height or 2×10^{12} m^3 should be sufficient to produce an observable effect. The above density is far above the ambient nighttime value and would have to be created in a time which several factors (to be discussed below) suggest to be of the order of a minute. Using an average ionization potential for air (I_{O_2} = 12.2 ev; I_{N_2} = 15.5 ev) of 15 volts, we easily arrive at a minimum energy requirement of 2.4×10^6 joules or a power requirement of 40 kwatt for 60 sec.

The release of electron clouds from rockets in the earth's atmosphere between 70 km and several thousand kilometers altitude has been carried out by a number of researchers in the past decade. While these electron clouds have been useful for ionospheric physics studies, they have exhibited no interaction with the magnetosphere because the releases have been smaller than the ones envisioned in this report and, more importantly, for the most part they have been neither at the right place nor at the right time. Most of the previous releases have been conducted at midlatitudes and predominantly near dawn or dusk and have succeeded in producing only on the order of 10^{21} electrons. We require on the order of 10^{24} electrons at auroral latitudes near midnight at an altitude of around 100 km. The few releases which had been carried out in the auroral zone for the purpose

of mapping ionospheric electric fields have all been above 150 km in altitude which is too high to couple magnetic field lines with the neutral atmosphere.

Most previous chemical releases have relied upon photo-ionization by sunlight to produce large numbers of electrons. Since 120 km altitude at auroral latitudes near midnight is not in sunlight we have considered a number of different methods of achieving the desired degree of ionization. The most promising seems to be an extension of the present technique involving the release of chemically reacting products. Another possibility is the use of energetic (of order 100 Kev) electron or ion beams to ionize the ambient air. Breakdown of the lower ionosphere using electromagnetic radiation or the use of x rays to ionize the air do not seems as practical. Further study is required to determine the most optimum method.

In Section 2 we shall discuss the relevant properties of the ionosphere during an aurora and give the criteria used which determines the required electron density, volume to be ionized, and time scale of the experiment. In Section 3 we give a preliminary evaluation of the several suggestions to produce the necessary ionization mentioned above and indicate the major uncertainty associated with each. Section 4 consists of a brief summary. In the Appendix we describe the calculation which is necessary to determine the efficiency of the ionization of air by using an energetic ion beam.

(ii) Requirements for Triggering an Aurora

Aurorae typically occur in the auroral zone usually within a few degrees of 66° magnetic latitude and generally between the late evening and early morning hours local time. Although there is a wide variety of displays, generally they appear to be around 5 to 10 km in thickness in the N-S direction but often extend for several thousand kilometers in the E-W direction. Their lower edge of visible light and presumably ionization generally is at an altitude of around 100 $\pm$ 10 km. The fact that intense auroral breakups consistently occur in the same location and represent the rapid deposition of large amounts of energy indicates that they are produced by the onset of an explosive instability. It has been suggested [Axford, et al, 1965] that the energy source of an aurora may lie in the sunward flow of high energy plasma in the equatorial plane of the magnetosphere around $L = 6$. It is likely that some type of disturbance of this flow in the equatorial plane is responsible for provoking the instability which results in an aurora. It may be possible to create such a disturbance by slowing down with respect to the flow a sufficient number of magnetic flux tubes; the method we suggest is to tie their feet in the ionosphere by increasing the ambient conductivity significantly. This has the effect of coupling the magnetic field lines more strongly with the neutral atmospheric particles and thus increasing their drag. An alternative view suggests that the increased conductivity will greatly alter the ambient or equilibrium voltage gradients which

may result in the lowering of energetic particle mirror points and hence initiate increased precipitation which could then sustain the increased ionization. While it is not at all certain that increased ionization in the ionosphere will provoke an aurora, the possibility of doing so with reasonable rocket payloads or power requirements makes it too intriguing to be overlooked. Should such an attempt be successful, the opportunity then exists for increasing our understanding of auroral phenomena as well as shedding light on the dynamic aspects of the flow in the magnetosphere.

While the possibility of triggering an aurora provides an exciting goal, useful scientific information would also be available from such an experiment if this spectacular result is not achieved. At a minimum, the change in ionospheric ion density will locally modify the ionospheric current patterns. Measurement of these currents would provide some information about the interaction of the magnetospheric flow patterns with the ionosphere. One would also expect at least measurable changes in precipitation due to the disturbance of the field line motion. Monitoring of these changes would again provide information which may suggest interactions between the magnetospheric flow and natural ionospheric irregularities. Furthermore, ionization over such a large scale as 10 km would complement experiments which have been performed by chemically releasing smaller electron clouds at the same altitude range at various times of the day. As examples, investigations of electron diffusion rates, drifts and distortion of the electron cloud, recombination phenomena, and various decay modes

of the electron density could be carried out as well as studies made of the effect of the ionospheric winds and the effect of the electron cloud on communications.

We now obtain an estimate of the size of the region to be ionized. The minimum scale size on which the equatorial flow as such can be disturbed is probably a gyro-diameter of a proton of typical energy (1 Kev) in the earth's magnetic field at $L = 6$ ($\sim 160\gamma$) . This distance is 57 km; the equivalent length in the ionosphere is reduced by the square root of the ratio of the magnetic field intensities which results in a value of 3.2 km. Hence, tying an area of 10 x 10 sq. km. will represent intercepting the flow over a length corresponding to 3 proton gyro-diameters in the equatorial plane. A substantiation of the estimate is the observed fact that aurorae are typically several kilometers in thickness, possibly indicating a tendency towards a minimum scale size. If one were to ionize a larger area, extending the long dimension in the N-S direction would intercept more of the equatorial flow and would probably increase the possibility of triggering an aurora.

The total amount of ionization which might be required to trigger an aurora is uncertain. The most reliable dimension of the ionization cloud is probably the 5 to 10 kilometer size in the N-S direction as described above. It would also seem that the scale size in the E-W direction should be larger than an equatorial proton gyro-radius and hence comparable to that of the N-S direction if the gyrating particles in the equatorial plane are to be prohibited from

passing through the frozen flux tubes. The remaining uncertainties are the determination of the most appropriate altitude at which to create the ionization, the required vertical thickness of the ionization, and the required degree of ionization. We first discuss the appropriate criteria theoretically and then compare our deductions with observations.

The Pedersen and Hall conductivities, σ_P and σ_H, which are the conductivities perpendicular to the magnetic field and parallel and perpendicular respectively to the electric field, are given by

$$\sigma_P = \left[\frac{(\omega\tau)_i}{1 + (\omega\tau)_i^2} + \frac{(\omega\tau)_e}{1 + (\omega\tau)_e^2}\right] \sigma'$$

$$\sigma_H = \left[\frac{(\omega\tau)_i^2}{1 + (\omega\tau)_i^2} - \frac{(\omega\tau)_e^2}{1 + (\omega\tau)_e^2}\right] \sigma' \qquad (2.1)$$

with

$$\sigma' = \frac{n_e e}{B} = 2.7 \times 10^{-4}\left(\frac{n_e}{10^5 \text{cm}^{-3}}\right)\left(\frac{B}{0.6 \text{ gauss}}\right)^{-1} \text{mho m}^{-1}$$

Above 80 km $(\omega\tau)_e >> 1$ while $(\omega\tau)_i(\omega\tau)_e > 1$ above 95 km. Hence, above 95 km the Hall current is due predominantly to the electrons while according to Eq. (2.1) the Pederson current in the N-S direction

is predominantly due to ions. As it is difficult to create persistent ionization below about 95 km we shall take it to be a lower bound for our ionization cloud. An upper limit to the altitude above which we cannot tie the magnetic field lines to the neutrals is where $(\omega\tau)_i$ is of order unity or around 120 km for NO^+, as the ions rarely collide with neutrals at higher altitudes. If the criterion to be applied in order to achieve maximum effectiveness for line-tying magnetic field lines is that the Pedersen conductivity should be maximized, then Eq. (2.1) suggests that the ionization should be created at around 120 km altitude. The precise optimum altitude is uncertain but the above discussion indicates that close to but below 120 km is most appropriate. It is possible that the electron contribution to the Pedersen conductivity at these altitudes is considerably in excess of the value indicated by Eq. (2.1) due to anomalous or turbulent diffusion of electrons across magnetic field lines. Such increased electron diffusion is almost universally observed in laboratory plasmas when $(\omega\tau)_e >> 1$. In this case the Pedersen conductivity would become less dependent on altitude and 120 km would remain only as an upper limit.

The requirement of a significant change in the Pedersen conductivity provides a criterion for determining the necessery height-integrated density in the ionization cloud. According to a model by Boström [1964] the height-integrated Pedersen conductivity is on the order of half a mho for the undisturbed ionosphere. According to Eq. (2.1) a height-integrated density of 4×10^{11} electrons

cm^{-2} will increase the Pedersen conductivity by an order of magnitude above the ambient value. The thickness of this cloud of ionization is determined primarily by the requirement that the electron density be low enough so that the ionization will persist for times of the order of minutes. Experiments involving chemical releases indicate that electron densities on the order of 10^6 cm^{-3} persist for the required time [Marmo et al, 1961]. This fact indicates that the thickness of the ionization cloud should be several kilometers.

The theoretical discussion above agrees favorably with observations. In Fig. 1 is shown typical electron density profiles measured by rockets during discrete and diffuse aurorae [Baker and Ulwick, 1967]. Also shown for comparison are typical daytime and nighttime profiles. The distinguishing characteristic of the discrete aurora is the enhancement by several factors of the electron density for about 20 km centered around 115 km. A value of 5×10^5 cm^{-3} seems typical and is occasionally exceeded by a factor of two or three. We thus reach the conclusion that ionization with a height-integrated density of order 10^{12} electrons cm^{-2} with an electron density of about 10^6 cm^{-3} at a height of around 115 km is created during a natural aurora. It may be more than a coincidence that the penetration depth of the precipitated 10 Kev electrons corresponds to an altitude where the deposited ionization will have a maximum effect on the Pedersen currents and that the scale height is large enough so that the ionization is spread out which leads to a change of the Pedersen conductivity by more than an order of magnitude.

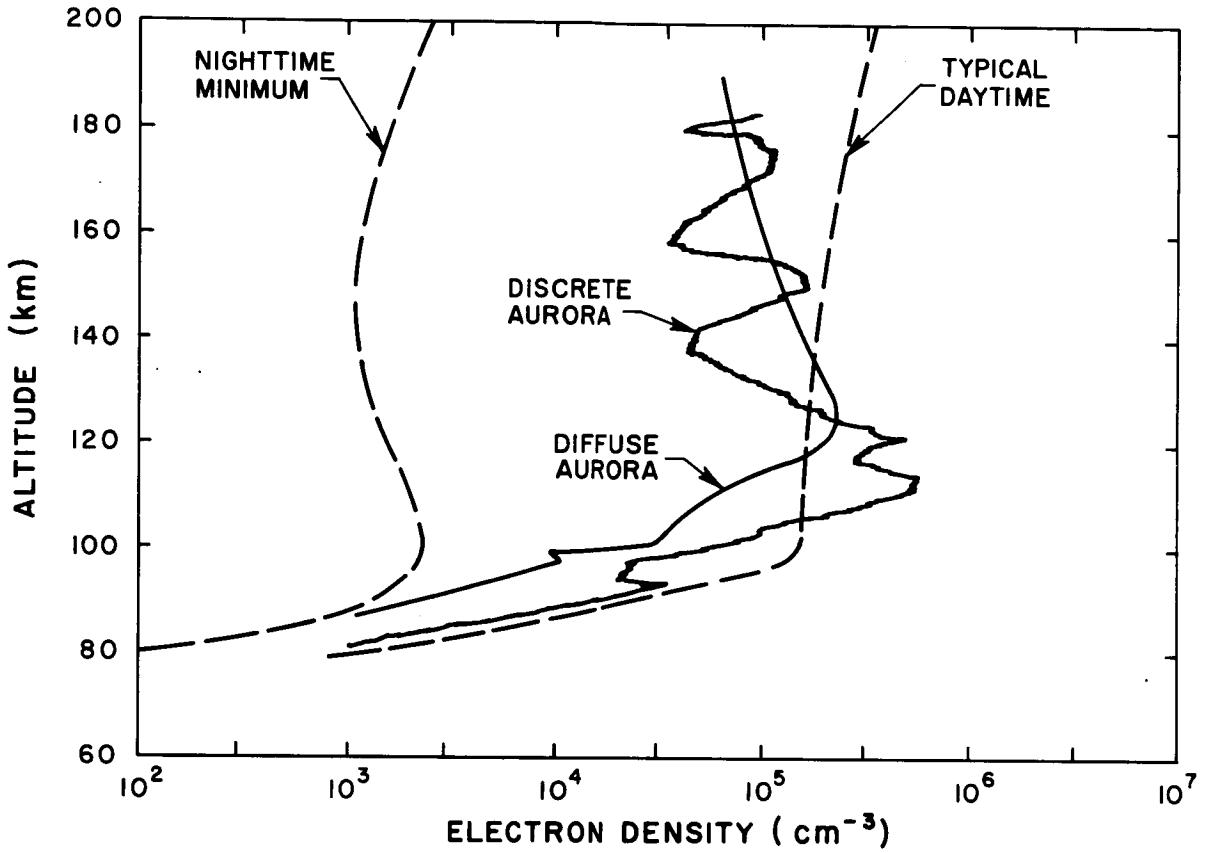

Fig. 1 Typical electron density profiles measured during discrete and diffuse aurorae (Baker and Ulwick, 1967). The dashed curves represent typical daytime and nighttime profiles.

Combining a height-integrated density of 10^{12} electrons cm^{-2} with a 100 square kilometer area leads to the previously mentioned requirement of 10^{24} electrons or about 2.4 Megajoules assuming a 100 % efficiency for ionizing air.

The time limitations of the experiment require two considerations: a/ the minimum length of time for which the regions of high electron density should be maintained; and b/ the rate at which the electrons are to be created. An estimate for the former time is given by the time it takes the stopping of the magnetic flux tubes to be communicated to the equatorial plane. The appropriate speed is the Alfvén speed which yields a time of about a minute for a lower limit. There is no reason to believe that the creation time of the cloud must be less than this limit.

Above 100 km, the principal loss of electrons is due to diffusion; the role of recombination is uncertain. A recombination coefficient in the range of 10^{-7} to 10^{-10} cm^3 sec^{-1} yields times for the electron density to decrease by a factor of two in the range of 5 to 5 x 10^3 sec. However, experiments conducted by detonating small canisters containing alkali compounds have shown [Marmo, et al, 1961] that small electron clouds (scale size $\sim$ 1 km) with densities in excess of 10^6 cm^{-3} have persisted near 115 km altitude for more than 10^3 sec. The conclusion was that the principle cause of decrease in electron density was diffusion with a diffusion coefficient of the order 10^7 cm^2 sec^{-1} indicated for electrons at an altitude of 115 km (varying inversely with the neutral density).

A time in excess of 10^3 sec results for the density of a 100 sq. km. cloud to decrease by a factor of two.

There are two factors which set upper limits to the time during which the required ionization can be produced. Aurorae are observed to drift northerly at a rate of about 100 m sec^{-1} which indicates a time limit of about a minute for a 10 km region. In addition, the time to rise and fall 5 km freely under gravity is also a minute. Hence, the maximum time for deployment of the necessary ionization is of order 60 sec yielding a power requirement of only 40 kwatt for 100 % efficiency of conversion of energy into ionization. In a chemical release there is no power requirement and the electron creation rate criterion is essentially inappropriate.

(iii) Creation of Electron Clouds in the Lower Ionosphere

We briefly discuss several possible methods which might be used to produce large electron clouds in the lower ionosphere.

a./ Production of Electron Clouds by Chemical Means

There are two aspects to the problem of creation of large electron clouds by chemical means. First is the problem of creating sufficient numbers of electrons per gram of chemicals while the second problem is that of distributing the ionized material over the desired 2×10^3 km^3 volume.

Small electron clouds about a kilometer in diameter around 120 km in altitude and having densities of order 10^6 cm^{-3} have been produced by exploding small canisters containing an alkali

metal. In a series of experiments summarized by Marmo, et al [1961], 50 moles of an alkali compound typically produced 10^{21} electrons for an overall yield of 3×10^{-5} electrons per atom. The primary reason for such low yields is that the canister used burst at around 300-500 atmospheres after only 3-5 % of the chemical had reacted. The thermal coefficient of ionization (the number of electrons per reacted atom) was given as 10^{-3} after the rapid expansion at the thermal speed to the ambient pressure produced a cloud about 200 m in radius. If the chemical had undergone complete reaction (implying 5000 atm pressure), the temperature would have been higher yielding more electrons per atom in addition to increasing the number of atoms reacted. Assuming a nearly 100 % reaction and the same thermal yield results in a figure of 10^{-3} electrons per atom as a reasonable overall efficiency coefficient including recombination during the expansion. Since we require for our purposes about 2 moles of electrons, the weights of chemicals necessary is of order 300 kg, which is within the limits of feasibility for a modest sized program. Rosenberg and Golomb [1963] have reported a chemical yield of near 100 % by adding a high explosive to cesium nitrate and aluminum. Best estimates indicate that around 2.5×10^{22} electrons were produced by detonating 18 kg mixtures at high altitude indicating that for our purposes we would require around a 700 kg payload.

More recent investigations [Friedman, et al, 1963; Friedman and Macek, 1965] have reported much higher electron yields per gram of reactant achieved by burning strands of compressed material rather

than by exploding canisters. Theoretical thermodynamic estimates predict yields for both systems on the order of 10^{20} electrons gm^{-1}. Experimental results obtained in the laboratory by Friedman, et al [1963] indicate that actual yields from the cesium nitrate and aluminum mixture were below the theoretical estimates by about a factor of four. Friedman and Macek [1965] reported experimental results almost an order of magnitude below theoretical estimates for the tetracyanoethylene, hexanitroethane and cesium azide mixture primarily because the actual temperature was below the assumed adiabatic value and the presence of unburned CN readily attached electrons. In summary, indications are that around 50 kg of material is sufficient to produce the necessary 10^{24} electrons for our purposes, an order of magnitude below the amount required by detonation.

We now turn our attention to the problem of spreading the desired ionization over the large volume required. In the earlier burst releases at high altitudes, the neutral clouds which were produced were observed to expand by diffusion to a size of 1 or 2 km in a minute. The electrons diffused more slowly and maintained a density of order 10^{6} cm^{-3} which was observed to persist for 10^{3} seconds. An ambipolar diffusion coefficient for the charged particles at 115 km is indicated to be about 5×10^{6} cm^{2} sec^{-1}. However, we cannot achieve our goals by just scaling up the number of electrons and the volume by a factor 10^{3}. If the electron diffusion is fast enough to spread itself over the desired volume in

a time of order one minute, the magnetic field lines will not be tied by the resulting ionization. If, on the other hand, the electrons expand rapidly without diffusing, they are essentially moving field lines aside. It is possible that turbulent diffusion could be relied upon to distribute the charge component of the cloud rapidly and still allow the ionization to effectively tie down the magnetic field lines after its dispersal. The mixing of the ionized material must be accomplished by using a large number of small electron sources. Each of the smaller electron clouds thus produced could rapidly diffuse to produce a large volume of ionized air through which the magnetic field cannot move freely. Approximately twenty-five such clouds with a 1 km radius would be a minimum requirement for covering a 100 sq. km area with sufficient ionization. The scattering and ignition of a large number of chemical sources of electrons via a rocket payload should not be a difficult problem.

b./ Ionization of Air Using a High Energy Electron or Ion Beam

High energy electron beams provide the most efficient method of producing ionization. Each high energy electron expends only 32 ev in ionizing an air molecule and hence, a 100 Kev electron beam will produce approximately 3×10^3 ion-electron pairs resulting in an overall efficiency of 45 % or a requirement of less than an ampere of current for a minute. From the standpoint of a low power requirement and the fact that the technology of

electron guns is very advanced, the use of electron guns seems very promising. There is a possible charging problem in that a rocket which emits an electron current must reach some positive potential in order to attract to it an equal current from the surrounding medium. A preliminary investigation [Linson, 1967] indicates that a few kilovolts is sufficient and hence the beam energy is not significantly degraded. If more than one rocket is used, charging considerations are even less of a problem. A more serious and fundamental objection arises in that the earth's magnetic field limits the excursion of the beam perpendicular to the field. The gyro-radius of a 100 Kev electron in a 1/2 gauss magnetic field is only 20 meters. While the rocket trajectory can be used to cross field lines in one dimension, it seems possible to produce only a thin vertical sheet of ionization but not a cubic volume of order 10^3 km^3. The only way of overcoming this limitation would be to use a number of rockets spaced close to each other so that these sheets of ionization could diffuse rapidly into each other. Based on the previously mentioned diffusion rates, four or five such sheets could be sufficient.

The advantage of an ion beam over an electron beam for creating a large volume of enhanced electron density is that its gyro-radius in the earth's magnetic field is larger, but it suffers from the relative disadvantage of a shorter range and a smaller fraction of its energy going into ionization. We shall show that, unlike electrons of comparable energy, the principal energy loss

of a heavy ion at and below the several hundred kilovolt range is due to elastic collisions with neutrals which determines its range and results in the major part of its energy being used to heat the air. The charging problem is much less severe than in the case of an electron beam as a flux of low energy electrons can easily neutralize an ion beam.

The gyro-radius of an ion with M proton masses at an energy of E ev is

$$r_G = 2.9\sqrt{M \cdot E}\ \text{m} = 0.91\sqrt{M\left(\frac{E}{10^5}\right)}\ \text{km.}$$

For an ion of order 100 Kev, a minimum mass of $M \cong 7$ is indicated for a gyro-radius of about 2.5 km. A spinning rocket could ionize air in a circle with a diameter about 4 r_G by shooting tangentially instead of radially. A larger area could, of course, be ionized by using additional rockets simultaneosuly. The upper limit to the energy range which we consider for an ion beam is set by the limitations of ion gun technology. Breakdown considerations suggest that energies substantially greater than 200 Kev are impractical.

Ions with energy E less than $E_c = 28 \times M$ Kev have velocities less than that of the least bound (15 ev) electron in the N_2 molecule. At such velocities ions are not efficient ionizers and their principal energy loss is due to elastic collisions with neutrals. Experimental information on elastic scattering and ionization cross

sections of heavy ions at energies below E_c is presently meager but an area of increasingly active research. It is generally true that the elastic cross-section is a decreasing function of energy and is lower by more than one order of magnitude than that of typical ionization cross-sections which are increasing functions of energy below E_c. However, the energy loss in an elastic collision between heavy particles far exceeds the mean energy transferred in an ionizing collision. Indeed, we find that the energy loss rate, $\frac{dE}{ds}$, and hence the range, $R(E)$, of a heavy ion is determined predominantly by its elastic collisions. The total number, $N(E)$, of ion-electron pairs produced by a single ion is easily determined from a knowledge of the mean free path, $\ell(E)$, between ionizing collisions by the formula

$$N(E) = \int_0^E \frac{1}{\ell(E')} \frac{ds}{dE'} dE' \quad . \qquad (3.1)$$

In order to obtain quantitative expressions for these variables, we have turned to a theory for elastic cross-sections due to O.B. Firsov [1958] and another theory for inelastic or ionizing cross sections [Firsov, 1959] by the same author. In the Appendix we discuss these theories, indicate their limitations and evaluate the mean energy loss in an ionizing collision and the mean free path $\ell(E)$ which allows us to evaluate the integral given

by Eq. (3.1). Estimates of the range are also carried out in the Appendix and are shown in Fig. A. 1 for an ion traveling through air at a density of 1.4×10^{12} cm^{-3}, typical for 115 km. The results of the calculations give the number of electrons produced as a function of energy and atomic number of the energetic ion. Some representative examples are shown in Fig. 2 from which we find that the number of ion-electron pairs produced per incident ion of atomic number Z and energy E ev in the 100 Kev range is given very closely by

$$N(E) \cong 400 \left(\frac{19}{Z}\right) \left(\frac{E}{10^5}\right)^{1.37} . \qquad (3.2)$$

Table I shows the results of the calculations for Cs^+ and Na^+. The general statement which one can make is that there is a distinct advantage in using small Z both from the standpoint of increased range and efficiency for producing ionization.

In the calculations in the Appendix we have neglected the effect of secondaries, double ionization, and stripping, each of which will increase the number of electrons produced. In particular, secondaries (both ions and electrons) can significantly increase the number of ion-electron pairs produced by as much as a factor of two or more in some cases. The energy loss due to ionization has also been neglected as being small; this approximation is worse for the more efficient low Z ions. It should also be stressed that

Firsov's theory does not include any effects peculiar to the particular interacting pairs which depends on atomic structure. For instance, it is known experimentally that alkali ions ionize noble gases nearest them in atomic number more easily than the theory predicts [Flaks, et al, 1966]. In addition, there are peculiarities which the theory cannot anticipate, such as the fact that Na^+ is a less efficient ionizer than would be expected [Flaks, et al, 1966]. However, Firsov's [1959] theory does show general agreement with experimental results; a comparison of its predictions with experimental values is shown in Fig.A.2. There is no reason to choose alkali ions over any others; the choice of ion should depend on practical considerations such as ease of operation in a high voltage gun. It is obvious that higher energy at the same power is desirable both from the point of view of increased range and efficiency.

The use of an ion beam would require rockets. The payload is primarily determined by the weight of the energy storage devices. If an efficiency of 10 % can be achieved, the figures given in the introduction indicate a minimum energy requirement of 2.4×10^7 joules. Present day technology indicates that a storage capacity approaching 10^5 joules/lb for special energy cells which can discharge their energy at a kwatt/lb is attainable. The minimum payload is thus indicated to be around 250 lbs without considering the practical aspects of energy storage and release and the equipment necessary for the creation of a high energy ion beam. Such a small payload makes this suggestion an interesting possibility.

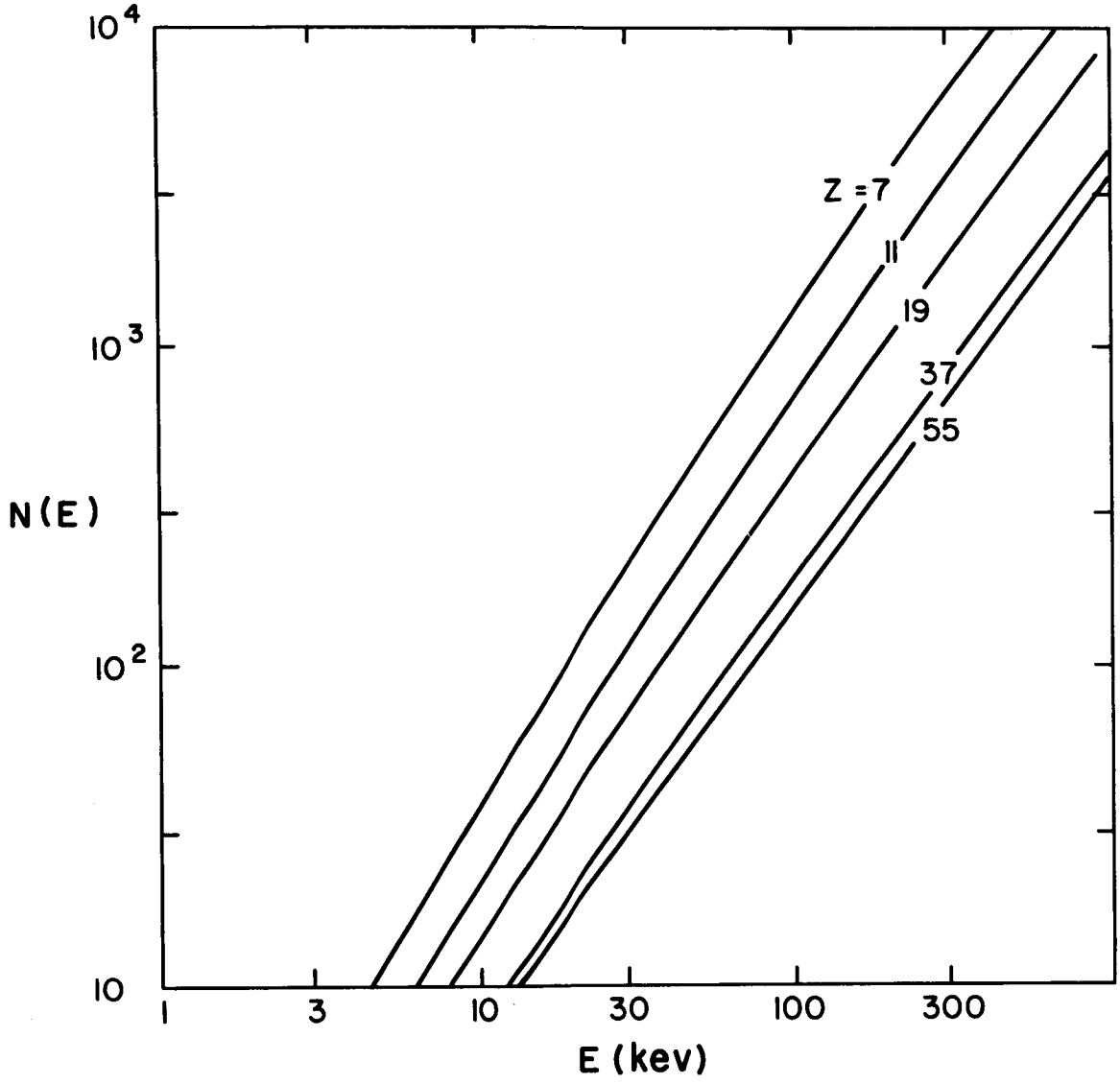

Fig. 2 Number of electrons produced by each ion as a function of energy for several representative ions.

Table I. Characteristics of Heavy Ion Ionization

Energy	Ion	Range	Larmor Radius	Ion - e^- pairs	Energy/ electron	Efficiency
E ev	Z	$\sim .19 \frac{(Z+7)^{4/3}}{Z^2} \left(\frac{E}{10^5}\right)$ km	$.91\sqrt{M\left(\frac{E}{10^5}\right)}$ km	$\sim 400\left(\frac{19}{Z}\right)\left(\frac{E}{10^5}\right)^{1.37}$		$\sim \frac{114}{Z}\left(\frac{E}{10^5}\right)^{0.37}$ %
100 Kev	Cs^+	1.5 km	10.5 km	150	670 ev	2.2 %
100 Kev	Na^+	7.1 km	4.5 km	700	140 ev	10.5 %

c./ Ionization of Air Using Electromagnetic Radiation

We are uncertain about the prospects of breaking down air at a pressure p of 4×10^{-5} mm Hg (the pressure at 115 km) and will confine ourselves to a few remarks which seem pertinent. The plasma frequency in an electron cloud of n electrons cm^{-3} is $f_p = 9 \times 10^3 \sqrt{n}$ cps. Radiation at frequencies f between $f_e = 1.3 \times 10^6$ cps which is the electron gyro-frequency in a magnetic field of 0.46 gauss and 9×10^6 cps which is the plasma frequency is reflected from an electron cloud of 10^6 cm^{-3} and cannot be used to break down air. Hence, we consider the two cases of radiation above and below these limits separately. Another important parameter is the elastic collision frequency of electrons with neutrals which is given approximately by $\nu \sim 3 \times 10^8$ p.

It appears that frequencies above 9 Mc are impractical. If a transmitter is carried by a rocket, breakdown would be most likely to occur near the transmitter where field strengths are the highest. Thus, a local, high density, electron cloud would be produced which would no longer absorb additional radiation when its plasma frequency exceeded the operating frequency. Transmission from the ground is also impractical as the most efficient energy transfer to the electrons occurs when the operating frequency is equal to $\nu/2\pi$. But this condition would be met at or below an altitude of 60 km for $f > 9 \times 10^6$ cps. Again, the air would break down (if sufficient power were transmitted) at lower altitude than desired and the resulting electron cloud would increase in density

until it would reflect the incident radiation.

In a magnetic field, a right-hand polarized wave commonly called a whistler due to its dispersion characteristics, can propagate below the plasma frequency if it is also below the electron gyro-frequency which is 1.3×10^6 cps for the ionosphere. The appropriate dispersion relation for whistlers, valid for frequencies above the ion gyro-frequency (about 400 cps), propagating at an angle θ with respect to the magnetic field, and obeying the condition $f_e^2 \sin^2\theta << 2|f_p^2 - f^2|$ is [Stix, 1962]

$$(kc)^2=(2\pi f)^2\left[1+\frac{f_p^2}{f(f_e\cos\theta-f-i\frac{\nu}{2\pi})}\right]\sim(2\pi f)^2\left[1+\frac{f_p^2}{f(f_e\cos\theta-f)}+i\,\frac{f_p^2\nu}{2\pi f(f_e\cos\theta-f)^2}\right] \tag{3.3}$$

where the last expression is appropriate for $\nu << 2\pi(f_e\cos\theta - f)$. In Eq. (3.3) c is the speed of light and k is the complex wave number. At 10^6 cps the free space wave length is 300 m and waves traveling within 40° of the magnetic field can propagate. The above dispersion relation tells us that the absorption of wave energy is increased as the operating frequency approaches the gyro-frequency from below. The absorption is also proportional to the ambient electron density and inversely proportional to the atmospheric neutral density. This fact indicates that if transmission is from the ground, maximum absorption takes place at the lower edge of the

ionosphere (around 100 km) where $f_p \sim 10^6$ cps and $\nu \sim 10^5$. From Eq. (3.3) we obtain a typical absorption distance as

$$(\text{Im } k)^{-1} \sim \frac{2c(f_e \cos - f)^{3/2}}{\nu f_p \sqrt{f}} \sim 1 \text{ km}$$

for waves traveling parallel to the magnetic field at a frequency of 10^6 cps. As the electron density increases above 10^4 cm^{-3} this distance decreases which makes it difficult to penetrate the ionosphere significantly at modest power levels. A lower transmitting frequency increases the penetration but is difficult to focus due to its large free space wavelength.

The above considerations indicate that it would be difficult to create ionization at the desired altitude by electromagnetic radiation. We have not considered the problem of the coupling of the radiation into the ionosphere which is important as the power which is actually absorbed is reduced if the radiation is predominantly reflected from the bottom of the ionosphere. The possibility of irradiating the ionosphere from above where the collision frequency is less has not been investigated. Furthermore, we have not considered the important problem of breakdown of the air or the efficiency with which the absorbed radiation is converted into ionization. The possible use of electromagnetic radiation to accomplish our goal requires further study.

(iv) Summary

From what we have presented here, it seems as though it may be possible to produce sufficient numbers of free electrons on a large enough scale in the lower ionosphere to have geophysical effects. The efficient use of payloads of the order of hundreds of kilograms may achieve the ultimate goal of triggering an aurora. The most likely method for production of these electrons at 115 km appears to be by chemical deployment or with the use of high energy electron or ion beams. The principal advantage of chemical releases is their simplicity. Alkali clouds also have the added advantage of having a significantly smaller recombination coefficient which results in a longer lifetime for the electrons. The use of electron beams probably would require more than one rocket in order to spread the ionization out over the required area. The efficiency of ion beams is increased by the use of ions of lower atomic number and higher energy. Increasing the energy of the beam not only increases its overall efficiency but also increases its range which allows more flexibility for operation at slightly lower altitudes. The possibility of using electromagnetic radiation in the radio frequency range needs to be investigated further.

It is possible that increased coupling of the magnetic field lines to the ionosphere could be obtained by producing ionization at lower altitudes. In support of this it has been reported that the lower edge of discrete aurora usually lies in the range of 100 ± 10 kilometers. The practical limitation for the maintenance of

ionization is set by the decreasing lifetime of the electrons as one moves to lower altitudes. One would have to rely on initiating increased precipitation in order to maintain the ionization. Since the e-folding distance for the exponential atmosphere is 7 km, the use of high energy heavy ions for producing ionization much below the altitudes we have been discussing becomes impractical due to their shorter range. The use of chemical releases then appears to be the most promising method of producing large numbers of electrons at lower altitudes, but their successful deployment becomes more difficult due to slower diffusion.

ACKNOWLEDGEMENTS

We gratefully acknowledge useful discussions with Dr. C. Kennel and F. Coroniti.

This work was supported by the National Aeronautics and Space Administration, in part under Contract No. NASw-1400 and in part by the Environment Modification Study Group.

(v) APPENDIX

We apply the theories of O.B. Firsov in order to obtain estimates for the elastic [Firsov, 1958] and ionization [Firsov, 1959] cross sections so that the integral given in Eq. (3.1) can be evaluated to give the total number of electrons produced by an energetic ion. In the following we consider collisions of an arbitrary ion $Z \geq 7$ with a nitrogen atom ($Z = 7$, $M = 14$). For elastic scattering, Firsov [1958] gives the expression*

$$\sigma_{el}(E) = 6.7 \times 10^{-16} \frac{Z(M + 14)}{(Z + 7)^{1/3}} \frac{1}{E} \left[\frac{E_o}{E} \ell n\left(1 + \frac{E}{E_o}\right)\right] cm^2 ,$$

$$E > E_{min} = 0.34 \cdot Z \cdot (Z + 7)^{1/3}(M + 14) \text{ ev} \sim 10\left(\frac{Z}{54}\right)^{7/3} \text{kev} \qquad (A.1)$$

$$E_o = 21 \times Z(Z + 7)^{1/3} (M + 14) \text{ev} \sim 100 \left(\frac{Z}{24}\right)^{7/3} \text{kev} .$$

---

* Firsov introduces the function $\psi(Z_1, Z_2) \sim (Z_1^{2/3} + Z_2^{2/3})^{1/2}$. We find that ψ differs by less than 2 % from $1.1(Z_1 + Z_2)^{1/3}$ for $1 < Z < 56$ and we use the simpler expression in the following equations.

The factor in brackets is unity for $E < E_o$ while for greater energies it gives the more rapid decrease than E^{-1} in the elastic cross section due to the coulombic character of the nuclear scattering. For $E < E_{min}$ the cross section rapidly approaches its gas kinetic value. The mean energy loss for elastic scattering is $2M_T M(M_T + M)^{-2}E$ where M_T is the mass of the stationary target particle. If the elastic scattering is assumed to be due to a hard sphere of cross sectional area given by Eq. (A.1), we easily obtain an energy loss rate roughly independent of energy of

$$\frac{dE}{ds} = 3.8 \times 10^{-14} n \frac{Z}{(Z + 7)^{1/3}} \frac{M}{M + 14} \left[\frac{E_o}{E} \ell n\left(1 + \frac{E}{E_o}\right)\right] ev\ cm^{-1} \qquad (A.2)$$

where n is the density of neutral molecules ($= 1.4 \times 10^{12}$ at 115 km). Molecular scattering has been taken into account by doubling the atomic cross section given by Eq. (A.1). Neglecting the slowly varying factor in brackets, we obtain a pessimistic estimate for the range of a heavy ion at 115 km of

$$R = 0.19 \frac{(Z + 7)^{1/3}}{Z} \frac{M + 14}{M} E \text{ meters} \qquad (A.3)$$

which is shown plotted as a function of Z in Fig. A.1. Note the substantial increase in range for $Z < 20$. The plot is shown for $Z \geq 7$ as Firsov's statistical theory is valid only for many electron atoms.

For ionizing collisions, Firsov [1959] calculates the energy transferred to the electrons in a single ionizing collisions between heavy atoms or ions to be

$$\mathcal{E} = \frac{x\mathcal{E}_i}{[1 + 0.304(Z + 7)^{1/3}r]^5} \text{ ev} \qquad (A.4)$$

where r is the impact parameter in $\mathring{A}$, $\mathcal{E}_i$ is the ionization energy of the least bound electron which we take to be 15 ev, and x is the ratio of the velocity of the ion normalized by a characteristic velocity which can be expressed in terms of the energy as

$$x = \frac{5.94 \times 10^{-2}(Z + 7)^{5/3}}{\mathcal{E}_i}\sqrt{\frac{E}{M}} \sim \frac{1}{6}(Z + 9)\sqrt{\frac{E}{10^3}} \qquad (A.5)$$

$x \cdot (E \times 10^{-3})^{-\frac{1}{2}}$ is shown in Fig. A.1 as a function of Z. There is a lower limit to the energy for which we can expect Firsov's theory to be realistic as he assumes rectilinear motion for the nuclei. The maximum energy transferred in an ionizing collision is xE_i according to Eq. (A.4). If we arbitrarily demand that the incoming ion must itself have 5 times this energy in order to apply the theory, we obtain a minumum value of x given by

$$x_{min} = \frac{1.18 \times 10^{-3}\ (Z + 7)^{10/3}}{M} \qquad (A.6)$$

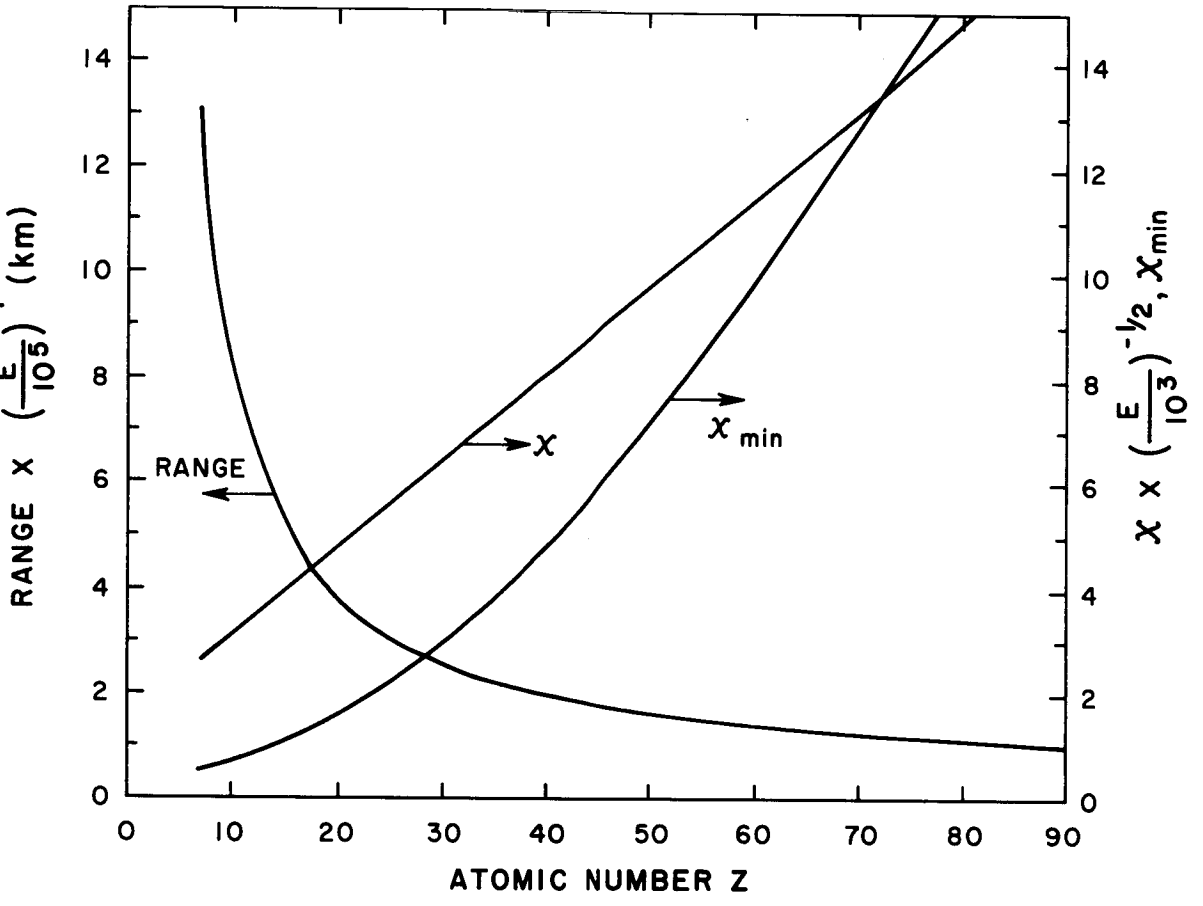

Fig. A.1 Range of a 100 kev heavy ion of atomic number Z according to Firsov's [1958] theory. On the right-hand scale are shown the parameter x for a kev ion defined by Eq. (A.5) and the minimum value of x for the validity of the theory for the inelastic cross section [Firsov, 1959].

below which we cannot expect the theory to be accurate. x_{min} is also shown as a function of Z in Fig.A.1 where the corresponding critical energy is seen to vary from around 100 volts for low Z to around 1.5 Kev for heavy ions.

Firsov obtains a universal curve for ionizing collisions by arguing that as long as the minimum ionization energy is transferred, an electron will be ejected by the Auger process with a high probability. Setting $\mathcal{E}$ equal to $\mathcal{E}_i$ in Eq. (A.4) and solving for πr^2, we obtain Firsov's [1959] expression which when multiplied by two gives for the molecular ionization cross section

$$\sigma_i = 8 \times 10^{-16} \left(\frac{25}{Z+7}\right)^{2/3} [x^{1/5} - 1]^2 \text{ cm}^2 \quad . \qquad (A.7)$$

In recent years there has been increased experimental activity in measuring cross sections for various interactions involving heavy ions in the Kev range. We show in Fig. A.2 a typical comparison [Flaks, et al, 1966] of experimental values involving several combinations of incident and target particles with Firsov's universal curve. It seems as though the Firsov cross section predicts roughly the dependence on velocity and is within a factor of two of measured values for large energies. We shall make use of his expression for our analytic calculations.

We are now in a position to evaluate the mean energy loss $\bar{\mathcal{E}}$ in an ionizing collision as a function of x. After a simple calculation we obtain

$$\bar{\varepsilon} = \frac{x^{3/5} + 2x^{2/5} + 3x^{1/5} + 4}{10} \varepsilon_i \qquad (A.8)$$

which is shown plotted in Fig. A.3. Since at worst only a few times the ionization energy is lost per ionizing collision, we see that heavy ion ionization is a relatively efficient process. The limitation which occurs is that elastic collisions are responsible for the energy loss of heavy particles.

Knowing the ionization cross section from Eq. (A.7) and the energy loss rate from Eq. (A.2), we can calculate the number of electrons produced by each primary heavy ion by using Eq. (3.1). The result can be given in the form

$$N(E) = \frac{(M + 14)E}{M \cdot Z \cdot (Z + 7)^{1/3}} F(x); \quad F(x) = 0.147\left([x^{1/5} - 1] + \frac{1}{5} - \frac{2x^{1/5}}{11}\right) \qquad (A.9)$$

which is shown as a function of energy for some representative ions in Fig.2. This calculation of N(E) has neglected the contribution to the total number of electrons produced by secondaries (both ions and electrons) and has neglected the contribution of the energy loss due to ionization as being small compared to the elastic energy loss.

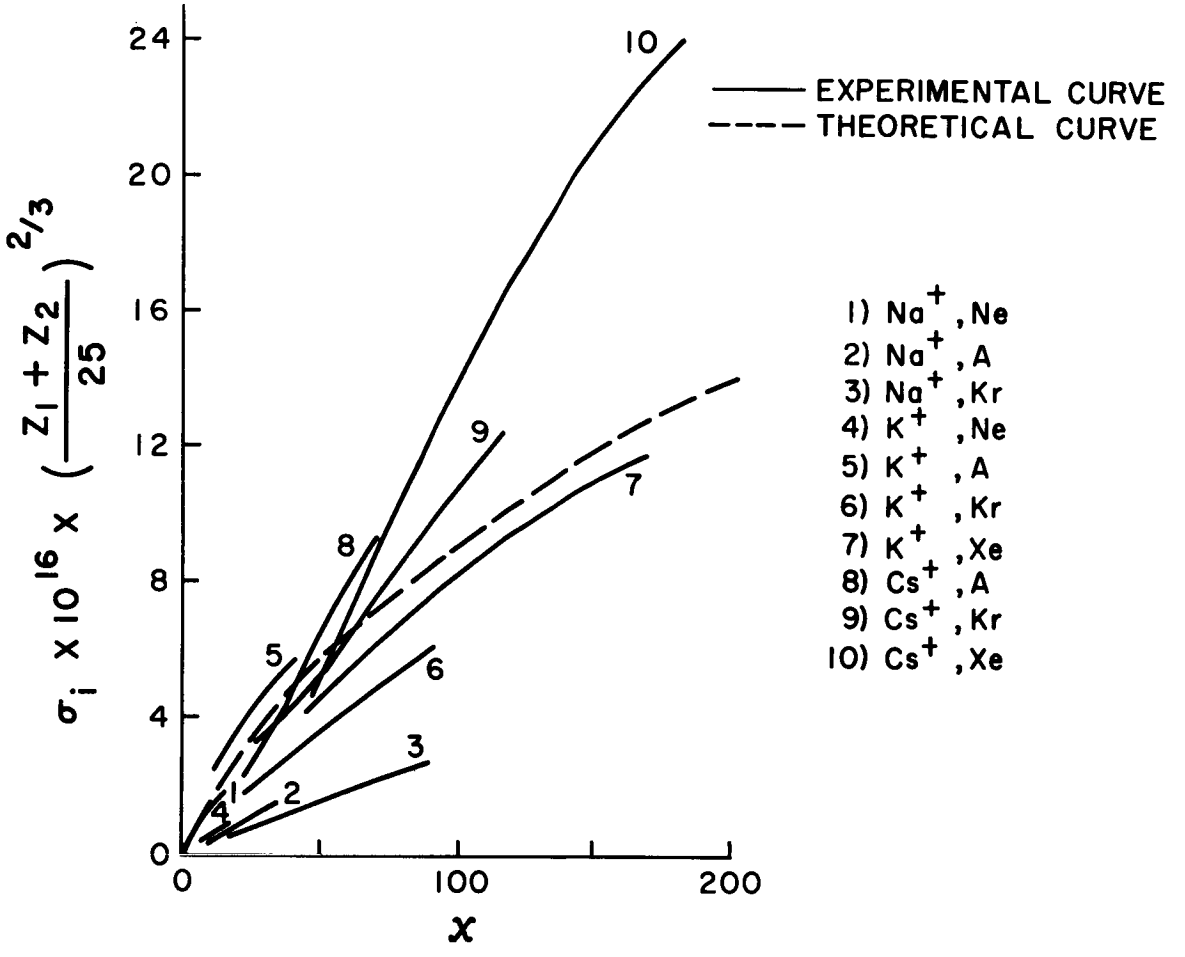

Fig. A.2 Comparison taken from Flaks, et al [1966] of experimentally measured ionization cross sections for various interacting species with the universal (dashed) curve due to Firsov [1959].

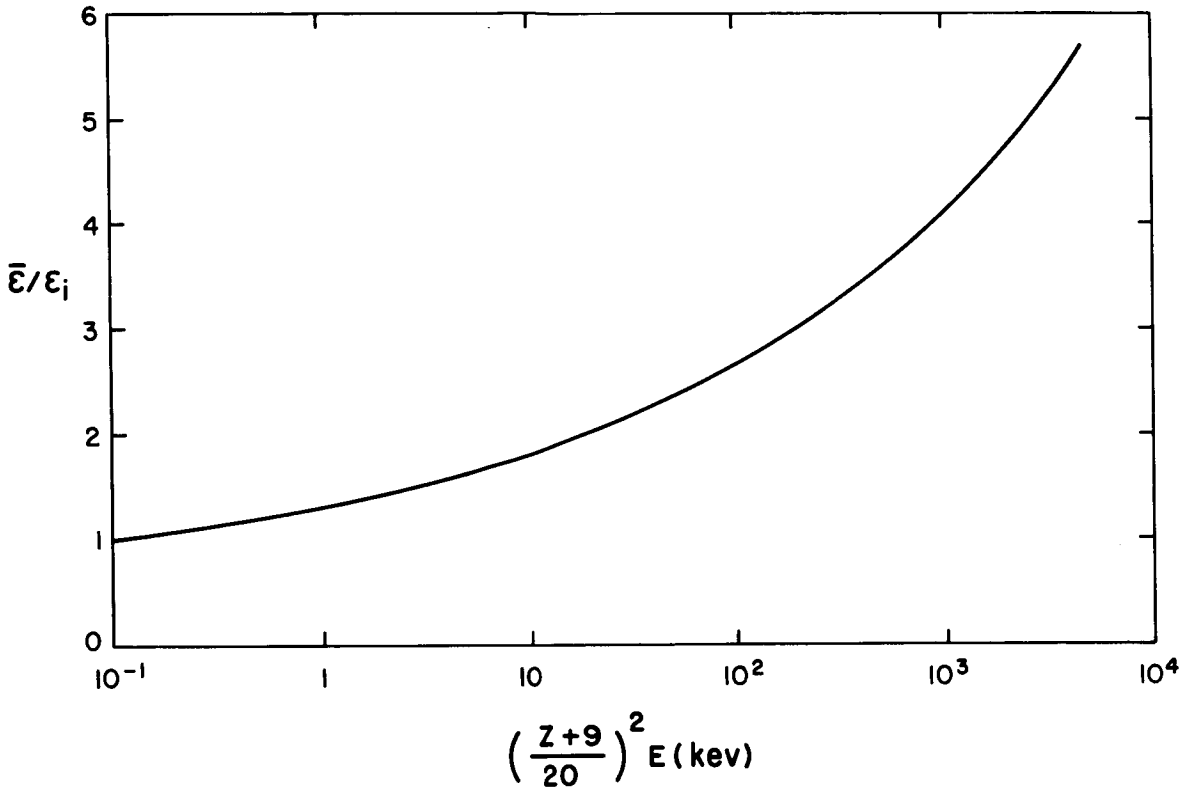

Fig. A.3 Mean energy transferred in an ionizing collision as a function of energy according to the theory of Firsov [1959].

REFERENCES

Axford, W.I., Petschek, H.E. and Siscoe, G.L., "Tail of the Magnetosphere", J. Geophys. Res. 70, 1231-1236, 1965.

Baker, K.D. and Ulwick, J.C., Paper GA72 presented at the 48th Annual Meeting of the Amer.Geophys.Union in Washington, D.C., April 17-20, 1967.

Boström, R., "A Model of the Auroral Electrojets", J. Geophys.Res. 69, 4983-4999, 1964.

Firsov, O.B., "Scattering of Ions by Atoms", Sov.Phys. JETP 34, 308-311, 1958.

Firsov, O.B., "A Qualitative Interpretation of the Mean Electron Excitation Energy in Atomic Collisions", Sov.Phys. JETP 36, 1076-1080, 1959.

Flaks, I.P., Kikiani, B.I. and Ogurtsov, G.N., "Ionization of Gases by Alkali Ions", Sov.Phys.Tech.Phys. 10, 1590-1595, 1966.

Friedman, R., Fagg, L.W., Millar, T.K., Charles, W.D. and Hughes, M.C., "Study of Electron Generation by Solid Propellant Technique", in Progress in Aeronautics and Astronautics, Vol. 12, pp. 379-393, Academic Press, 1963.

Friedman, R. and Macek, A., "A Novel Chemical System for Generation of Electron-Rich Gases", Tenth Symposium (International) on Combustion, pp. 731-741, The Combustion Institute, 1965.

Hinteregger, H.E., Hall, L.A. and Schmidtke, G., "Solar XUV Radiation and Neutral Particle Distribution in July 1963 Thermosphere", Space Research V, pp. 1175-1190, North-Holland, 1965.

Linson, L.M., "Spherical Probe Characteristics at Large Positive Potentials in a Magnetic Field", Paper 5C-8 presented at Ninth Annual Meeting of the Division of Plasma Physics, Austin, Texas, November 8-11, 1967 (to be published).

Marmo, F.F., Pressman, J. and Aschenbrand, L.M., "Electron Clouds: A General Survey", Planet Space Sci. 3, 139-157, 1961.

Rosenberg, N.W. and Golomb, D., "Generation and Properties of High Altitude Chemical Plasma Clouds", Progress in Aeronautics and Astronautics, Vol. 12, pp. 395-408, Academic Press, 1963.

Stephenson, S. Town, "The Continuous X-Ray Spectrum", Handbuch der Physik 30, 337-370, 1957.

Stix, T.H., The Theory of Plasma Waves, pp. 38-40, McGraw-Hill, 1962.

6. STUDY OF MAGNETOSPHERIC ELECTRIC AND MAGNETIC FIELDS BY TRACER TECHNIQUES

Edward W. Hones, Jr.

University of California, Los Alamos Scientific Laboratory

Los Alamos, New Mexico

(i) Introduction

One of the great hindrances to the attainment of a full understanding of the particle population in the magnetosphere has been the inability to make measurements of the electric fields (both periodic and quasi-static) in the magnetosphere. By contrast, it has been possible to measure the magnetic fields in space and consequently the magnetic structure of the magnetosphere is known in quite some detail, though even here, lack of precise knowledge regarding the path followed by a magnetic field line poses difficult problems in magnetospheric physics.

Electric fields have, in the past, been inferred from ionospheric current systems. Two basic current systems are the S_q system and the DS system. The S_q was early suspected to be driven by tidal motions in the ionosphere caused by the sun's heating of the atmosphere. A dynamo theory for this current system based on such a model has evolved and explains the observed current system with considerable accuracy.

By contrast, the source of the DS system is not yet understood though for many years it has been suspected that it results in

some way from the action of the solar wind upon the outer regions of the magnetosphere. The S_q system is strongest at low and middle latitudes, while the DS system exists at auroral and high latitudes. The DS system is intimately related to the many phenomena -- visual aurorae, magnetic activity, cosmic radio noise absorption, etc., observed in the auroral zone.

In the last several years techniques for measuring electric fields by measuring the $\overline{E} \times \overline{B}/B^2$ drift of clouds of barium ions have been developed and some measurements of electric fields at low latitudes and at auroral latitudes have been made. Furthermore, there have been efforts to measure electric fields by electronic methods from rockets and satellites and there appears to be some hope that such techniques will ultimately enjoy considerable success.

This paper will deal with the magnetic field and the quasistatic electric fields in the magnetosphere, the present state of knowledge regarding them, and various techniques for studying them. The discussion will be concerned with fields associated with higher latitudes, partly because the nature of the fields here is more complex than at lower latitudes and partly because it is in this region that the initial phases of the solar wind's interaction with the magnetosphere occur.

(ii) The Magnetic Field of the Magnetosphere

The magnetic field measurements made by satellites within the magnetosphere have been of great value in development of knowledge of magnetospheric structure. They have revealed something of

the nature of the magnetopause, they have revealed the neutral sheet and other features of the structure of the tail, they have shown significant inflation of the magnetic field to occur at distances rather close to the earth (3 to 4 R_e) in quiet times. However, the measurements leave unanswered a question which is of great importance in developing an understanding of a variety of geophysical phenomena -- particularly high latitude phenomena; what path does a line of force follow through the magnetosphere between its intersections with the earth? As some examples: at what magnetic latitude in the noon meridian plane is the division between lines that cross the equator in the noon meridian and those that are swept back into the tail? What are the paths of field lines which emanate from the auroral oval? Where do lines of force which pass through the neutral sheet in the tail touch the earth? These are typical of the questions which are asked repeatedly in efforts to decide among various modes of solar wind-magnetosphere interaction which have been proposed.

It is certain that the field line configuration varies with time due to changing conditions in the solar wind and to the changing orientation of the earth's magnetic axis. So one wants to be able to trace field lines at many locations in quick succession and to do so over extended periods of time.

(iii) <u>The High Latitude Electric Fields</u>

Until very recently no direct measurements of the electric fields in the magnetosphere had been made. Knowledge of the quasi-

stationary electric fields was derived from ionospheric current systems, which, in turn, were deduced from magnetic perturbations observed at the ground. Electric fields derived in this manner are subject to many uncertainties: The magnetic perturbations are measured by a few (10 to 20) stations and the equivalent current system is produced by interpolation between these widely scattered stations; currents are generally assumed to be confined to a thin sheet in the ionosphere, whereas it is likely that currents flow, also, along lines of force; electric fields in the ionoshpere are deduced from the currents by making use of the computed integrated conductivity which is a complex altitude-dependent mixture of Hall and Pedersen conductivities; extrapolation of ionospheric electric fields to the distant magnetosphere is usually done assuming that the electric field along the magnetic lines is negligible.

The difficulties of deriving the magnetospheric electric fields from the high latitude current system can be illustrated by noting the uncertainty associated with the very first step of the procedure, namely the deduction of the equivalent current system in the ionosphere from magnetic activity. Figure 1 (from Akasofu et al, 1965) shows two such current systems. The earlier one, A , is a two cell system, having a strong westward electrojet in the post-midnight hours, and a strong eastward electrojet in the pre-midnight hours, each with its system of return currents. The newer model, B , has a single westward electrojet flowing through the entire auroral oval, being most intense near midnight. When translated into

magnetospheric electric fields these two current systems lead to distinctly difference concepts regarding the interaction of the solar wind with the magnetosphere. System A suggests that solar wind plasma enters the distant tail of the magnetosphere and flows forward toward and around the earth nearly symmetrically. System B , on the other hand, suggests that solar wind plasma enters the afternoon-evening section of the magnetosphere, flows behind the earth and out through the morning section of the tail.

The need for more direct means of determining magnetospheric electric fields is evidently very great. Here again, as with magnetic field line tracing, the time variability of the electric fields makes it imperative that the measuring techniques allow great flexibility -- many measurements should be made in quick succession over large distances. This suggests, of course that measurements from a satellite are generally the most desirable. Aggson (1967) has developed an electronic measuring device and has flown it on a satellite (ATS-1). Though this first attempt did not meet with complete success, there seems to be considerable hope for ultimate success. A basic problem with electric field measurements by electronic means from a moving satellite's motion across magnetic field lines generates an electric field $(- \bar{v} \times \bar{B})$ which can be one or two orders of magnitude greater than the electrostatic fields (perpendicular to the magnetic field) to be measured, depending upon the altitude of the satellite and the direction of the electrostatic field. If there are, in addition, time-varying photo-electric voltages and ram-voltages induced on the

satellite, determination of the magnitude and direction of the ambient electric field may be rather inaccurate.

Releases of barium ions above $\sim$ 200 km altitude have recently provided successful and apparently quite accurate measurements of electric fields in the auroral zone. Foppl et al (1967) reported on the release of barium ion clouds on five successive nights over Kiruna, Sweden. The rockets which carried the barium bombs (to an altitude of $\sim$ 230 km) also carried an instrument which measured the electron density profile through the ionosphere. The observed drift speed and direction of the ion cloud provided a measurement of the electric field (perpendicular to B) and the electron density measurement together with standard values of ionospheric ion and neutral composition provided an indication of the Pederson and Hall conductivities through the ionosphere. From these quantities currents were calculated and were compared with ionospheric currents deduced from magnetic disturbances observed at the ground near the drifting ion cloud. Good agreement was found between the currents deduced from the two independent observations, indicating that the electric fields deduced from the drifting ion clouds were quite accurate.

Despite (or better, perhaps, because of) their success the barium releases just mentioned indicated that a more versatile system for measuring electric fields whose direction reversed within distances of 100 km or less. What is really needed in order to unravel the mysteries of the solar wind - magnetosphere interaction is

the big picture of the electric field -- that is, a snap-shot of an appreciable portion of the whole system taken in a short time (i.e., in a few minutes). For example a latitudinal profile of the field direction and intensity at a given local time would help immensly in deciding whether the electric field pattern is that indicated by current system A or B in Figure 1. and would thus tell a great deal about the flow of the solar wind plasma through the magnetosphere.

(iv) Tracer Techniques

In the above section it has been indicated that tracing of high latitude magnetic field lines and determination of the pattern of electric fields at high latitude are of vital importance of theories of the interaction of the solar wind with the magnetosphere. There are, conceptually, a number of ways to do these measurements. The following is a discussion of the use of barium ions and of positrons as tracers by which the measuremtns might be attempted.

(v) Barium Ion Clouds as Tracers

We shall discuss below, hypothetical experiments in which barium ion clouds, generated by a "barium ion engine" are used as tracers or probes to trace magnetic field lines and measure electric fields in the magnetosphere (Hones, 1965). First, however, we shall discuss some concepts regarding barium ion clouds in general.

The use of barium ion clouds as "probes" to study fields and the behavior of plasmas in space has been pioneered during the past few years by Lüst's group. In a specially designed chemical reactor barium metal and CuO are burned causing something like 5 % of the barium metal to be released as barium atoms with kinetic energy $\approx$ 0.3 ev. These are subsequently ionized (within a few seconds to $\sim$ 100 seconds) by sunlight. The cloud of ions is then visible by scattered sunlight. Such barium clouds have been created at altitudes ranging from $\sim$ 150 km to $\sim$ 2000 km (Haerendel et al, 1967). Following their release, the ion clouds drop downward along the magnetic field lines under the influence of gravity. They also drift across the magnetic field and it has been found that, for clouds above $\sim$ 200 km, where the effect of neutral winds is small, the cross-fields drift is largely an $\frac{\bar{E} \times \bar{B}}{B^2}$ drift and thus is a fairly accurate indication of the magnitude and direction of ionospheric electric fields (Foppl et al, 1967).

Since the barium ion cloud is visible by scattering sunlight and for optimum seeing, must be viewed against a dark sky, its use at low altitudes, i.e., a few hundred kilometers, is limited to the twilight regions of the earth. In tracing magnetic field lines, however, the ion clouds would generally be outside the earth's shadow. They would be seen against a night sky background from any point on earth at which the solar depression angle is greater than $\sim$ 15 degrees. Thus, the only region of the magnetosphere in which field lines could <u>not</u> be traced by barium ion clouds is a cone of $\sim$ 15 degrees half-angle

centered on the sun. So, most regions of interest, including the front neutral points are accesible to line-tracing by barium ion clouds. In measuring magnetic electric fields, it may be necessary, in order to minimize the effect of self-shielding of the cloud, to confine their use to regions no more than $\sim 10^4$ km from the earth where the number density and temperature of the ambient particles are similar to those of the cloud. It is thought that the magnetic field lines are approximate equipotentials over their entire length, so measurement of electric fields at $\sim 10^4$ km, together with knowledge of the paths of field lines outward into the magnetosphere from there would permit mapping of the electric fields in the distant magnetosphere. This restricition of cloud heights to $\sim 10^4$ km does not seriously limit the usefulness of barium ion clouds for electric field measurements because a large fraction of the field lines of interest (particularly the auroral and higher-latitude lines) still would allow placement of an ion cloud in the sunlight against a light sky.

The essential requirement of a barium ion cloud is that it must be bright enough to be observed. We shall find that ion clouds produced by a barium ion engine are not bright enough to be observed photographically so would have to be tracked visually. While this may not be as attractive as photographic tracking, it should yield perfectly adequate measurements because of the repeatability of cloud injections with the barium ion cloud. The rate, α, at which an ion will scatter sunlight is:

$$\alpha \quad \text{(photons/sec)} = \frac{\pi e^2}{m_e c^2} \, f_{mn} \, \lambda^2 \, \phi_\lambda \, u \qquad (1)$$

where e = electron charge

m_e = electron mass

c = velocity of light

f_{mn} = oscillator strength for the transition between levels m and n

λ = wavelength

ϕ_λ = solar photon flux per unit wavelength interval (continuum) outside the earth's atmosphere

u = residual intensity at bottom of the solar Fraunbrofer line.

Once ionized bariums (BaII) has a resonance line at $\lambda = 4554$ angstroms for which the oscillator strength ≈ 1.0. $\phi_{4554} = 5 \times 10^{21}$ $(cm^2 - sec - cm)^{-1}$ and $u \approx 0.2$. These numbers give $\alpha = 1.8 \text{ sec}^{-1}$. The value which has been used by Lüst's group is $\sim 1 \text{ sec}^{-1}$. The latter value will be used in the following discussion though it is uncertain.

The ion cloud, observed visually or photographically through a telescope from the ground, must have at least the brightness of the night sky against which it is observed. Observations would logically be made through a filter. A 30-angstrom bandwidth $\sim$ 60 % transmission is readily attainable (Schklovskii et al, 1960). The night sky background, G, is $\sim 5 \times 10^4$ photons/cm^2-sec-ster-angstrom (Allen, 1955). The intensity of light at the surface of an ion cloud is

$$\frac{\alpha N_{\perp}}{4\pi} \quad \text{photons/cm}^2\text{-sec-ster} \; . \tag{2}$$

where $N_{\perp}$ = number of ions/cm^2-column .

Thus the brightness threshold established by the above criterion requires a value $N_{\perp} = \frac{4\pi \times 30 \times 5 \times 10^4}{1.0 \times 0.6} \approx 3 \times 10^7$ ions/cm^2-column. One must also consider the sensitivity of the detecting instruments. The photon intensity, from a distant ion cloud, at the focus of an imaging device such as the eye, a camera, or telescope is:

$$\frac{N_{\perp}\alpha}{16F^2} \quad \text{photons/cm}^2 - \text{sec} \quad . \tag{3}$$

where, the "F-number" of the device is the ratio of the focal length to the diameter of its objective lens and the other symbols have the same meaning as above. Notice that, for $F \gtrsim 1.0$, equation (3) is about equal to equation (2). That is, the photon intensity at the image is about equal to the surface intensity at the cloud. Since objective lenses with $F \gtrsim 1$ are attainable, we can assume an image brightness equal to the cloud's surface brightness (equation 2) in all subsequent considerations.

A photographic film of high sensitivity requires $\sim 10^9$ photons/cm^2 for an appreciable grain density. We shall find that due

to the smallness of the clouds in the hypothetical experiments to be discussed and the rapidity of their motion, it would be necessary to limit photographic exposure times to $\sim$ 1 sec. This would require that the cloud surface brightness be $\sim 10^9$ photons/cm^2 sec-ster to be photographable.

The eye requires only $\sim 10^5$ photons/cm^2-sec at the retina to discern a diffuse light source in perfect darkness. Thus, the eye, with the help of an imaging system of $F \lesssim 1$ could see, against a perfectly black sky, a cloud of surface brightness $\lesssim 10^5$ photon/cm^2 -sec-ster. This is much less than the brightness 1.5×10^6 photons that the cloud must display to equal the night sky brightness through a 30 angstrom filter.

The essential results of the above discussion are:

(a) The barium cloud must have a brightness at least equal to that of the night sky seen through a 30 angstrom filter, requiring $N_1 \lesssim 3 \times 10^7$ ions/cm^2-column;

(b) The threshold brightness defined by (a) is well above that required for visual observing through a good telescope;

(c) The threshold brightness for photographing the clouds in $\sim$ 1 sec is $\sim 10^9$ photons/cm^2-sec-ster and requires $N_1 \lesssim 10^{10}$ ions/ cm^2-column, a number not attainable with barium ion engines.

(vi) Production of Ion Cloud by Barium Ion Engine

Ion engines have been made which produce close to one ampere of mercury ions of a few Kev energy. The ion beam is made electrically neutral by injecting electrons from a filament near

the exit of the engine. Modifications of such an engine to produce similar beams of barium ions are relatively straightforward and probably could be accomplished for several hundred thousand dollars. Ion engine producing 10 amperes are in the early development stage and these, too, could be modified for barium ion production. Of course, it would be possible to mount several 1-amp engines in parallel to get several amperes without awaiting the development of larger engines. Below, we consider the feasibility of tracing magnetic field lines and measuring electric fields by means of short bursts of barium ions projected in a desired direction relative to the magnetic field from a magnetically-oriented satellite in a polar orbit several hundred to several thousand kilometers above the earth. The ion bursts would be triggered by ground command. This technique offers the opportunity to make many thousands of measurements at desired times and locations during the life of the satellite and satisfies, to a certain extent, the need for extensive field measurements which was discussed in an earlier section of this report.

(vii) Magnetic Field Line Tracing

There are two degrees of sophistication which might be aspired to in studying magnetic field line paths through the magnetosphere. Ideally, one would like to trace out a line in detail, noting its complete path between conjugate points. Such an ideal measurement can be approached by barium in clouds from an ion engine, and will be the principle subject of this section. However, we acknowledge

that, short of the ideal case, it would be very valuable simply to shoot particles (e.g., electrons) up a field line and see whether they return to earth in the opposite hemisphere and in approximately how long, or whether they fail to return to earth. This type of measurement would tell whether the line were open or closed (for the type of particle used) and its approximate length. There are obvious problems associated with detection of the returning particles. These will not be discussed here, however, since this type of magnetic field line "tracing" is not the subject of this paper.

A barium ion cloud, if projected along a field line with enough energy to overcome gravity (> 90 ev) will be free to travel the whole path of the line. To be useful, however, for actual line-tracing experiments the cloud must be visible at the maximum extent of the line and its motion along the field line must be fast compared to the velocity <u>across</u> field lines caused by ambient electric fields. The latter condition requires that ion energies be one Kev or more. Such ions would take about 1000 seconds to reach the equatorial crossing of field lines of interest. In this time typical auroral zone electric fields might move the cloud as much as 10 or 20 degrees in longitude. The ions from the current chemical releases ($\lesssim$ 0.3 ev) are of no use in tracing field lines unless they are released near the maximum extent of the line. This requires carrying the source to high altitude and even then, the clouds's path would be strongly influenced by electric fields due to its small velocity.

Other means of giving barium ions enough velocity to trace field lines are (a) to generate them in an atomic bomb as suggested by Harrison (1962) or to project them upward along the field from a shaped explosive charge, a scheme which is being considered by Lüst's group. The use of a barium ion engine, as suggested here, is a much less violent method and is not a one-shot affair but provides the opportunity for thousands of repetitions from a single vehicle.

We shall now consider the performance of a line-tracing experiment in which a neutralized beam of barium ions is projected up a magnetic field line from a magnetically oriented polar-orbiting satellite at $\sim$ 300 km altitude. The directed energy of the ions is 6 Kev ($v \gtrsim 100$ km/sec) and their thermal energy is 30 ev. Table 1 from Knauer (1967) lists the expected properties of such a beam, powered by solar-cells and rechargable batteries, and thus appropriate for repeated use on a satellite. Figure 2 (Knauer, 1967) is a schematic representation of the source. The transverse energy density of the beam as it emerges from the source is much greater than the magnetic field energy density so the cloud will quickly expand to a larger diameter. The lower limit of this expanded size is that at which the beam's transverse energy density equals the magnetic field energy density. Taking $B = 0.5$ gauss, one finds that the beam will promptly expand to a diameter of $\sim 90\, j^{1/2}$ centimeters, where j is the ion current of the beam in amperes. The electron gyro radius is small compared to this size (i.e., $\sim$ 30 cm) while the ion gyro radius is large

($\sim 1.6 \times 10^4$ cm). The ions are restrained from moving far out of the $\sim$ 100 cm diameter beam, however, by a sheath of positive charge which is quickly formed. Further expansion could come about through various possible diffusive processes. The atmospheric density at 300 km is $\sim 10^9$ particles cm^3, so that collisional mean free path is $\sim 10^7$ cm. Thus, each ion of the beam will suffer only about one collision, and each electron $\sim$ 30 collisions, with the neutral atmospheric particles as they leave the atmosphere. The diffusion of the column due to these collisions is not insignificant and might increase the diameter by a factor of two or more. (This collisional diffusion could be reduced or eliminated, of course, by ejecting the beam at higher altitude.) Diffusion by coulomb scattering among the electrons and ions of the cloud itself is another cause of "collisional" diffusion, and one which might be effective over a greater portion of the cloud's path. However, this can be shown by the methods of Spitzer (1956) to be negligible. Thus, in the absence of other "anomalous" diffusion processes, the cloud would expand initially to a diameter of a few times ($90\ j^{1/2}$)cm, the ions being restrained from executing their full gyro orbits by space change. Anomalous diffusion processes might cause the column to assume a diameter much larger than this, however, and for the present purposes, we assume (we believe, conservatively) that this maximum size will be the ion gyro-diameter, 3×10^4 cm. Below we will present estimates of beam currents required to trace lines based upon these minimum and maximum beam diameters.

TABLE 1

Ba^+ Source and Accelerator

A 20 cm diameter Kaufman thruster, converted from mercury to barium, can be expected to possess the following properties:

. Ion Beam Current	$\approx$ 1 A	. Thruster Weight (including propellant)	$\approx$ 8 lb
. Ion Beam Energy	2 to 10 Kev	. Power Conditioning Weight	$\approx$ 40 lb
. Thermal Ion Energy	$\approx$ 30 ev	. Control Unit Weight	$\approx$ 1 lb
. Peak Power [a]	4 to 14 kw	. Battery Weight[a,b] (100 W/lb)	30-57 lb
. Average Power[a,c]	1 to 19 kw	. Solar Panel Weight	$\approx$ 10 lb

[a] Depending upon ion beam energy

[c] For pulsed operation, 1 sec duration, 10 sec interval

[b] Total of 10^3 pulses, 1 sec duration, 10 sec interval

[c] To recharge battery in 24 hours

After the expansion to the final diameter (which we assume takes place in a few seconds, within a few hundred kilometers above the earth), the cloud will expand further only as the tube of force which contains it grows, i.e., $\propto r^{3/2}$, where r is the geocentric distance. The cloud will also grow in length, due to the velocity spread of the ions, at a rate

$$\frac{dL}{dt} \approx \frac{kT}{mV_o} \approx 0.25 \text{ km/sec}$$

Table 2 indicates the minimum current, j_{min}, required for observation of an ion cloud produced by a one-second burst from the source. This information is given for two possible values of the initial cloud diameter: 300 cm and 3×10^4 cm. It is given, also, (a) for the cloud just after its expansion to its initial diameter; (b) for the same cloud as it crosses the equator at 5 R_E and (c) for the cloud as it crosses the equator at 10 R_E. Line tracing becomes important for lines as close as ~ 5 R_E because inflation of the magnetic field has been observed at distances of 3 or 4 R_E and the ATS satellite has shown quite large distortions of the field at 6.6 R_E (Paul Coleman, private communication). For each position the diameter and length of the cloud are given, both in linear and angular units. The table shows that if the cloud initially expands to 300 cm, a 2-ampere current will suffice to make it observable at 10 R_E. The angular width (0.4 seconds of arc) is very small, however, and a telescope with $\geq$ 30 cm diameter objective lens would be required to resolve the cloud at its greatest distance. If the cloud expands initially

TABLE 2

Dimensions of Ion Clouds Created by 1-Second Burst of 6 Kev Ba Ion Engine

and Minumum Current Required for Observation of Clouds

Initial (∿300 km alt) B ∿ 0.5 gauss					Equator at 5 R_E B = 2.4×10^{-3} gauss Time to reach equator = 500 sec					Equator at 10 R_E B = 3×10^{-4} gauss Time to reach equator = 1000 sec				
Linear Dia (cm)	Angular Dia (sec)	Linear Length (km)	Angular Length (min)	j_{min} (amp)	Linear Dia (cm)	Angular Dia (sec)	Linear Length (km)	Angular Length (min)	j_{min} (amp)	Linear Dia (cm)	Angular Dia (sec)	Linear Length (km)	Angular Length (min)	j_{min} (amp)
300	2	100	1200	.015	4200	0.3	225	25	0.47	1.2×10^4	0.4	350	20	2.1
3×10^4	210	100	1200	1.5	4.2×10^5	30	225	25	47.	1.2×10^6	40.	350	20	210.

to 3×10^4 cm, reasonable currents will not permit its observation even at 5 R_E, if one observes through a single diameter of the cloud. However, the satellite moves $\sim$ 8 km per second (which is many times the beam diameter) in its orbit a 300 km and if the 1-sec injection takes place as the satellite moves equatorward, the later-injected parts of the cloud will tend to overtake the first-injected parts. This feature will increase the cloud thickness along the line of sight from certain observation points. With experience in using such an orbiting ion source, it might become possible to plan injection location, times, and durations so as to improve, considerably, the observability of the cloud over that calculated by the simplified arguments above. Consideration of the geometry field lines leaving the earth from the auroral region and above also shows that over much of its path the cloud could be observed nearly end-on from particular ground locations, increasing by as much as a factor of 10, or more, its line-of-sight thickness. In particular, a ground station directly under the release point would, initially, see the cloud nearly end-on and so, even the cloud of 3×10^4 cm initial diameter would be readily observable initially. The angular motion of the cloud as observed from the cloud will be slow, making visual tracking relatively simple. It is to be noted, also, that the orbital period of the satellite is $\sim$ 1 ½ hours, during which a ground station moves $\sim$ 22 degrees in longitude. So a single observing station, in the auroral zone, could observe two or three cloud-launches per night with particularly good initial perspective of the cloud at each launch.

The clouds discussed above consist of $\sim$ 1 amp-sec, or about 1 milligram of ions. It is good to have such small amounts of barium per injection if one contemplates many injections. How do these very small amounts compare with the amounts which have been used in chemical bursts and what evidence do the latter provide regarding the above calculations of the visibility of the clouds from a barium ion engine? The cloud of April 22, 1966 (Haerendel et al, 1966) contained a total of 255 grams of Ba. Of these, 5 % or 1.8 grams ($\sim$ 6 x 10^{22} atoms) became ionized. The cloud was 2000 km long and at least 5 km wide and was easily observed without a filter at dusk. (The solar depression angle at launch was only 6 degrees). N_1 for this cloud was $\sim$ 6 x $10^8/cm^2$-column, 20 times greater than we require in the above calculations. The use of a filter, alone, ignoring the probable high background of the sky at the time of the burst, gives easily this factor of 20. We conclude, from this comparison, that the results listed in Table 2 are substantially correct.

If a barium ion cloud expands, initially, to a diameter of only a few hundred centimeters, as in the first line of Table 2, it provides a powerful means of studying the magnetic field topology in most regions of interest in the magnetosphere. If, however, it expands to the larger diameter (line 2, Table 2) its use at large distances is probably not feasible, though experience with use of such clouds may reveal techniques for providing adequately bright clouds at certain desired points along their trajectory. It does not now seem possible to say which of these two initial diameters is the

more nearly correct. The very fact that cross-field diffusion of ion clouds is not amenable even to order-of-magnitude calculations despite the many laboratory experiments that have been performed suggests that barium ion clouds projected into the magnetosphere by an ion engine under rather precisely controlled conditions, might provide information of basic importance to plasma physics.

(viii) Measurement of Electric Fields

Electric field measurements would be accomplished by injecting, from a satellite orbiting over the poles at $\sim 2\ R_E$, low energy ions whose drift velocity due to the gradient and curvature at the magnetic field is very small compared to that expected due to electric fields. The larger distance of the cloud above the earth in this experiment is required because the cloud will hover near its point of injection and prolonged observation of it outside the shadow of the earth requires this greater height. Barium ions would have a kinetic energy of ~ 20 ev by nature of the satellite's orbital velocity (5.3 km/sec). This energy and direction of ejection from the source would be controlled, however, so as to limit the cloud's spreading along the magnetic field lines. Under the competing actions of gravity and the magnetic gradient parallel to the lines the ions will spread out along the lines of force and it can be shown that, for barium ions injected perpendicular to the magnetic field with kinetic energy, W_o, within a few thousand kilometers from the earth's surface at high latitude, the kinetic energy parallel to the lines, $W_{||}$, is

$$W_{\|}(r) \approx W_o \left[1 - \left(\frac{r_o}{r}\right)^3\right] - \frac{90}{r_o}\left[1 - \frac{r_o}{r}\right]$$

where r_o is the geocentric distance at which injection takes place. $W_{\|}$ and W_o are in electron volts; r and r_o are in the earth radii. This equation determines the value of r at which $W_{\|} \to 0$, i.e., the height to which barium ions, injected with energy W_o at r_o, will rise or fall after injection. One finds that ions injected at $r_o = 2$ with energy near 15 ev will neither rise nor fall; by controlling their energy to within ~ 0.1 ev it should be possible to limit their total spread along the lines to ~ 100 km.

The radius of curvature of a 15 ev barium ion at $r = 2$ R_E is ~ 1 km. Thus a burst of ion current of intensity j amperes and duration Δt seconds will distribute 6.3×10^{18} $j\Delta t$ ions in a region ~ 2 km east-west, about 5.3 Δt km north-south, and ~ 100 km. high. From a point on earth directly underneath it this region subtends and angle of ~ 4 minutes of arc (i.e., one-tenth the diameter of the full moon). The column density, $N_{\perp}$ of the cloud from a point directly underneath it is $\sim 6 \times 10^7$ j ions/cm^2-column. For $j = 1$ ampere this is twice the threshold for visual observation. $N_{\perp}$ could be increased by injecting the cloud at lower altitude, but this would, in general, reduce the time for observation of the hovering cloud.

Electric fields perpendicular to $\overline{B}$ would be derived from the measured $\overline{E} \times \overline{B}/B^2$ drift of the cloud. In order for the ion cloud

to be useful in making quantitative evaluations of electric fields, its lifetime against deterioration by better-known phenomena such an ion electron recombination and diffusion by coulomb scattering must be long -- hopefully several hours.

The ion electron recombination time at 6000 km altitude, where the ambient electron density is only $\sim 10^3/cm^3$ is at least several days and possibly much longer. The ion density in the cloud is $\sim$ 5 to 10 ions/cm^3, much less than the ambient electron density, so the cloud will not seriously perturb the environment.

Estimates of the slowing-down and "deflection" time of the cloud ions were derived from the equations of Spitzer (1956). Here we will simply indicate the values of parameters used and the results of the calculation. The "field particles" consist of 10^3 electrons/cm^3 and 10^3 protons/cm^3 both at temperature 10^3 °K . The barium ions have, initially, 15 ev kinetic energy. Making use of Spitzer's equation (5-9), (5-18), and (5-22) and his Tables 5.1 and 5.2, we find that t_D , the time for a 90° deflection of a barium ion, is $\sim 3.6 \times 10^5$ seconds, or about 4 days. But t_D varies directly with the third power of the ion velocity and as the ions are slowed down by coulomb interactions with field particles, t_D shorten rapidly. Spitzer's equation (5-28) gives $\sim$ 2 hours for t_s , the slowing down time for the barium ions. This, then, is the effect most severely limiting the lifetime of the cloud. For, as the ions are slowed by coulomb interactions their deflection

time decreases and they also fall to lower altitude where the field particles are even more numerous. It appears, then, that useful cloud lifetimes may be limited to an hour or so in the experiment as described here.

(ix) Positrons and Tracers

Positrons are attractive for use as tracers because when they come to rest in matter they annihilate with an electron, forming two half-mev gamma rays which are emitted in opposite directions. Detection of the coincident pair of half-mev gamma rays in a suitably situated pair of scintillation detectors then permits positive identification of the stopping and annihilation of the incident positron. Hones (1964) considered a hypothetical experiment in which positrons are injected in the "slot" between the radiation belts at 2.5 R_E and their subsequent behavior studied with a positron detector on a satellite. The postulated detector was heavily shielded against the energetic background particles in the slot and it was found that to obtain a true count rate of 30 counts/sec (10 times the background rate of 3 counts/sec) 3×10^{21} positrons were required.

In the present study, a different location is chosen for injection of the artificial belt -- namely at 6.6 R_E, (the geostationary orbital distance) and the injection is to take place from a satellite in an equatorial geostationary orbit. The electron background at the equator at $L = 6.6$ is obtained from Vette et al (1967) and is tabulated below.

TABLE 3

Electron Flux at L = 6.6

E(Mev)	Integral Flux > E(cm^2-sec)$^{-1}$ *
0.1	6×10^7
0.3	3×10^7
0.5	1×10^7
0.7	4×10^6
1.0	1×10^6
1.5	1×10^5
2.0	1×10^4
2.5	1×10^3
3.0	1×10^2
3.5	1×10^1
4.0	1×10^0
5.0	1×10^{-2}

The Bremsstrahlung spectrum generated by these electrons in beryllium (the outer shielding of the hypothetical detector of Hones (1964)) was calculated by the equations of Petschek (1963). This spectrum is shown in Figure 3. Shown also is the Bremsstrahlung spectrum deduced by Hones (1964) for the electron spectrum in the slot. The integral Bremsstrahlung flux above 1 Mev in the detector at the geostationary orbit is $\sim 10^{-3}$ of that in the slot. For this reason the accidental counting rate of the same detector is reduced to very low levels and

* These are the maximum values, found at $\sim$ 0900 L.T.

it is assumed in the following that a true count rate of 0.1 count/sec could be detected.

Aside from the greatly improved background there is a good reason, from the standpoint of magnetospheric physics, for injecting fast, electron-like particles in this region. These lines of force connect nearly with the auroral zone, and so studies of the behavior of such tracers in this region might provide valuable insight to auroral processes. In this study, no effort is made to conceive experiments with specific detailed objectives. Rather, it is our purpose only to determine the feasibility of injecting a detectable quantity of positrons.

As mentioned above, consideration of the background count rate for the hypothetical detector of Hones (1964) leads to the conclusion that one could hope to detect a positron flux which would give a count rate of $\sim$ 0.1 counts/sec. This turns out to be a flux of $\sim$ 20 positrons/cm^2-sec or a positron density of $\sim 10^{-9}/cm^3$. The volume of a shell 100 km thick (the gyro diameter of a 1 Mev positron) at 6.6 R_E is $\sim 10^{27}$ cm^3, so $\sim 10^{18}$ positrons are required to fill the shell uniformly to a detectable flux level.

Hones (1964) found that 10 kg of reactor-irradiated copper would yield 3×10^{21} positrons. Thus, only $\sim$ 10 grams would be required here if such a source were used. However, one wonders whether the small quantity of positrons required here could be produced by an electron accelerator. The Marquardt Corporation (1966) has conducted a feasibility study for placing in a geostationary orbit a 10 Mev electron

accelerator. An 850 pound payload could provide a total of 3×10^{19} electrons in a total operating time of 10 minutes. To produce positrons with this accelerator, one would place a sheet of dense material (e.g., lead) about one radiation length thick (0.5 cm) in the electron beam. Bremsstrahlung gamma rays produced by electrons would produce electron-positron pairs. What is the efficiency of positron production? Seward (1966) quotes the value 2×10^{-3} escaping positrons/Mev of gamma energy absorbed in a lead shell. If we assume a conversion plate of lead 0.5 cm thick in the electron beam, we can say that roughly 5 Mev of gamma rays are produced in the stopping of each electron and thus find a conversion efficiency of $\sim 10^{-2}$ positron per electron. Thus, the Marquardt accelerator would produce a total of only 3×10^{17} positrons which would not provide one shell-filling. It does not seem, therefore that accelerator produced positrons provide an attractive possibility for magnetosphere experiments.

Seward (1966) finds that a specially designed nuclear bomb of $\sim$ 100 kT yield could produce up to 2×10^{24} positrons. This is 1000 times as many as Hones required for detection in the slot. Both nuclear bombs and irradiated copper, although they represent sources strong enough to establish detectable shells of positrons in the magnetosphere, are costly because a rocket launch is required for each shell. In the outer magnetosphere (e.g., at 6.6 R_E) the lifetime of the shell would probably be quite short so it appears that positron injections here might be an unnecessarily expensive way to study particle behavior.

(x) Conclusions

A barium ion engine, of one-ampere current, developed at moderate cost by modification of an existing ion engine, could create barium ion clouds which would probably be bright enough to permit electron field measurements and other low-altitude studies of the magnetosphere, such as cross-field diffusion of plasmas. It is possible, too, that such an ion source would permit tracing of magnetic field lines to distances 5 to 10 earth radii. The latter possibility, a unique feature of visible clouds of energetic ions, depends upon the extent to which the ion cloud expands across the magnetic field as it leaves the source. This question does not appear to be amenable to theoretical determination and may require, for its answer, actual observation of the behavior of ion beams ejected in space such as those of the SERT tests. Ion engines of 10-ampere current are in the design stage and conversion of such an engine to barium ion production would greatly enhance the possibilities of this technique for magnetospheric field measurements.

Quantitites of positrons which would make a detectable shell in the trapping region of the magnetosphere (where the shell should have a long life) require a nuclear bomb or a very hot source of irradiated copper. Much smaller quantities suffice to provide a detectable shell at the outer edge of trapping (e.g., L = 6.6) and these can be provided by a small piece of irradiated copper that should be relatively easy to handle. However, here the lifetime of

the shell will be short and it is doubtful whether the benefits of positron injection would warrant the cost and effort involved in the establishment of each shell. An electron accelerator probably cannot create enough positrons to establish a detectable shell even at $L = 6.6$.

REFERENCES

Aggson, T., Goddard Space Flight Center, private communication, 1967.

Ahern, J.E., A.I. Bratton, W. H. Buford, R.W. Kenney, A.K. Stazar, and I.A. Sofen, A design concept for electron injection in space, Marquardt Corporation Report MR 20381, November 1, 1966.

Akasofu, S.I., S. Chapman,and C.I. Meng, J.Atmosph. Terr.Phys. 27, 1275, 1965.

Allen, C.W., Astrophysical Quantities, Athlone Press, Univ. of London, 1955.

Foppl, H., G. Haerendel, L. Haser, R. Lüst, F. Melzner, B. Meyer, H. Neuss, H.H. Rabben, E. Rieger and J. Stocker, Preliminary Results of Electric Field Measurements in the Auroral Zone, Max-Planck-Institut für Extraterrestishce Physik, Preprint, 1967.

Haerendel, G., R. Lüst and E. Rieger, Motion of artificial ion clouds in the upper atmosphere, Planet. Space Sci., 1967.

Harrison, E.R., An experiment to determine the nature of the earth's distant magnetic field, Geophysical Journal of the Royal Astronomical Society, 6, 462-467, 1962.

Hones, E.W., Jr., On the use of positrons as tracers to study the motions of electrons trapped in the earth's magnetosphere, J. Geophys.Res. 69, 182-185, 1964.

Hones, E.W., Jr., On the use of electrical ion sources for ion tracer experiments in the magnetosphere, Univ. of Iowa, Department of Physics and Astronomy Report, 65-31, 1965.

Knauer, W., Exploration of geomagnetic cavity with accelerated barium ions, Hughes Research Laboratories Brochure 67M-7958/B5363, 1967.

Petschek, A.G., Interpretation of satellite detector counter rates, J. Geophys.Res. 68, 663-665, 1963.

Schklovskii, I.S., V.S. Esipov, V.G. Kurt, V.I. Moroz, and P.V. Schlegov, An Artificial comet, Soviet Astronomy, A.J., 3, 986 May-June 1960 (English Translation).

Seward, F.D., A nuclear bomb as a source of positrons for space experiments, University of California, Lawrence Radiation Lab. Report UCRL-14784 Rev.1, 1966.

Spitzer, L., Physics of Fully Ionized Gases, Chapter 5, Inter Science Publishers, Inc., New York, New York, 1956.

Vette, J.I., A.B. Lucero and J.A. Wright, Models of the trapped radiation environment, Vol.III: Electrons at synchronous altitudes, NASA SP-3024, 1967/

FIGURE CAPTIONS

Figure 1 (a) Earlier model current system (schematic) for polar magnetic substorm; view from above dp north pole; the direction of the sun is indicated.

(b) New model current system (schematic) proposed by Akasofu, Chapman and Meng. (From Akasofu et al, (1965).

Figure 2 Schematic diagram of Kaufman thruster (ion engine) such as would be used as barium ion source (Knauer, 1967).

Figure 3 Computed Bremsstrahlung spectra behind beryllium shield of positron detector at $L = 6.6$ and $L = 2.5$.

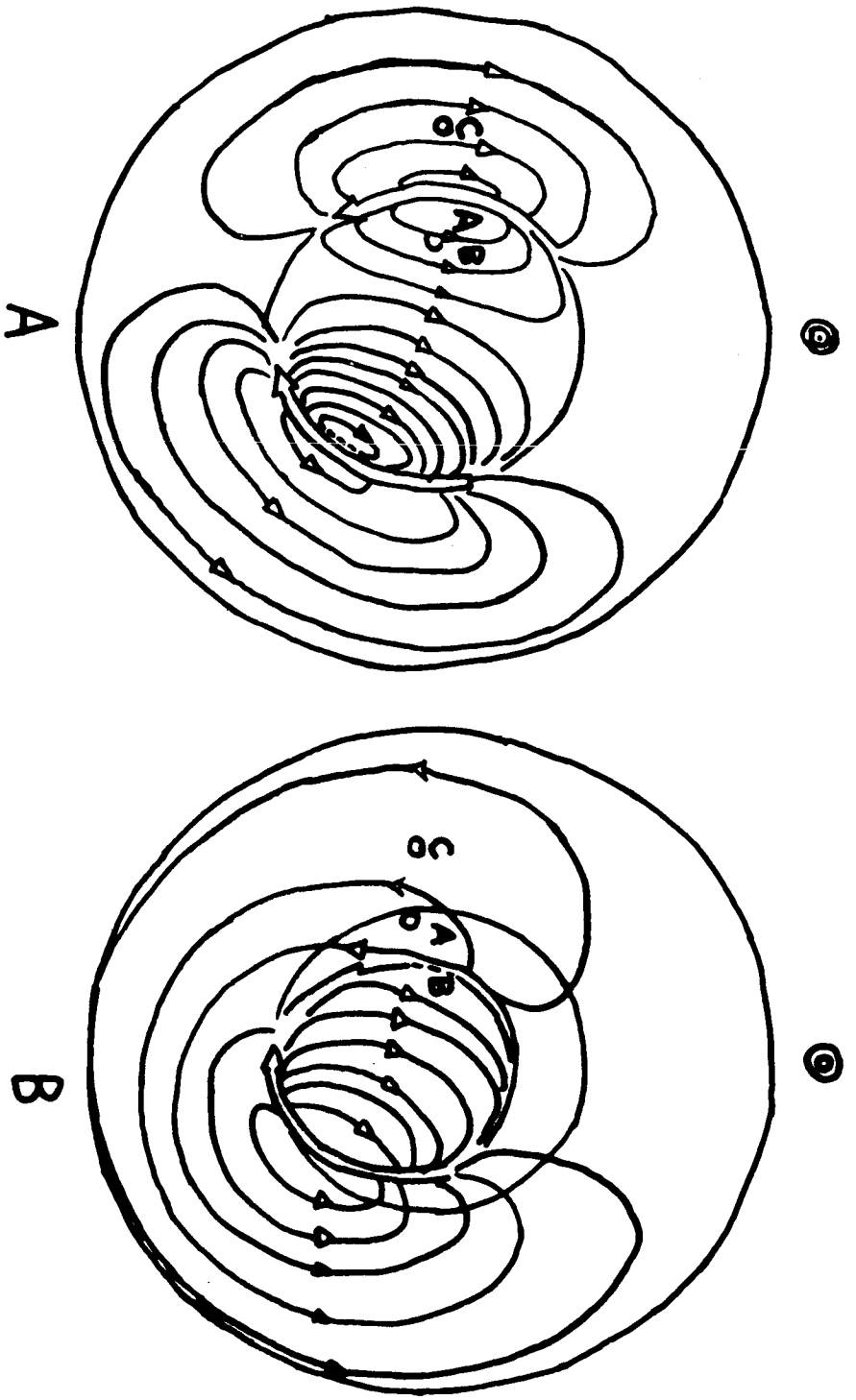

Figure 1.

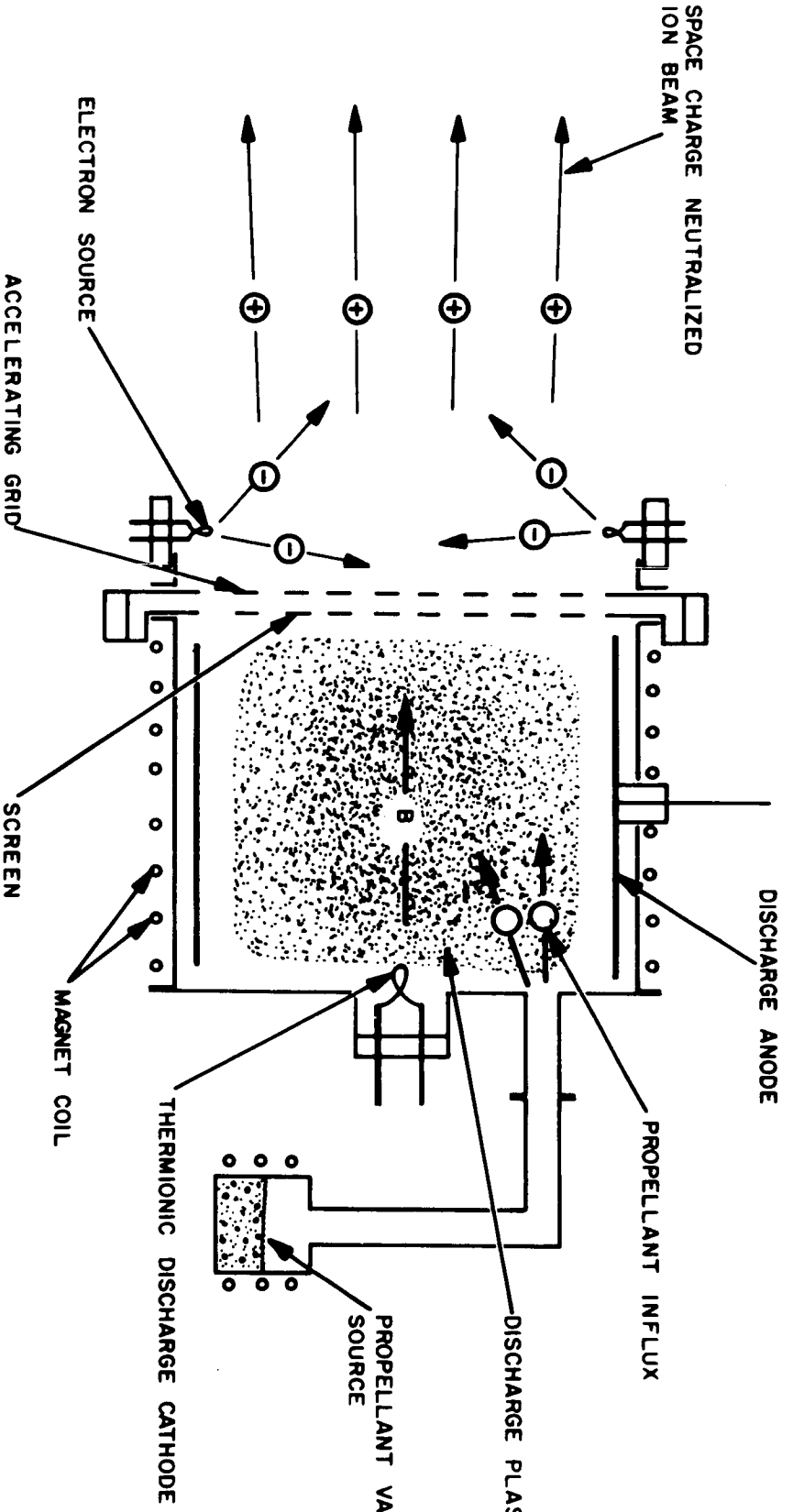
SPACE CHARGE NEUTRALIZED ION BEAM
ELECTRON SOURCE
ACCELERATING GRID
SCREEN
MAGNET COIL
THERMIONIC DISCHARGE CATHODE
PROPELLANT VAPOR SOURCE
DISCHARGE PLASMA
PROPELLANT INFLUX
DISCHARGE ANODE
B

Figure 2.

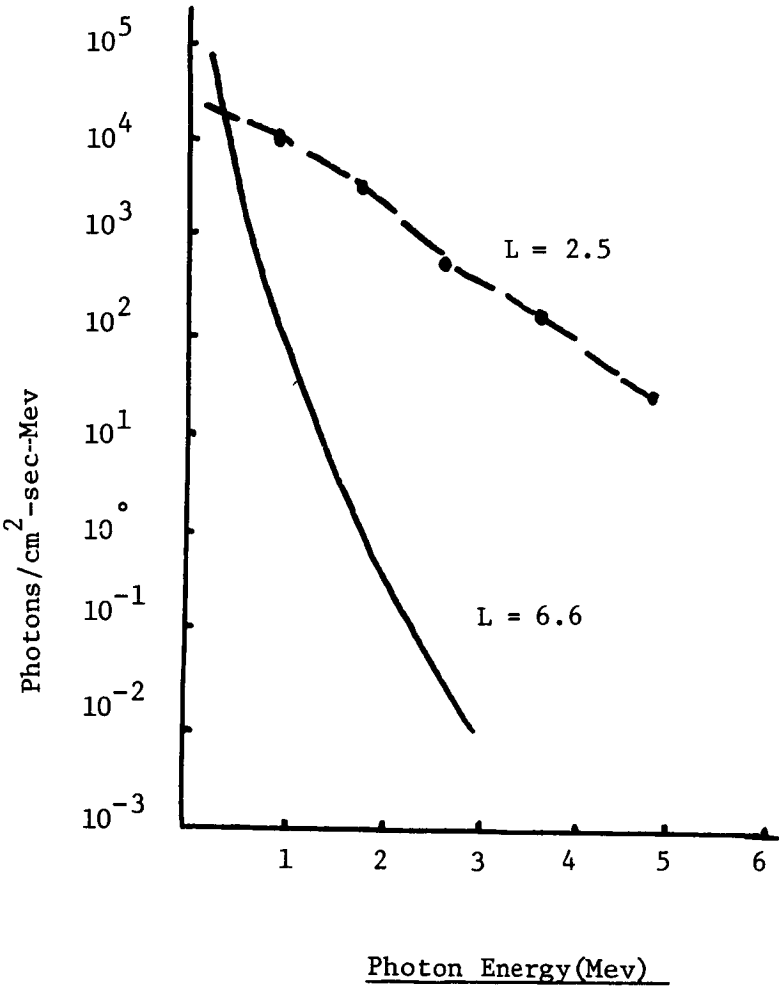
Photons/cm^2-sec-Mev
10^5
10^4
10^3
10^2
10^1
10^0
10^{-1}
10^{-2}
10^{-3}
L = 2.5
L = 6.6
1
2
3
4
5
6
Photon Energy(Mev)

Figure 3.

7. MODIFICATION OF THE MAGNETOSPHERIC CONVECTION PATTERN BY MASS INJECTION

Harry E. Petschek

AVCO Everett Research Laboratory

Everett, Massachusetts

The basic energy source and driving mechanism for most of the phenomena which are observed to occur within the magnetosphere beyond about L equal 3 or 4 is generally believed to be the solar wind. These phenomena include the aurora, the production and precipitation of higher energy particles, the emission VLF noise and the distortion of the magnetosphere into a long tail. The most likely mechanism for coupling solar wind energy to the internal magnetosphere is that drag at the magnetosphere boundary allows the solar wind to drive an internal convection pattern within the magnetosphere.[1-4] While the precise nature of this coupling is still subject to some controversy, there is significant evidence that the coupling exists and is responsible for many of the features observed within the magnetosphere.The observed elongated magnetic field in the tail is direct evidence that some shear force is acting on the magnetosphere boundary. The data on low energy particles on the nightside suggests that a flow towards the earth is bringing these particles towards the nightside.[5] The well-known observation that aurorae are predominantly a nighttime phenomena indicates

that the energy is coming into the magnetosphere from the night-side. Even the fluxes of particles of several MeV are known to be affected by disturbances in the over-all flow field.[6] All of these phenomena indicate that the convection pattern plays a crucial role in determining the over-all balance of the internal magnetosphere. One may therefore anticipate that modifying this convection pattern would produce significant changes in the number of observable phenomena.

The purpose of this report is to indicate that such modification is feasible over local regions with modest present day payloads and conceivably over the entire magnetosphere if the full payload of an Apollo-size vehicle could be utilized.

If a mass of ionized material comparable to the ambient mass were added to a region of the magnetosphere at a velocity different from the natural velocity, the velocity of this region would be momentarily changed. This would correspond to a significant change in the flow pattern locally. This disturbance would last for the time required to re-accelerate the added mass to the natural flow velocity. The possibility of actually changing the convection flow either locally or globally by injecting mass depends on the fact that the total mass of the magnetosphere is surprisingly small. Taking the density of one proton per cubic centimeter and a volume corresponding to a cube 30 earth radii on a side, the total mass is about 10 tons. Since even this mass is within the rocket capability

which will exist in the next few years, the requirement of providing sufficient mass of material can easily be met. Indeed, as will be discussed below, significant changes in local regions of auroral flow should be achievable with modest present day rockets. The problem which is not as easily resolved is the method of distributing the mass over the large volumes required.

As an example we consider a possible modification of the flow in a local region in the auroral zone. Consider a cloud of neutral cesium released in a circular orbit at $L = 6$, on the equator, and on the nightside of the earth. If sunlight is not eclipsed by the earth, the cesium will be ionized by solar radiation with a time constant of 1.6×10^3 seconds.[7] During this time thermal expansion of the cloud at a temperature of a few hundred degrees centigrade will allow it to reach a diameter of about 10^3 km. The undisturbed convection velocity at this point is about 10 km/sec and roughly in the azimuthal direction. The first atoms which become ionized could therefore be dragged by the magnetic field to a distance of about 2×10^4 km ($\sim \frac{1}{2}$ rad.) away from the neutral cloud. Since the magnetic field lines remain rigid, the mass should be compared to the mass along the entire length of the field line $\sim 10^5$ km. The volume of interest therefore extends 10^5 km along the field line, 2×10^4 km azimuthally, and 10^3 km in the radial direction. Taking a density of one proton per cubic centimeter, this corresponds to an ambient mass of 10 kg.

The release of a few tens of kilograms of neutral cesium should therefore be sufficient to produce significant changes in the

local convection flow. The region affected would have roughly the dimensions given above. The azimuthal extent might be somewhat less since the velocity of the field lines which have been weighted down by the early ionization would already be somewhat reduced. The duration of the event would be determined by the time required to accelerate the added mass to the normal velocity. A rough estimate of this time would be that another comparable mass of convection flow must go by the region and impart its momentum to the cesium. Since we have taken the mass which flows by in the ionization time the acceleration time would be comparable to the ionization time or about 1.6×10^3 seconds.

The effects of the release of a few tens of kilograms of cesium should produce significant changes in several standard observables. For example, the ionospheric current pattern at the base of the affected field line should be modified and readily observable with ground magnetometers near the base of the field lines involved. The modified density may form a whistler duct. Since natural ducts are rare in the auroral zone such an artificial duct would be easily identified and monitored. Satellites flying through the cloud should be able to detect the cesium ions with particle detectors. A cesium ion moving at the convection velocity would have an energy of about 1 Kev. Finally, the disturbance in density velocity and shear may produce instabilities which modify particle precipitation. This precipitation could be observed with polar satellites or balloons or might even have sufficient intensity to produce a large scale visible aurora.

As a second example, modification of the tail is somewhat more difficult than the example just given for the auroral zone. Firstly, because of the larger dimensions involved, a larger mass is inquired. Secondly, the distribution of the added mass over these large volumes is more difficult. Thirdly, since the magnetic field is significantly distorted by the flow, the interaction of the flow with the added mass can lead to further magnetic field distortion and more complicated flow phenomena may result. An entire cycle of the convection pattern requires of the order of 10^4 sec. If significant effects are to be achieved the mass should probably be added in a time comparable to or smaller than this. On the other hand, in order to allow the mass to spread over a large volume, long times are desirable. Lithium has an ionization time by solar radiation of about 10^4 seconds[7] and would spread by thermal expansion to a diameter of about three earth radii.

Consider a cloud of lithium released at about 30 earth radii within the tail, but away from the neutral sheet. The volume occupied by the lithium during the ionization time would be 2×10^4 km both along the field lines and perpendicular to the flow and magnetic field, and the magnetosphere length $\sim 2 \times 10^5$ km along the flow direction. A density of one proton per cubic centimeter, which may be slightly high for the tail, corresponds to $\sim 10^2$ kg. Since in this case the field lines can be bent by the flow, one might expect that the field lines going through the cloud would continue

to move while being retarded within the cloud. The resulting slingshot effect would accelerate the added mass more rapidly than was estimated previously. The resulting concentration of the momentum and energy should result in a geometrical perturbation of the neutral sheet and possibly a modification of the earthward flow which it produces.

If 10^3 kg were added at such a location the mass would be sufficient to retard the entire length of the field lines on which the lithium has been placed even taking the slingshot effect into account. This should reduce the velocity toward the neutral sheet and the rate of field line reconnection over the three earth radii width of the region. This in turn should produce noticeable modifications both locally in the tail and along these streamlines into the auroral zone. Modification of ionospheric currents and auroral precipitation would be expected. Finally, if ten such clouds were simultaneously released distributed at three earth radii intervals across the tail the entire tail would be decelerated and changes should occur over the entire auroral zone and tail.

One of the major uncertainties associated with such experiments at the present time would be production of the ionized gas cloud. The ionization times quoted were taken from theoretical calculations based on ionization by solar radiation. More recent experiments with barium clouds have indicated that considerable uncertainty in these ionization times exists.[8] It is not clear at the present time whether or not these difficulties are peculiar to the chemistry of barium and would not apply to the alkali gases

suggested in this report. It should, however, be borne in mind that the experiments suggested do not depend critically on the chemical species which is injected except that the ionization time should be in the appropriate range. It seems likely that the element with the appropriate ionization time can be found. Furthermore, some variability exists; in particular, the injection in the auroral zone could be carried out at higher latitudes than the equator which, for the same ionization time, would allow a wider spread in L value. The problem in ionization time is therefore one of finding a release mechanism and a suitable chemical species to fit the required ionization times.

The above examples serve to show that addition of mass in the range of several tens of kilograms up to several tons should produce modifications of the convection pattern over local or global regions. While these estimates should be reasonably accurate as far as predicting a modification of the convection pattern, it is very difficult to estimate what further effects should occur. Modification of the convection pattern would clearly produce modifications in the ionospheric current patterns. The expectation that further significant effects on particle precipitation, creation of aurorae and VLF emissions will occur rests on two basic concepts. Firstly, that the convection pattern is the basic driving source for phenomena within the magnetosphere and therefore modifying it should produce significant changes. Secondly, many features of the magnetosphere such as aurorae, particle precipitation, and VLF emissions

appear sporadically indicating that the magnetosphere is easily triggered into such phenomena, thus suggesting that a disturbance which is artificially produced might also trigger these phenomena.

REFERENCES

1. Dungey, J.W., Interplanetary magnetic field and the auroral zones, Phys. Rev. Letters, 6, 47-48, 1961.

2. Axford, W.I. and C.O. Hines, A unifying theory of high-latitude geophysical phenomena and geomagnetic storms, Can.J.Phys., 39, 1433-1464, 1961.

3. Levy, R.H., H.E. Petschek and G.L. Siscoe, Aerodynamic aspects of magnetospheric flow. AIAA, 1964; AIAA Journal, 2, 2065-2076, 1964.

4. Axford, W.I., H.E. Petschek and G.L. Siscoe, Tail of the magnetosphere, J. of Geophysical REs., 70, No. 5, March 1, 1965.

5. Frank, L.A., JGR, 72, 185, (1967).

6. McIlwain, C.E., JGR, 71, 3623 (1966).

7. Marmo, F.F., J. Pressman and L.M. Aschenbrand, Planet. Space Sci. 3, 139 (1961).

8. Föppl, H., G. Herendel, L. Haser, J. Loidl, P. Lütjens, R. Lüst, F. Melzner, B. Meyer, H. Neuss and E. Rieger, Artificial strontium and barium clouds in the upper atmosphere, Planet. Space Sci. 1967, Vol. 15, pp. 357-372.

8. WAVE-PARTICLE INTERACTION EXPERIMENTS

R.A. Helliwell

Radioscience Laboratory, Stanford University

Stanford, California

ABSTRACT

It is proposed to modify the environment of the magnetosphere by injecting whistler-mode waves from transmitters located on the ground and in satellites. Both longitudinal and transverse resonance between charged particles (principally electrons) and the waves would be employed to produce changes in the waves and the interacting particles. Injected waves may be amplified or attenuated. Radiation at new frequencies may be stimulated. Particles may experience changes in pitch angle and energy.

Observations of such wave-induced phenomena should aid in understanding the physics of the interaction processes and provide a basis for systematic modification of the wave and particle environments. In addition, new diagnostic tools for the study of both the energetic and thermal particle environments may emerge.

For an initial wave-particle interaction experiment, a polar orbiting satellite is suggested, with the geocentric distance ranging from about 2 to 4 earth radii. A frequency range of 1 kHz to 300 kHz is suggested. Two to three mutually orthogonal electric dipoles would be driven in various ways to excite waves

in the range 1 kHz to 300 kHz. A transmitter power of at least 1 kw is desired. Broadband receivers excited by loop antennas would be employed to detect stimulated emissions and echoes. Auxiliary experiments in the satellite include sounding of the magnetosphere in both the whistler and "HF" modes together with particle detection (pitch angle and energy distribution) in the 100 ev to 300 kev range. Complementary measurements of waves and particle effects would be made on the ground at the ends of the field lines of interest.

(i) Introduction

In this paper we explore briefly some possible ways of modifying the environment of the magnetosphere by injecting whistler-mode waves. Strong interaction between the waves and energetic particles is expected to occur over a wide range of particle energy because the wave velocity in the whistler-mode is relatively low ($\sim$ 0.1c). Interaction modifies the characteristics of both the waves and the particles. In the proposed experiments interactions would be stimulated by signals transmitted from the ground or from a space vehicle. The resulting wave and particle phenomena would be measured by suitably located radio receiver and particle detectors.

Wave-particle interaction experiments are interesting for several reasons. Perhaps most important at this time is their potential contribution to a better understanding of magnetospheric physics.

With improved understanding may come new methods for measuring the parameters of energetic particles, and possibly those of the background thermal plasma as well. Wave-particle interaction experiments will also aid in assessing the feasibility of controlling the properties of trapped particles using electromagnetic waves. Experimental evidence supported by theory, indicates that the growth of electromagnetic waves through the transverse resonance instability leads to significant lowering of the mirror points of the interacting electrons. Some of these electrons enter the 'loss cone' and are absorbed or 'dumped' in the ionosphere, where they may cause detectable radio wave absorption and various auroral effects.

Ability to control the dumping of electrons would naturally lead to other experiments involving trapped particles. With sufficient wave power it might be possible to reduce significantly the level of dangerous radiation reaching astronauts. In addition to dumping, it may even be possible to accelerate energetic particles, thereby providing a new tool for the study of this little understood process. Controlled acceleration could also lead to other experiments, for instance the mapping of the earth's field through the enhancement of energetic particle fluxes over a narrow range of L values.

Another area of possible application for wave-particle interactions is the control of wave generation, amplification and attenuation for the benefit of VLF communication and navigation systems. At high geomagnetic latitudes it is known that the level

of natural noise at VLF is often determined by emissions form the magnetosphere and ionosphere rather than by impulses from lightning. Suppression of these emissions, either continuously or on a scheduled intermittent basis, could mean a significant increase in signal-to-noise ratio. Ability to use the amplifying properties of particle streams could lead to new communication techniques involving satellite and ground stations.

Before discussing proposed wave-particle interaction experiments, we shall review briefly the relevant background. In section (ii) we look at the mechanisms of propagation of whistler-mode waves. In section (iii) we describe the principal known interaction phenomena and in section (iv) their various interpretations. In section (v) we outline some suggested experiments and discuss their requirements and interfaces. In section (vi) we discuss experiment requirements. It must be emphasized that these suggestions are not intended to be comprehensive, but rather to indicate the kind of interesting experiments that might be done by injecting waves. Other ideas will surely come forth as more thought is given to the problem.

(ii) Propagation Paths

To excite an interaction the waves must be able to propagate from the source to the region of interest. We consider now the accessibility of various regions of the magnetosphere to whistler waves from sources on the ground and in space.

Sources on the ground, such as man-made transmitters and lightning discharges, can illuminate the lower boundary of the ionosphere by direct transmission and via multiple reflections between earth and ionosphere. Some of the incident energy leaks into the ionosphere, being guided approximately along the magnetic field lines of the earth. Those components that encounter an enhancement of field-aligned ionization can be ducted and conveyed to the opposite hemisphere where they exit into the earth-ionosphere waveguide. They may then propagate a considerable distance away from the exit point before their intensity drops below the threshold of detection. The ray paths of waves not so ducted simply deviate slowly from the field line, following a 'non-ducted' path which is determined by the overall distribution of refractive index.

A characteristic of typical non-ducted propagation as determined by ray tracing in a model magnetosphere is that the wave normal tends to bend more slowly than the earth's field. Thus the direction of wave propagation (with respect to the earth's field) tends to become more transverse as the wave propagates. If the wave frequency is below the lower hybrid resonance frequency (see section (iii)). the wave normal can reach 90° , at which point the wave is reflected [Kimura, 1966; Thorne and Kennel, 1967]. One phenomenon in which this process occurs is the so-called magnetospherically reflected (MR) whistler [Smith and Angerami, 1968]. The MR whistler shows a number of components which are interpreted as successive reflections between magnetospheric reflection points

in the vicinity of the lower hybrid resonance frequency. The wave normals of the reflected components of MR whistlers are close to 90°, implying a relatively large longitudinal electric field component. After several reflections the calculated ray paths are found to follow the earth's field rather closely [Kimura, 1966]. Often associated with MR whistlers are strong emissions [Smith and Angerami, 1968]. One of the objects of a wave injection experiment would be to stimulate such emissions. MR whistlers have been seen only within the plasmasphere and within $\pm$ 30° of magnetic equator.

One of the limitations of ground sources for interaction experiments is the restricted range of wave normals which can be excited in the ionosphere. Because of the high refractive index of the ionosphere, wave normals in the transmitted wave are initially confined to a narrow cone (usually only a few degrees in a half angle) about the vertical. This limits the paths that a ray entering the ionosphere at a certain latitude can take. Nevertheless, if we neglect reflection effects at the plasmaphere boundary, it appears that one can always find a starting point from which a ray may reach a given point in the magnetosphere.

By placing the transmitter in the magnetosphere, the refractive index is increased causing the range of accessible wave normals and corresponding ray paths to increase. This means that more paths can be excited and a wider range of interaction conditions achieved. Of especial interest is the possibility of causing the

signal and any associated emissions to return to the satellite in the manner of a boomerang, following reflection in the region of the lower hybrid resonance. Such a reflection would not involve an exact retracing of the path of the incident wave but rather a rapid turn-around, with the return path passing close to the former path. Using ray tracing in a model magnetosphere, the path of the boomerang mode has been found to follow closely the path of the earth's field [Edgar, private communication]. A schematic diagram of the boomerang mode is shown in Figure 1.

Ducted signals can also be excited by a satellite transmitter but normally only when the satellite is within a duct. By contrast, a transmitter on the ground can simultaneously excite many different ducts because the energy leaks into the ionosphere with nearly vertical wave normal. However the ground transmitter should be reasonably close (say within 500 km) to the entrances to the ducts to ensure adequate signal strengths.

The two principal sources of wave injection, ground transmitter and satellite transmitter, have both advantages and disadvantages. With a ground source it is possible in principle to excite all available ducts on a continuous basis. Thus the monitoring of drifting ducts [Carpenter and Stone, 1967] is best carried out from the ground. A disadvantage of the ground source is the high injection loss produced by attenuation in the earth-ionosphere waveguide and coupling across the lower boundary region of the ionosphere. In addition, if the region is at a high

altitude, there is a divergence loss connected with the spreading of the lines of force of the earth's field. However these losses are at least partially compensated by the relatively high powers available from some ground stations. In a typical experiment where the magnetospheric path started at a distance of 2000 km from the ground transmitter and the satellite (OGO-I) was near the equator at $L = 2$, the nighttime magnetic field intensity from NAA, radiating 10^6 watts on 17.8 kHz, was roughly $10^{-3}\gamma$ [Heyborne, 1966]. This signal level is comparable to the intensity of strong natural noise frequently observed with the same satellite.

With a satellite transmitter on the other hand, it should be possible to produce the required signal levels at reasonable distances from the satellite with a few hundred watts of power, since the waveguide and coupling losses are no longer present. Furthermore, a satellite source, as indicated above, is capable of exciting the full range of wave normals, thus allowing examination of regions inaccessible to ground sources.

A disadvantage of the satellite source compared with the ground source is the fact that the satellite is normally moving rapidly and hence it is not possible to monitor continuously a particular path of propagation.* This limitation is especially striking in experiments requiring ducting propagation. Thus a satellite crossing

---

* A possible exception is the path from a synchronous satellite; however, it is believed that the magnetosphere at synchronous altitude ($6.6\ R_E$) does not co-rotate with the earth.

a duct with a diameter of 50 km at a speed of 10 km a second could observe ducted signals for only 5 seconds. Since echo times may range from less than one to nearly ten seconds, depending on frequency and path, this method of study has limited application. A considerable improvement would result if the satellite followed an orbit which was somewhere aligned with the axis of the duct.

Recent satellite observations [Heyborne, 1966] show that signals from ground VLF stations are often cut off above a certain latitude. The cutoff appears to occur near the plasmapause (typically near $L = 4$) for moderate disturbance, and has tentatively been attributed to D-region absorption. In this situation a satellite transmitter would appear to provide the only reliable means of injecting waves into the region beyond the plasmapause.

The radiated power required to produce a certain signal level at a certain point in the magnetosphere can be determined if the directivity of the antenna and the ray trajectories from the transmitter are known. Since this information is not available, we shall make a very crude estimate based on admittedly over-simplified models. For dicussion purposes we shall assume that a signal power density of 10^{-11} watts/m^2 is desired in the interaction region which is located 5000 km from the satellite transmitter. This signal level corresponds to that of relatively strong narrowband noise as measured with OGO-I at frequencies of a few kHz.

For non-ducted propagation assume the power density varies inversely with the square of the distance from the source. Then the

total power required from an isotropic source would be $4\ (5 \times 10^6 m)^2 \times 10^{-11}$ watts = 3,140 watts. Because of the anisotropy of the magnetosphere at VLF, we can expect some guiding even in the absence of a duct. For example if we neglect the effects of ions and take $f << f_H$, the angle between the ray and the earth's field has a maximum value of $20°$. If we assume the energy is uniformly distributed over this 'ray-cone', the directive power gain is about 10 db, and the required power is reduced to 314 watts.

In ducted propagation wave power is guided along the lines of force of the earth's field when the angle between the wave normal and the earth's field is less than the so-called 'trapping' angle. (It depends on the percentage enhancement ionization in the duct and on f/f_H.) Because the wave is trapped, the wave power density does not vary inversely with the square of the distance from the source as in a homogeneous medium but inversely as the effective cross-sectional area of the duct. For a typical duct with a wave normal trapping angle of 20°, the maximum ray angle for $f << f_H$ is about 10°. For simplicity assume that the radiated energy is proportional to the size of the ray cone in solid angle. Then the power trapped is about one-fourth of that radiated. Now for a typical duct at $L = 5$ the cross sectional area in the equatorial plane is about $10^{11} m^2$ [Angerami, private communication]. The total radiated power required is then $4 \times 10^{11} \times 10^{-11} = 4$ watts.

Although such crude calculations cannot be used as a basis for design, they do suggest that experiments based on use of ducted signals should require significantly less power than 'non-ducted'

experiments. More quantitative study of the antenna pattern and ray divergence is required.

(iii) Wave-Particle Interaction Phenomena

In this section we review briefly the principal wave-particle interaction phenomena that have been observed on the ground and in satellites. Most of the phenomena to be discussed are electromagnetic emissions observed in the frequency range 300 to 300,000 Hz [Helliwell, 1965]. (However it is known from recent observations, both on the ground and in satellites, that emissions can be observed at higher and lower frequencies.) Detailed information on changes in particle parameters resulting form interaction processes is very limited [Oliven and Gurnett, 1966] even though the theory has received considerable attention [Kennel and Petschek, 1966].

For our present purpose it is useful to consider wave effects in one of two phenomenological categories. First are those in which an input signal is either amplified or attenuated, but whose frequency-time variation and bandwidth remain essentially unchanged. Second are those in which an emission occurs spontaneously or, if triggered, whose spectral character differs markedly from the spectrum of the triggering signal. It should be noted, however, that there is actually no sharp distinction between these classes, since observed interactions may show the properties of both.

In the first class we have whistlers, originating in lightning, whose observed dispersion fits cold plasma theory but which show marked amplitude changes not readily explained in terms of cold plasma theory. An example is the 'long-enduring' whistler echo train [Helliwell, 1965] that may show several hundred discrete echo components of nearly the same amplitude. This phenomenon requires either a lossless duct with perfect reflectors at the ends, or an amplification process somewhere on the path. Another example is the sharp high-frequency cutoff observed on ducted whistlers at one-half the electron gyrofrequency [Carpenter, 1968]. This effect has been attributed both the failure of the ducting mechanism [Smith, 1961] and to cyclotron damping by resonant electrons [Liemohn, 1967]. On the other hand, non-ducted whistlers of the 'MR' type show sharp low- and high-frequency cutoffs which have been attributed to Landau damping by resonant electrons [Thorne, private communication]. Also in the first class are man-made signals from stations such as Omega (10.2 kHz) which show clear evidence of amplification with little or no change in spectrum [Carpenter, 1968].

In the second class are the relatively broadband noise known as auroral hiss and the narrowband noise known as discrete emissions (e.g., chorus). Both may appear spontaneously, while the latter are often triggered by natural or man-made signals.

Because of their apparent susceptibilty to control, we shall review the characteristics of triggered narrow-band emissions in some detail. Many natural emissions of the narrow-band type are observed to be related to whistlers or other emissions. An emission

may be triggered by a whistler at any frequency within its range, but not with equal probability at all frequencies. The bandwidth of triggered emissions may range from less than 1 % to greater than 10 % of the center frequency. Two broad categories of triggered emissions are recognized, one associated with ducted signals and the other with non-ducted signals.

Triggered emissions associated with ducted signals most commonly start at the upper cutoff frequency of nose whistlers, which usually is very close to one-half the minimum gyrofrequency on the path of propagation [Carpenter, 1968]. Triggered emissions observed on the ground are believed to originate in whistler ducts, since, as pointed out earlier, ducting aids the transmission of whistlers out of the ionosphere and into the earth-ionosphere waveguide. Furthermore, the presence of the duct helps to keep the direction of propagation of the triggering signal aligned with the earth's field, a condition favoring emission growth through the transverse resonance instability. However the generation process is not limited to ground-observed ducts, since the OGO I and III VLF experiments see the same type of discrete VLF emissions occurring spontaneously over wide ranges of L-value.

The reason for the frequent triggering of ducted emissions at one-half the minimum gyrofrequency is not understood, but it is thought that wave particle interactions as well as the failure of ducting at this frequency must be involved [Carpenter, 1968]. The satellite experiments to be proposed should provide useful new data on these puzzling phenomena.

The duration of an emission triggered by a ducted whistler may on occasion exceed 30 seconds, a time much longer than the mirroring period of any resonant particles. This suggests that the generation region tends to remain fixed in space, rather than moving with the particles as some authors have suggested. Recent observations of the upper cutoff frequency of whistler mode noise made with the OGO-I satellite support previous suggestions that the region of generation is located close to the top of the line of force that passes through the satellite [Dunckel and Helliwell, in preparation]. These and other facts point to a mechanism based on gyro-resonance between electrons streaming in one direction and whistler mode waves propagating in the opposite direction.

Another type of narrow band triggered emission is that seen in satellites associated with MR whistlers [Smith and Angerami, 1968]. Although these emmisions tend to start at the tops of the MR traces, their frequencies are well below half the minimum gyrofrequency on the path. It has been suggested [Thorne, private communication] that these emissions are evidence of growth associated with the longitudinal resonance (negative Landau damping), since the wave normal angles of the parent whistlers are close to 90°. An experiment similar to that suggested for study of the transverse resonance would be desirable here.

Discrete VLF emissions can be triggered by single frequency transmissions from VLF stations. These have been called artificially-stimulated emissions (ASE). Their occurrence is highly sensitive to the duration of the triggering signal. In one series of experiments

on 14.7 kHz, the Morse code dots (50 msec in length) produced virtually no triggering, whereas the Morse code dashes (150 msec in length) produced variable-frequency, narrowband emissions most of the time [Helliwell et al, 1964]. The onset time of the triggered emissions was delayed with respect to the starting time of the triggering dash by about 100 msec.

Another example of emission phenomena, seen only in satellites, is the so-called lower hybrid resonance noise. This has been observed over a range of altitudes, principally in the vicinity of 1000 km. The frequency f_r of the lower hybrid resonance (LHR) given by

$$\frac{1}{M_{eff}}\,\frac{1}{f_r^2} = \frac{1}{f_o^2} + \frac{1}{f_H^2}, \quad \text{where } M_{eff} = \Sigma \frac{\alpha_i}{M_i}, \; \alpha_i = \text{fractional}$$

concentration of the i^{th} ion, M_i = the relative mass of the i^{th} ion, f_o = electron plasma frequency, f_H = electron gyrofrequency. For a typical model of the ionosphere and magnetosphere, this frequency ranges from < 1 kHz to $\sim$ 8 kHz. Emissions of the LHR type are characterized by a relatively sharp low frequency cutoff and a variable bandwidth. In addition, they appear often to be enhanced or triggered by whistlers of both the shorth path (0_+) and long path (1_-) variety. Excitation of the LHR noise apparently could be effected either from the ground or from a satellite.

Occurrence patterns of wave-particle interaction phenomena are complex. However, some broad distinctions can be developed

from available data. Thus broadband hiss is seen mainly in the auroral zones on the nightside of the earth and is thought to be associated with the open field lines. Discrete emissions, including chorus and so-called mid-latitude hiss, tend to be a daytime phenomena and are seen mainly in the region of closed field lines. Discrete emissions observed on the ground appear to exit from the ionosphere along preferred paths (i.e., ducts), whereas those observed in satellites seem to show no preferred paths. Thus it appears that many of the regions in space as well as certain phenomena are observable and controllable only from within the ionosphere or magnetosphere.

(iv) Interaction Mechanisms

The mechanisms of principal interest in this study are those related to the longitudinal and transverse resonances. The condition for longitudinal resonance is given by $v_{\|} \cos\Theta = v_p$, where $v_{\|}$ = streaming velocity of particles, Θ = angle between wave normal and earth's field, and v_p = phase velocity of wave. Longitudinal resonance is involved in Cerenkov radiation and in collective phenomena analogous to traveling wave tube amplification. In order for longitudinal resonance to be effective there must be a significant longitudinal component of the wave electric field and this is achieved only with a non-zero wave normal angle. The larger the wave normal angle, the larger the longitudinal electric field component. However, even at large wave normal angles, the

electric field tends to be shorted out in the direction of the earth's magnetic field and so is often relatively small. From the given resonance condition and the known parameters of the magnetosphere, the resonant particle energies are estimated to be a few kev. In the F region the resonant energy may drop to a few hundred ev. Emissions triggered by MR whistlers are thought to be evidence of a collective interaction at the longitudinal resonance taking place near the equator [Thorne, private communication].

For years it has been thought that incoherent Cerenkov radiation would be too weak to account for the level of observed emissions. However, Jørgensen [1968] has found recently that the parameters used in the early calculations were unrealistic. His estimates of Cerenkov radiation from electrons in the auroral zone are in relatively good agreement with observations of auroral hiss made both on the ground and in polar orbiting satellites. Modfying the Cerenkov process using longitudinally resonant waves would be worth some study as a possible experiment to be carried out from a satellite that crosses lines of force passing through the auroral zone.

The other interaction mechanism that has received considerable attention is based on the transverse resonance between waves and particles. Here the wave phase velocity and particle streaming velocity are oppositely directed so that the particle sees an upward-shifted Doppler frequency equal to its own natural gyrofrequency. This mechanism has been employed by a number of authors to explain the generation

of emissions [Dowden, 1962; Brice, 1964; Bell and Buneman, 1964; Helliwell, 1967] and related particle perturbations [Kennel and Petschek, 1966]. The condition for transverse resonance of non-relativistic electrons is given by

$$v_{||} \cos \Theta = v_p(1 - f_H/f) \quad ,$$

where $v_{||}$ = streaming velocity of electrons, Θ = angle between wave normal and earth's field, v_p = wave velocity, f_H = electron gyrofrequency, f = wave frequency $(f < f_H)$.

It is seen that the required particle velocity increases as the wave frequency is lowered. It has the same magnitude, but opposite sign, as that for the longitudinal resonance when $f = f_H/2$. Thus at frequencies low compared with the gyrofrequency, the resonant electrons must have higher energy for transverse resonance than for longitudinal resonance.(In both cases the energy of the resonant electrons increases with their pitch angle.) It is not surprising, therefore, that emissions linked to the transverse resonance are those which are common at relatively high normalized wave frequencies, such as one-half the gyrofrequency. With the transverse resonance, interaction occurs strongly at zero wave normal angle, and hence this mechanism is especially attractive for explaining interactions involving ducted whistlers. (Ducted whistlers must have small wave normal angles in order to be trapped in a duct.) Energies of interest in the transverse resonance will range from a few kev to several hundred kev.

Much of the literature dealing with the transverse resonance

instability has been based on a small-signal assumption and broadband electromagnetic wave energy. With such a model, Kennel and Petschek [1966] have been able to link the loss rate of electrons due to pitch angle scattering to the intensity of broadband noise generated by the interacting particles. In this process increased particle flux tends to increase the wave output which in turn increases the pitch angle scattering and reduces the wave growth rate. Thus the particle flux tends to remain constant in value while the wave amplitude and the precipitation rate may vary over wide ranges.

Recently the transverse resonance has been employed in the study or narrowband coherent signals whose spatial variations in phase are assumed to be matched to those of the resonant electrons. Under this condition strong phase bunching is encountered which is believed to result in a conversion of particle energy to wave energy [Helliwell, 1967]. Using this principle of phase matching, it is found that the time rate of change of frequency of oscillation can be directly related to the spatial gradient of electron gyrofrequency. For particles moving down (up) the line of force, the frequency rises (falls) with time. Consideration of the phase bunching mechanism suggests that if the intensity of the bunching wave exceeds a certain value, the power delivered to the wave will fall off, giving rise to a natural limiting process. Application of conservation of energy to this model indicates that if the flux of resonant electrons should differ from the equilibrium value for a fixed interaction region,

then the region of interaction would drift at the velocity required to establish equilibrium. Such drift would cause the spatial gradient of gyrofrequency to change which in turn would alter the rate of change of generated frequency with time. Thus if the interaction region crosses the equator in the direction of the particle stream, the frequency of emission first falls, then rises, giving rise to the well-known spectral shape known as the 'hook'. The term 'drifting cyclotron oscillator' (DCO) has been applied to this mechanism.

Employing the (DCO) model, it has been possible to interpret the principal forms of variable frequency narrowband emissions. Furthermore it is found that the finite time required to produce phase bunching can account for the delay observed in the triggering of artificially stimulated emissions.

Associated with the transfer of energy between particles and waves is a change in pitch angle which can result in dumping. The qualitative relations between the particle energy changes and the wave energy changes for the transverse resonance interaction are shown in Table 1. It is seen that for electron waves growth is always acoompanied by an increase in the particle longitudinal energy, and of course a decrease in the particle transverse energy, causing the pitch angle to decrease. For a proton on the other hand, the pitch angle change is reversed and when the proton particle energy increases, the pitch angle decreases. The increased interaction time of the drifting cyclotron oscillator process, compared with incoherent wave interaction, may increase the amount of pitch angle scattering of the resonant electrons, possibly by as much as a factor of 10 [Bell,

private communication]. These ideas lead to the suggestion that a wave interaction experiment in which both the frequency and its variation with time were controlled, could provide new information on the longitudinal component of the gradient of the earth's magnetic field. In this experiment a wave train would be transmitted along a line of force and the resulting change in the pitch angle distribution observed at the satellite. The time required to observe the change would be a measure of the distance of the interaction region from the satellite. From the time derivative of transmitted frequency, the longitudinal variation of electron gyrofrequency would be obtained.

Another application of the transverse resonance occurs with relativistic particles whose mass increase causes their gyrofrequency to be reduced below that for thermal electrons. Thus it is possible to synchronize electron and wave at frequencies well below the gyrofrequency without requiring any Doppler shift. Energy can then be exchanged between the wave and electrons gyrating in the equatorial plane of the earth's magnetic field. By suitably changing the frequency of the exciting wave with time, it is possible to lock the electron to the wave and slowly change its energy [Helliwell and Bell, 1960; Bell, 1964]. The energy can either be increased or reduced. Repeated excitation of the given electron each time it drifts around the earth could in principle raise its energy by a factor perhaps as large as 10. It has been estimated that a ground transmitter radiating 10 megawatts in the frequency range of 23 kHz to 90 kHz might produce a detectable effect at a latitude of 40° geomagnetic

TABLE 1. RELATIONSHIPS BETWEEN CHANGES IN PARTICLE LONGITUDINAL AND TRANSVERSE ENERGY, WAVE ENERGY, AND PARTICLE PITCH ANGLE FOR TRANSVERSE-RESONANCE INTERACTION WITH WHISTLER-MODE SIGNALS. (Appeared as Table 5 in Brice [1964]).

Type of Particle	Whistler Wave Energy	Total Particle Energy	Particle Longitudinal Energy	Particle Transverse Energy	Particle Pitch Angle
Electron	Increases	Decreases	Increases	Decreases	Decreases
Proton	Increases	Decreases	Decreases	Increases	Increases
Electron	Decreases	Increases	Decreases	Increases	Increases
Proton	Decreases	Increases	Increases	Decreases	Decreases

[Bell et al, 1963]. Such high power in a frequency variable source is not presently available. An alternative to this source of power would be a satellite-borne transmitter which could apply strong fields directly in the equatorial plane.

(v) Suggested Experiments

Wave injection experiments can be performed with the transmitter located on the ground or on a satellite. With the transmitter on the ground, the satellite would observe both ducted and non-ducted signals and their associated emissions and would employ particle detectors capable of measuring the changes in spectrum and pitch angle distribution of the interacting particles.

Because of the difficulty in radiating much power from a ground transmitter below 10 kHz, an experiment involving a ground transmitter would be limited to altitudes less than about 3.5 earth radii ($f_H \approx$ 20 kHz). However this is a region that is known to be a source of emission and that is readily accessible to the ground sources. A possible experiment in this class would be to try to change the pitch angle distribution of certain electrons by transmitting suitable triggering signals from the ground. For transverse resonance, the satellite particle detector would be located in the same hemisphere as the ground transmitter, while for longitudinal resonance the satellite should be in the conjugate hemisphere. If the satellite were below the mirror points of most of the particles, then pitch angle scattering should cause a rather large change in particle flux. The measurements might be most effective if made on a polar-orbiting

satellite at an altitude of about 300 to 1000 km. If the satellite were in a duct, the associated emission could be observed on the ground at the conjugate point.

For more detailed studies of the wave generated in the duct, it would be desirable to have the satellite travel near the top of the line of force where the emissions are believed to be generated. Thus a satellite traveling in polar orbit roughly tangent to the field line (say $L = 4$) could successively observe different part of emissions being stimulated by successive pulses transmitted from the ground. Variations in the transmitted signal could be made to test the prediction of the DCO theory regarding the relation between the location of the generation region and df/dt.

In the second class of wave-particle interaction experiment the transmitter is placed in a satellite. Advantages over the ground transmitter are increased field intensity and access to a much wider range of wave normals. Here two orbits would be especially interesting, one polar at medium altitude ($R_E = 2$ to 4) and the other equatorial at synchronous distance (6.6 R_E) .

The medium altitude polar orbit appears to offer several advantages for a first experiment. The region between $R_E = 2$ and 4 is known to be an active emission region and is readily accessible to signals from ground or satellite. Particle activity is present much of the time in this region, but should be less variable than at greater altitudes, and hence the detection of wave-induced perturbations should be easier. The lower altitudes allow use of higher

frequencies and hence reduce the size of antenna required. Thus at $R_E = 2$, $f_{H_o} = 110$ kHz, so that frequencies up to 55 kHz or so should be usable. Furthermore the relatively high refractive index inside the plasmaphere helps further to reduce the length of antenna required. For example at a frequency of 16 kHz on the equator at $R_E = 3$ (assuming an electron density of 400/cc), the refractive index for zero wave normal angle is about 8, a leg of the corresponding half-wave dipole would then extend about 600 meters from the satellite.

After experience is gained from the medium altitude experiment, a synchronous orbit satellite would be desirable. It would be designed to stimulate interaction processes on lines of force passing through the auroral zones. (Observations in OGO's I and III demonstrate that whistler-mode noise is observable out to the magnetopause on the sunward side of the earth.) Ionospheric effects that might be produced by the precipitated particles include D-region absorption, micropulsations, auroral effects, etc. A preferred location for such an experiment would be the line of force passing through the conjugate ground stations at Byrd and Great Whale River. Real time telemetry of the ground data, via satellite perhaps, is suggested to avoid the long delays normally encountered in receiving data from the Antarctic. The highest frequencies involved in the synchronous orbit experiments would be about two to three kHz.

Finally, there is the class of experiments in which waves and particles are injected from the same spacecraft. For maximum injection along a given field line the satellite would follow an orbit roughly tangent to the field line. Both longitudinal and transverse

resonances could be employed. If both waves and particle streams were suitably pulsed, the position of wave-particle interaction along the field line could be varied. For longitudinal resonance, interaction would occur before the electrons reached their mirror point. Both waves and particles could probably be detected on the same spacecraft since the waves would tend to return via magnetospheric reflection. For transverse resonance, on the other hand, only the electrons could be expected to return unless the satellite were in duct.

As an example of a specific experiment, consider the injection of an electron stream with a broad energy spectrum but having a certain narrow range of pitch angles falling outside the loss cone. Short whistler-mode wave trains transmitted from the satellite would interact with resonant particles returning from their mirror points. By adjusting the df/dt of the wave train, the region of maximum interaction could be selected. Its exact position would then be determined by measuring the delay of the corresponding changes in pitch angle.

Essential to the success of any of these 'modification' experiments is a knowledge of the parameters of the magnetospheric plasma at the time the experiment is performed. The satellite should carry appropriate sensors for this purpose, including a magnetospheric sounder. The sounder and whistler-mode wave generator could be the same device since their characteristics are rather similar. The sounder would be used to excite whistler-mode echoes from the lower ionosphere (in the same and opposite hemispheres) at frequencies

below the gyro and plasma frequencies. It would also be used to bounce reflections off the surface of the plasmaphere above these frequencies (in the 'HF' mode). It should provide interesting data on the topology of the plasmapause and the outer edge of the through just outside plasmapause. According to Angerami and Carpenter [1966], the plasma frequency in the through may be as low as 10 kHz while that within the plasmaphere may be as high as 200 kHz. A sounder frequency range of 5 kHz to 500 kHz would therefore be desirable. Equipment parameters such as frequency, pulse length, repetition period and range should be made adjustable by command from the ground.

Particle parameters of interest include pitch angle and energy distribution. Because of their low mass, electrons are expected to play the dominant role in wave particle interactions, but perturbations of energetic protons are possible and should not be overlooked. For electrons, the energies of interest are estimated to range from 100 ev (F layer, low frequency, longitudinal resonance) to perhaps 300 kev (large pitch angle or transverse resonance at low f/f_H) . Detectors should have response times of a few milliseconds in order to study the known transient effects.

(vi) Experiment Requirements

With respect to the receiving type of experiment, experience is extensive and designs can be made with considerable confidence. The main problem is that a suitable ground transmitter is not yet available with the characteristics desired. An experimental version

of a possible transmitter is presently under development at Byrd Station in the Antarctic where a 150 kw source (2 to 300 kHz) is being used to excite a 21-mile horizontal electric dipole layed on the ice. Efficiencies are however low and the signal strengths observed at the POGO satellites above the transmitter have been relatively week. However, such a transmitter might be located at a lower latitude so that paths at and within the plasmapause could be excited more readily. It is believed that transmitter powers well in excess of 100 kw would be required to oduce useful new results with this type of experiment.

At the present time limited receiving experiments can and are being made with the aid of transmissions normally available from Navy VLF stations. However, adequate control of the frequency function is not available. Furthermore desired transmission can be obtained only when the transmitter is not being used for communication, thus it would be difficult to coordinate the ground transmission with the satellite position.

Receiving equipment in the satellite could be similar to that used on the OGO series in which the frequency ranges from 10 Hz to 100.000 Hz. Broadband and narrowband tunable receivers would be needed in the new experiments as well as in the present OGO experiments. Loop antennas would be employed to provide reliable measurement of field intensities. Power and weight requirements for the receiving equipment are nominal, being of the order of a few pounds and a few watts, respectively. Loop antennas of roughly 2 meters in diameter are satisfactory.

A satellite transmitter is a more difficult proposition. Very little experience has been obtained in the operation of transmitting antennas at whistler-mode frequencies. Data from the Alouette II topside sounder experiment shows that whistler-mode echoes from the ground are sometimes excited when the satellite is near the magnetic pole. In these experiments the frequency was around 200 kHz and the power delivered to the antenna was less than one watt. This experience is a basis for expecting that some of the experiments mentioned above could be performed using a long electric dipole and a transmitter putting out only a few watts. In addition to variable frequency, its characteristics should inclued variable pulse length, various forms of amplitude and frequency modulation, and variable power. The pulse length should be variable so as to test suggestions regarding the effect of duration of signal on emission stimulation. As a starting point for the antenna design, we might consider a circularly-polarized array made up of two orthogonal dipoles excited 90° out of phase. A third dipole, orthogonal to the other two, might be needed to insure efficient excitation of waves with large wave normals. Signals could be received on the same antennas as in Alouette II or on separate loop antennas to provide better field intensity calibration.

Satellite interfaces include up and down data links and interference problems. High bit rates comparable to those obtained in the OGO satellites (64 kilobits/s) are desirable if the details of spectral changes are to be recovered. An analog channel transmitting a bandwidth of about 30 kHz would be desired. A number of commands from ground to satellite are required in order to control both the

transmitter and receiver. If an electron gun is included, additional commands would be required for its operation. With respect to interference we find problems in both directions. VLF receivers must be protected against the noise produced in a normal spacecraft resulting from the operation of dc-dc inverters and other spacecraft systems. One suggestion is to place the inverter frequencies above the range of interest, say > 300 kHz. Positioning the VLF sensor well away from the main body is also helpful. Interference to other on-board experiments by the transmitter could be controlled by time sharing.

The payload sizes for the experiments outlined above are not yet known. Certainly the Alouette II payload is a minimum, and we can anticipate an increase by a factor of ten if we are to radiate a kilowatt at VLF. The antenna tuning requirement alone is expected to increase considerably the weight and heat dissipation requirements. A total power capability of ten kilowatts is likely to be required.

In preparation for the design of such experiments, it is important to study the behavior at VLF of long antennas in the ionosphere. Especially important is the problem of non-linear effects in the medium in the immediate vicinity of the antenna. The mechanical problems of paying out the conductor and stabilizing the system need to be studied. The trade-off between the antenna length and antenna input total power should be investigated.

The lowest frequencies generally require the greatest lengths. Thus at synchronous altitude for a frequency of 1 kHz and a refractive

index of 10, the wavelength is 30 km. A half-wave center-fed dipole would then require two booms each 7.5 km in length. A much shorter length may be usable provided sufficient power is available.

Extension of the single satellite type of experiment should be considered. Thus an additional satellite might be used to detect conjugate point effects produced by the transmitter. Another possibility would be to use a low-altitude polar orbiting satellite to study particle and wave effects stimulated by a transmitter in a synchronous satellite. In general, any VLF transmitter experiment should take advantage of the presence of satellites capable of receiving VLF waves and measuring particle effects.

Finally, it should be noted that supporting ground observations are an important element in any wave-particle interaction program. Ground observations of whistlers and VLF emissions provide diagnostic data on certain properties of the magnetosphere such as electron density, needed to interpret the interaction results. Furthermore, both wave and particle effects caused by the interaction in the magnetosphere can often be observed in some form from the ground.

A schematic drawing illustrating some of the suggested experiments is shown in Figure 1. Although the interaction regions are shown at the top of each line of force, they may occur elsewhere as well. In particular, the existence of LHR noise suggests that strong interaction may occur in the region of the 'turn-around' of the boomerang mode which occurs near the LHR frequency. Also of

interest, but not shown in Figure 1, are the 'short' boomerang paths that have their turn-around points in the same hemisphere as the satellite. To excite the boomerang mode the transmitter frequency must exceed the local LHR frequency and be less than the maximum LHR frequency on the field line through the satellite.

FIGURE CAPTIONS

Figure 1. Examples of wave-particle interaction experiments using a VLF transmitter in a polar-orbiting satellite (labeled S). The noon-midnight meridium is shown, with the position of the plasmapuse assumed to be the same on both sides. Shaded boxes show assumed region of strong wave-particle interaction (T = transverse or cyclotron resonance; L = longitudinal resonance). Unlabeled arrows show ray direction of satellite radiation and stimulated emissions. Arrows labeled 'e' show streaming direction of electrons perturbed by transverse interaction. Arrows labeled 'HF' show path of sounding signals at frequencies higher than the electron plasma and gyrofrequencies. S_1 = longitudinal resonance with auroral zone electrons below satellite ($f \lesssim 10$ kHz); weak excitation of transverse resonance at top of line of force, employing ducted propagation ($f \lesssim 1.5$ kHz); S_2 = transverse resonance with trapped electrons at top of line of force at plasmasphere boundary, waves trapped on knee ($f \approx 7$ kHz); S_3 = longitudinal resonance with non-ducted boomerang mode ($f \approx 3$ kHz); S_4 = strong excitation of longitudinal resonance ($f \approx 6$ kHz); S_5 = 'HF' sounding of plasmapause ($f \approx 10$ kHz - 300 kHz); S_6 = strong excitation of transverse resonance ($f \approx 7$ kHz).

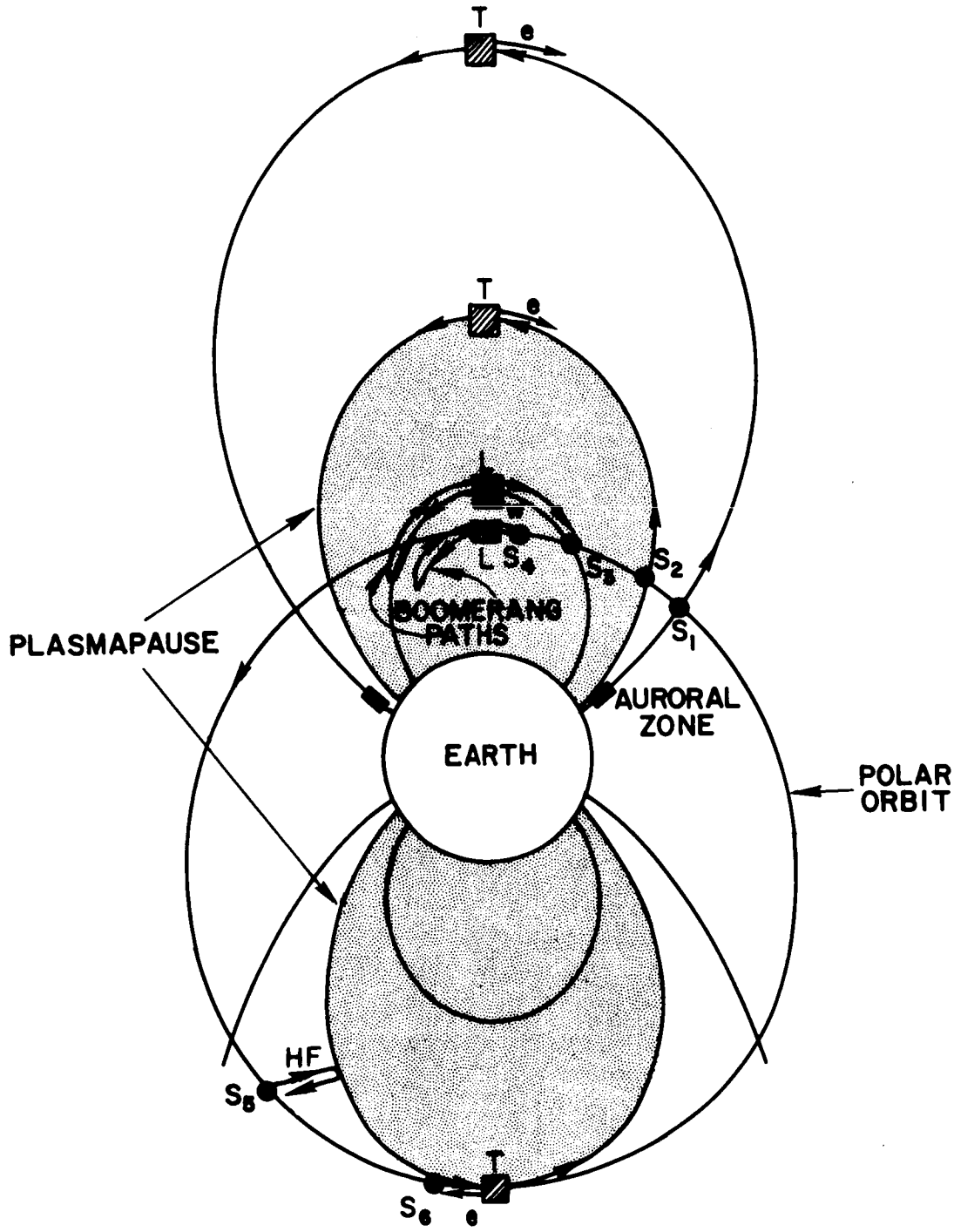
T
e
T
e
L
S_4
S_3
S_2
S_1
BOOMERANG PATHS
PLASMAPAUSE
AURORAL ZONE
EARTH
POLAR ORBIT
HF
S_5
T
S_6
e

Figure 1.

REFERENCES

Angerami, J.J. and D.L. Carpenter, Whistler studies of the plasmapause in the magnetosphere, 2, electron density and total tube content near the knee in the magnetospheric ionization, J. Geophys.Res., 71, (3), 711, Feb.1, 1966.

Bell, T.F., Wave-particle gyroresonance interactions in the earth's outer ionosphere, SEL-64-063, Radioscience Lab., Stanford Electronics Labs., Stanford University, Stanford, California, 1964.

Bell, T.F., and O. Buneman, Plasma instability in the whistler-mode caused by a gyrating electron streams, The Physical Review, 133, (5A), A1300-02, March 1964.

Bell, T.F., R.A. Helliwell, R.F. Mlodnosky, and R.L. Smith, Geocyclotron feasibility study, AFSWC-TDR-63-35, Air Force Special Weapons Center, Air Force Systems Command, Kirtland AFB, New Mexico, 1963.

Brice, N.M., Discrete very low frequency emissions from the upper atmosphere, SEL-64-088, Radioscience Lab., Stanford Electronics Labs., Stanford University, Stanford, California, 1964.

Carpenter, D.L., Ducted whistler-mode propagation in the magnetosphere; a half-gyrofrequency upper intensity cutoff and some associated wave growth phenomena, J. Geophys. Res., (in press), 1968.

Carpenter, D.L. and Keppler Stone, Direct detection by a whistler method of the magnetospheric electric field associated with a polar substorm, Planet Space Sci., 15, 395-97, 1967.

Dowden, R.L., Doppler-shifted cyclotron radiation from electrons: A theory of very low frequency emissions from the exosphere, J.Geophys. Res., 67, (5) 1745-50, 1962.

Dunckel, N. and R.A. Helliwell, Emission detected on the OGO-I satellite, (in preparation).

Helliwell, R.A., A theory of discrete VLF emissions from the magnetosphere, J. Geophys. Res., 72 (19), 4773-90, Oct. 1, 1967.

Helliwell, R.A., Whistlers and Related Ionosphere Phenomena, Stanford University Press, Stanford, California, 1965.

Helliwell, R.A. and T.F. Bell, A new mechanism for accelerating electrons in the outer ionosphere, J.Geophys.Res., 65,(6), 1839-42, 1960.

Helliwell, R.A., J. Katsufrakis, M. Trimpi and N. Brice, Artificially stimulated VLF radiation from the ionosphere, J. Geophys.Res., 69, (11), 2391-94, 1964.

Heyborne, R.L. Observations of whistler-mode signals in the OGO satellites from VLG ground station transmitters, SEL-66-094, Radioscience Lab., Stanford Electronics Labs., Stanford University, Stanford, California, 1966.

Jørgensen, T.S., Interpretation of auroral hiss measured on OGO-II and at Byrd Station in terms of incoherent Cerenkov radiation, J. Geophys. Res., (in press), 1968.

Kennel, C.F. and H.E. Petschek, A limit on stably trapped particle fluxes, J.Geophys.Res., 71, (1), 1-28, 1966.

Kimura, I., Effects of Ions on whistler-mode ray tracing, Radio Science, 1, (new series) (3), 269-83, March, 1966.

Liemohn, H.B., Cyclotron resonance amplification of VLF and ULF whistlers, J.Geophys.Res., 72, (1), 39-56, Jan.1, 1967.

Oliven, M.N and D.A. Gurnett, An association between discrete VLF emissions and 40 kev electron microbursts, Dept. of Physics and Astronomy, State University of Iowa, 1966.

Smith, R.L., Propagation characteristics of whistlers trapped in field-aligned columns of enhanced ionization, J. Geophys.Res., 66 (11), 3699-3707, 1961.

Smith, R.L. and J.J. Angerami, Magnetospheric properties deduced from OGO-I observations of ducted and nonducted whistlers, J. Geophys.Res., (in press), 1968.

Thorne, R., and C. Kennel, Quasi-trapped VLF propagation in the outer magnetosphere, J.Geophys.Res., 72 (3), 857-70, Feb.1, 1967.

APPENDIX

In the following few pages we have attached a memorandum kindly supplied to us by Dr. W. Hess (Director of Science and Applications) which gives useful information on the electrical power potentially available from the uprated Saturn I and Saturn V vehicles.

The numbers supplied in this memorandum should be regarded as subject to revision or change without notice. It is hoped they give some perspective however on the power requirements discussed in this report.

U.S. GOVERNMENT MEMORANDUM

Revised:October 25, 1967
Date: Oct. 5, 1967
In reply refer to: TB/10-4/28

TO: TA/Director of Science and Applications

SUBJECT: Electrical power potentially available from the Uprated Saturn I vehicle, Saturn V vehicle, and envisioned power supplies for earth orbital missions.

Since on either on Uprated Saturn I or a Saturn V launch, the SIB, SIC, and SII never attain earth orbit; only those stages (Saturn IV/Instrument Unit, Service Module, and Command Module) which would be used in an earth orbital mission are discussed herein. See figure 1 for the stack configurations.

The power available of any particular mission is a function of the mission's objectives and operational constraints. Since these are not firm at this time, the data levels presented herein are to be considered as representative. All power is nominally 28 volts d.c.

Saturn IV/Instrument Unit (S IV/IU)

The SIV/IU is separated into two dependent power units. These units are composed of silver-zinc batteries. The power is tabulated in table 1 for the various missions.

For future missions, Marshall Space Flight Center is considering extending the lifetime of the S IV and IU up to 25 hours. The use of solar cell panels and battery combinations for long duration missions is also being considered.

Service Module (SM)

The Service Module power is supplied by a bank of three fuel cells. They supply a total of 2850 watts for sustained operation with a maximum of 4200 watts for short periods. A battery for use in contingency deorbit and return is being seriously considered as an addition to the SM's power complement.

Command Module (CM)

The Command Module uses silver-zinc batteries. These batteries are primarily for re-entry use. See Table 1 for capacity.

TABLE 1

(28 volt power)

Mission	Booster		1. Mission Duration (days)	2. Mission Utilization (amp-hrs)	3. Provisioned Power (a) (amp-hrs)	4. Maximum Capability (amp-hrs)	5. Maximum Potentially Available (b) (amp-hrs)
AS-204	SIB	S IV	0.313	266	387	387	121
		IU	0.313	842	1,400	1,400	558
		SM	13.7	22,500	22,900	22,900	400
		CM	13.7	104	120	120	16
AS-501	S V	S IV	0.313	452	760	760	308
		IU	0.313	516	1,400	1,400	884
		SM	0.375	1,720	9,830	22,900	20,180
		CM	0.375	113	120	120	7
AAP-1	SIB	S IV					
		IU	0.273	493	810	1,050	557
		SM	26.8	56,450	73,150	73,150	16,700
		CM	26.8	83	120	120	37
AAP-3	SIB	S IV					
		IU	0.273	493	810	1,050	557
		SM	56	118,300	116,700	116,700	1,600
		CM	56	174	200	200	26

(a) Certain missions have off-loaded power systems, therefore, column 3 (Provisioned Power) can be less than column 4 (Maximum Capability).

(b) Column 5 (Maximum Potentially Available) is the difference between column 4 (Maximum Capability) and column 2 (Mission Utilization).

The electrical power as presented in table 1 is referenced to the expected vehicle performance. Deviations from expected performance, mission modifications, or objective changes greatly affect these values. The column labeled "Maximum Potentially Available" should be used as an indication whether additional batteries, fuel cells, etc., must be added to a given mission to satisfy a specific scientific need. The mission requirements as a whole must be analyzed for each configuration contemplated to insure that operational requirements can still be satisfied after the incorporation of scientific experiments.

An indication of the possible means of supplying power unavailable from the present systems is given in figures 2 and 3. These figures were abstacted from the USAF Systems Command Document entitled "Space Planners Guide". Exotic systems suchas nuclear reactors, chemical dynamic generators and solar dynamic generators are not practical in the context of the Saturn Apollo Applications Program.

o Figure 2 A indicates which type of system should be selected as a function of electrical output power and mission duration.

o Figure 2 B indicates the rate of discharge of a primary battery as a function of electrical energy, installed battery weight, and installed battery volume.

o Figure 2 C indicates the number of charge/discharge cycles available from a secondary battery as a function of electrical energy and installed battery weight.

o Figure 2 D indicates the realtionship of short period-high power drain sources as a function of system weight and electrical energy.

o Figure 3 A indicates fuel cell power output, for various mission durations, as a function of system weight.

o Figure 3 B indicates solar cell output, for various array configurations with optimum solar orientation, as a function of system weight.

o Figure 3 C indicates a radioisotope power output as a function of system weight.

Fred T. Pearce

Enclosures:
Figure 1, 2 and 3

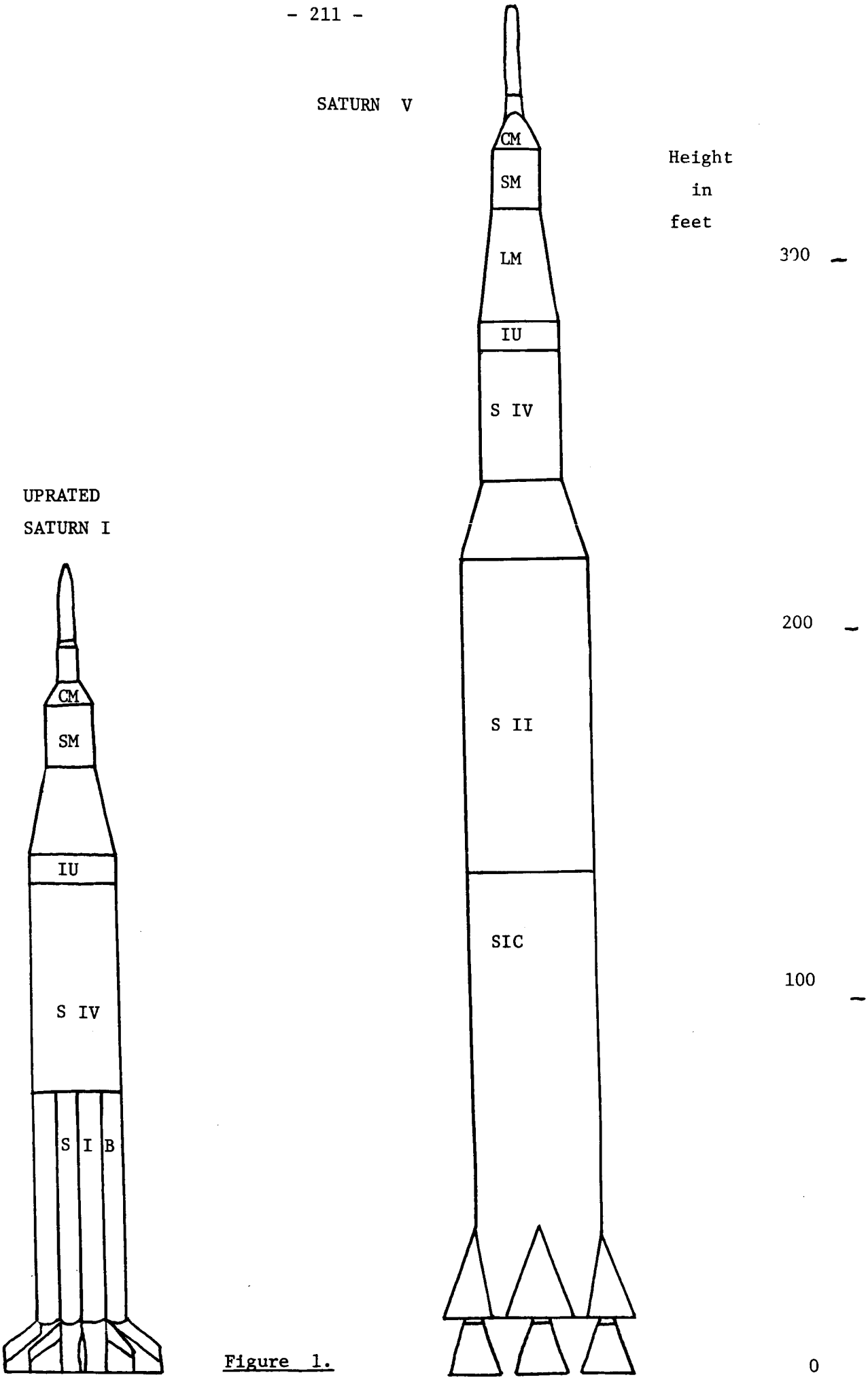
SATURN V
CM
SM
LM
IU
S IV
S II
SIC
Height
in
feet
300
200
100
0
UPRATED
SATURN I
CM
SM
IU
S IV
S I B

Figure 1.

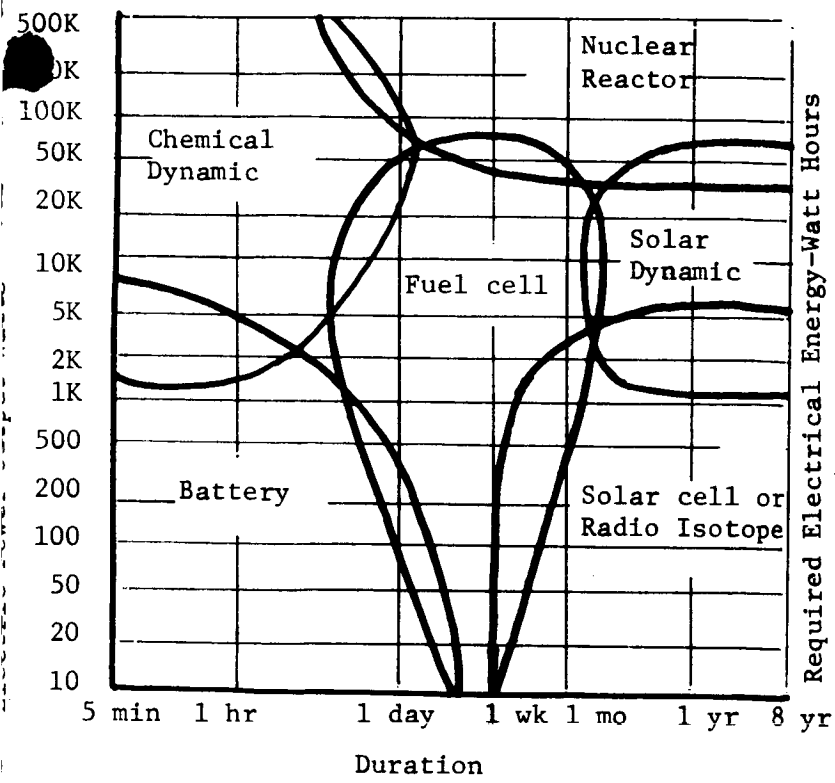

Figure 2 A Power Supply Operating Regimes

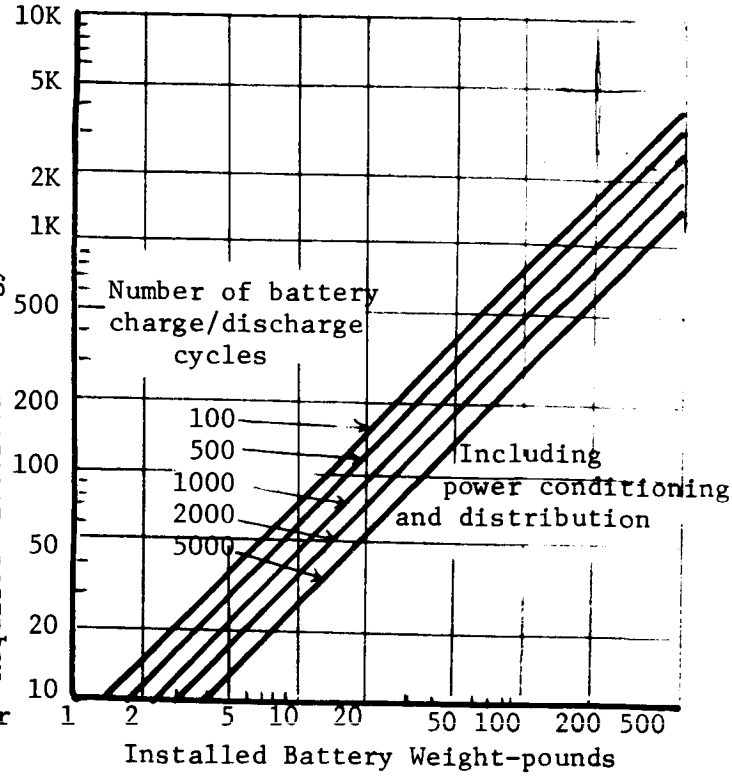

Figure 2 C Secondary Battery Weight

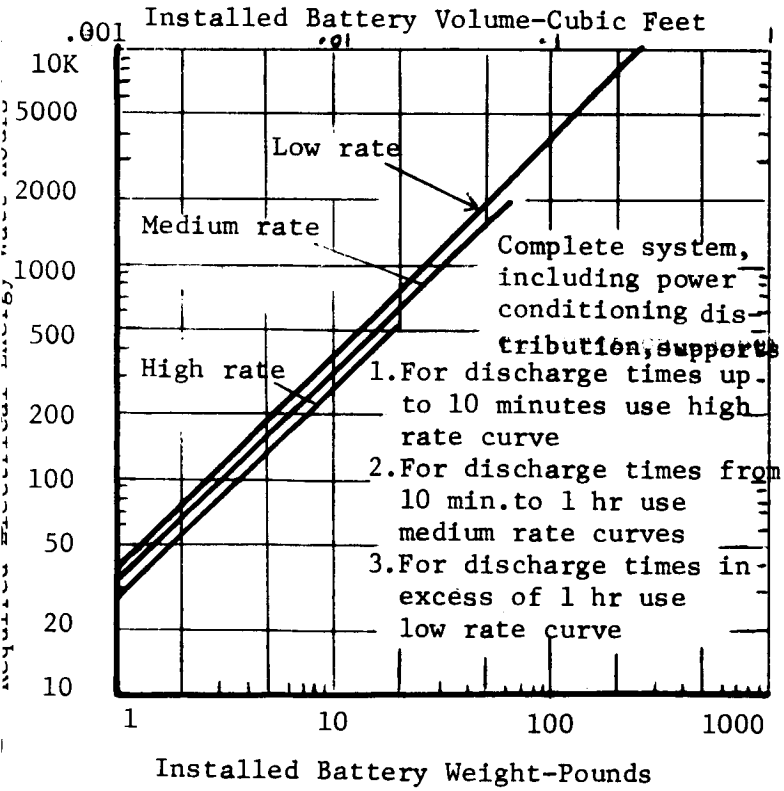

Figure 2 B Primary Battery Weight

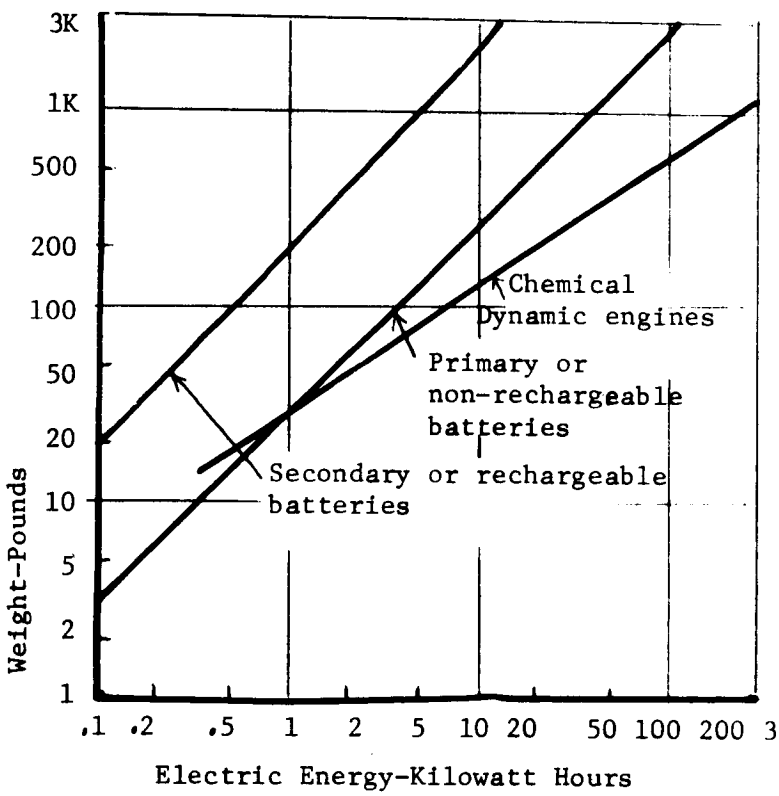

Figure 2 D Short Period-High Drain Power Source

Figure 2.

FUEL CELL, SOLAR CELL, AND RADIOACTIVE POWER SUPPLY PARAMETERS

FIFURE 3

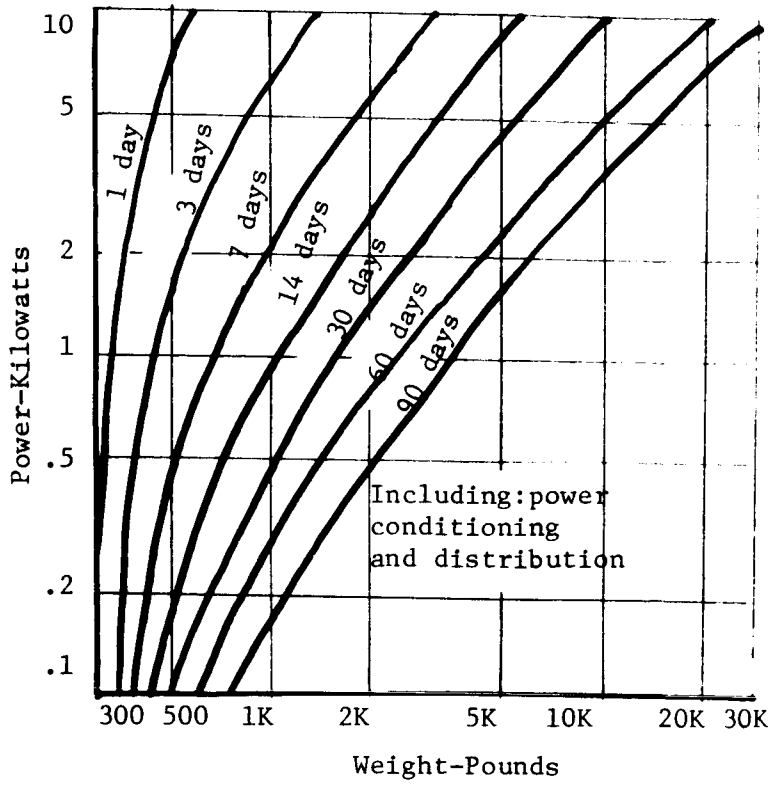

Figure 3 A Fuel Cell Weight

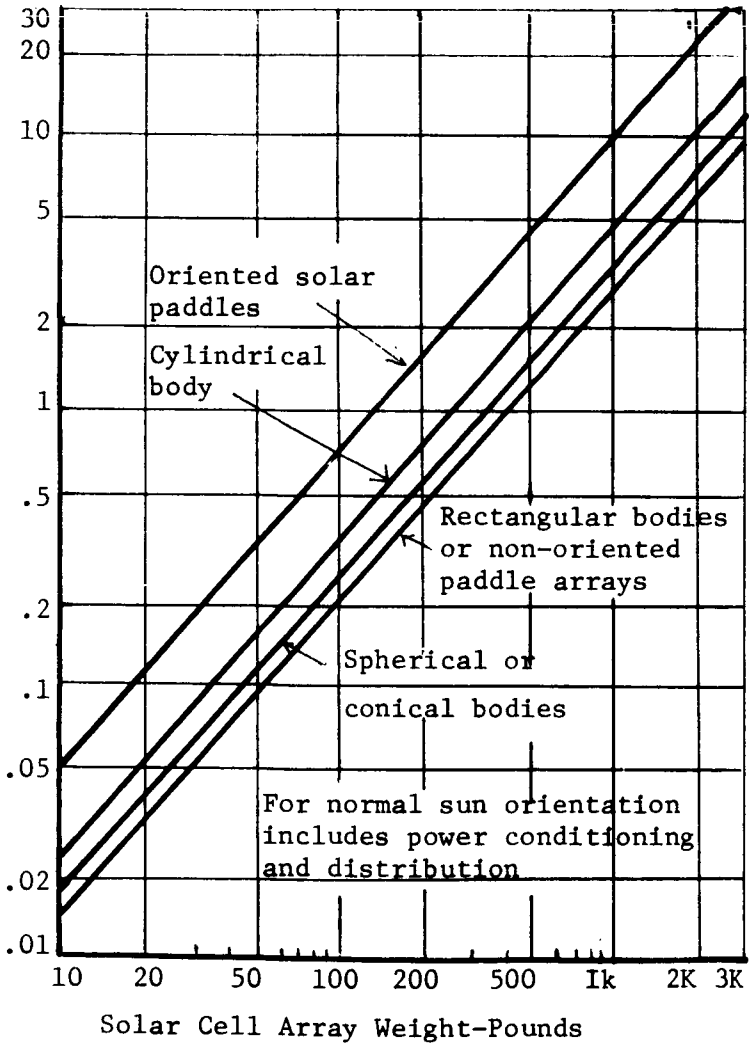

Figure 3 B Solar Cell Power System Weight

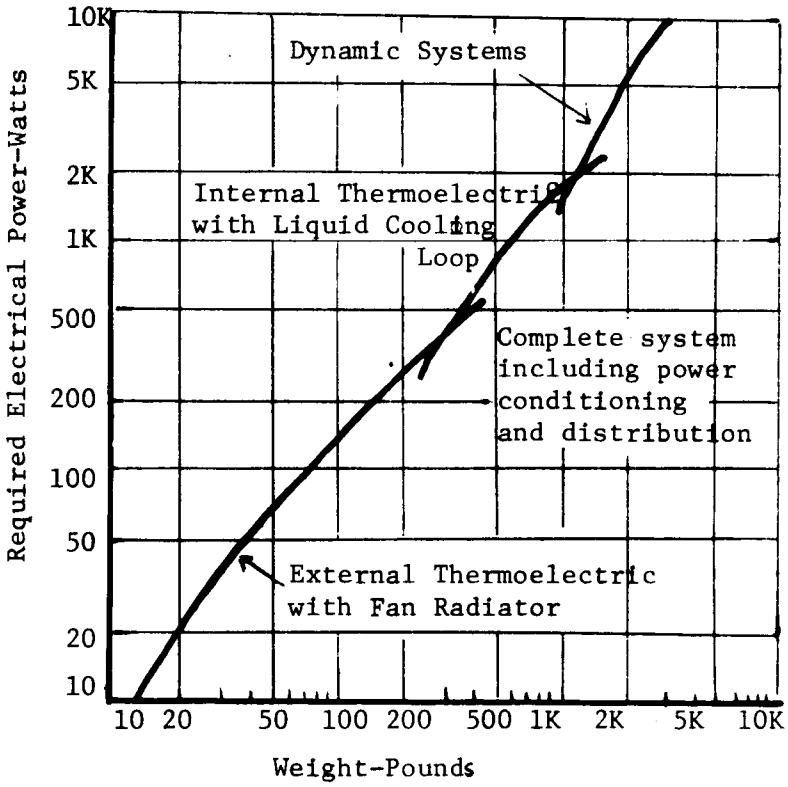

Figure 3 C Radioisotope Power Supply Weight